MATE: DELAYED CREDIT ASSIGNMENT FOR TEST-TIME ADAPTATION IN TIME-SERIES FORECASTING

Anonymous authors
Paper under double-blind review

ABSTRACT

Distribution shifts can undermine time-series forecasting accuracy after deployment. Test-time adaptation for time-series forecasting (TSF-TTA) can mitigate these errors, but a single correction mechanism can struggle with complex and abrupt shifts. Its effectiveness also varies across forecast leads and variable channels. Delayed target availability further complicates learning where and how strongly to apply each correction. We introduce MATE (Matured-Feedback Adaptive Test-Time Error Correction) to address these challenges. MATE separates correction generation from credit allocation under a full-window feedback protocol. It keeps the pretrained backbone frozen and constructs complementary corrections through a structured residual dictionary. As feedback matures, MATE accumulates credit statistics to guide lead–channel credit weights and regulate each correction's contribution. It also updates input and output calibrators using matured historical forecast errors to capture distribution shifts. Comparisons across datasets, forecasting backbones, and shift scenarios demonstrate broad forecasting gains. Mechanism ablations further support the effectiveness of position-specific correction control driven by matured feedback.

1 INTRODUCTION

Time-series forecasting supports critical decisions in energy, weather, and finance, yet evolving temporal statistics can undermine relationships learned during training (Gama et al., 2014; Liu et al., 2022). In streaming deployments, forecasts must continue as conditions change, while periodic offline retraining can leave emerging errors unaddressed between updates. Test-time adaptation for time-series forecasting (TSF-TTA) uses newly observed data to adjust forecasts during deployment (Kim et al., 2025; Grover & Etemad, 2025).

Auxiliary calibrators support such adaptation by adjusting a pretrained model's inputs or outputs while keeping its parameters frozen (Kim et al., 2025; Medeiros et al., 2025). Existing designs include contextual (Im & Kwon, 2026) and frequency-based corrections (Wang et al., 2026), with gating or shift-aware mechanisms regulating adaptation (Grover & Etemad, 2025). When multiple corrections are available, individually useful adjustments may become redundant or interfere in combination. This raises a credit-allocation problem: learning the weights of candidate corrections from their combined effect on historical prediction loss.

Correction utility can vary across forecast leads and variable channels: extending the latest observed level may help near-term predictions but miss longer-term changes, while the same adjustment may help one variable and overcorrect another. Learning these differences requires feedback, but forecast targets become observable only as the stream unfolds (Huang et al., 2026). Under the full-window feedback protocol adopted from FAC (Wang et al., 2026), a historical forecast becomes eligible for supervised updates only after all its targets arrive. When matured feedback is limited, estimating weights independently at every position restricts the evidence supporting each estimate. This motivates sharing evidence across positions while retaining differences in correction utility.

We address this problem with MATE (Matured-Feedback Adaptive Test-Time Error Correction), which separates correction generation from credit allocation. A structured residual dictionary generates candidates around a frozen backbone using output structure, historical forecast versions, and current observations. Once feedback matures, a credit controller accumulates second-order statistics from candidates saved at prediction time and base-forecast errors to evaluate correction com-

Reviewers: please read the Reviewer Guidelines (iclr.cc/Conferences/2027/ReviewerGuidelines) and the AI Policy for Reviewers (iclr.cc/Conferences/2027/AIPolicyForReviewers). If you used AI to expand, edit, or polish your review, please provide the input text to the LLM. Better still, consider skipping the LLM and submitting your original text: we, and the authors, are much more interested in your unedited thoughts than in what an LLM has to say. AI-assisted or not, you are putting your name and reputation behind your review: LLM-generated falsehoods, hallucinations or misrepresentations are subject to disciplinary action, which may include desk-rejecting all papers you have authored.

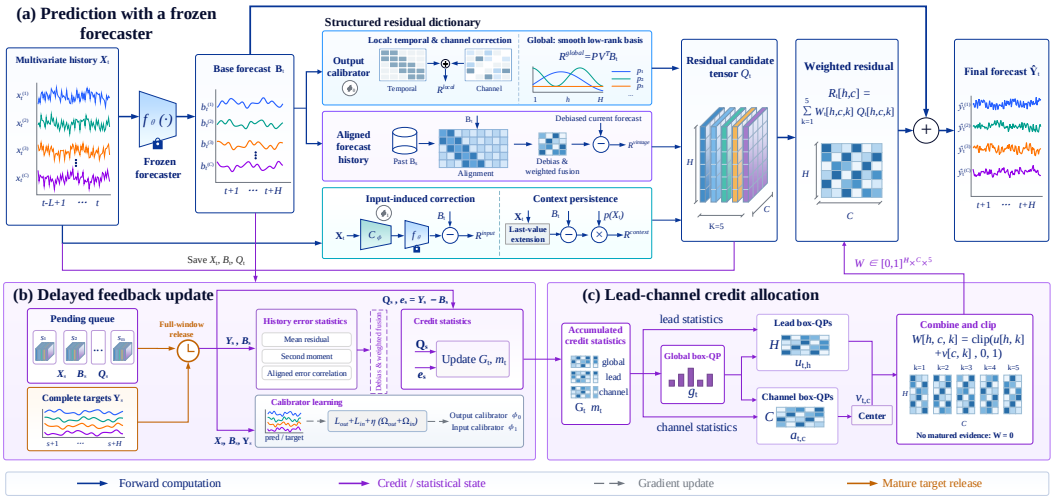


Figure 1: MATE framework. (a) Frozen-backbone prediction with weighted residual corrections. (b) Updates from fully matured feedback. (c) Credit allocation from global, lead, and channel statistics.

binations and account for interactions among residuals. It regularizes lead- and channel-dependent weights toward a shared global credit reference and combines them into structured lead–channel allocations. Our contributions are threefold:

- We separate candidate residual generation from feedback-driven credit allocation around a frozen forecaster under full-window delayed feedback.
- We develop a controller that evaluates saved residual combinations using second-order statistics and combines lead- and channel-dependent weights regularized toward a shared global reference.
- Across six datasets, four backbones, and five scenarios, MATE achieves the lowest MSE among compared methods in 396/460 configurations (86.1%) and the lowest mean MSE in every scenario. Ablations support the aggregate benefits of structured allocation, historical forecast versions, and current context.

2 Related Work

2.1 Online Time-Series Forecasting

Online time-series forecasting (OTSF) updates forecasting systems as streams evolve. FSNet combines fast adaptation and memory to learn recent patterns while reusing historical ones (Pham et al., 2023); OneNet ensembles temporal- and variable-dependency predictors using online feedback (Zhang et al., 2023). They emphasize learning representations and weighting existing predictors, respectively.

Both depend on feedback availability. Delayed-feedback online learning formalizes how waiting for outcomes affects decisions and updates (Joulani et al., 2013). Act-Now and DSOF revisit online forecasting and evaluation through label decomposition and dual-stream learning, respectively, emphasizing that information use must respect observation arrival order (Liang et al., 2024; Lau et al., 2025). ADAPT-Z further addresses multi-step feedback delay through feature adjustment (Huang et al., 2026). These studies establish why feedback timing is part of the adaptation problem, while targeting different components from the lead–channel credit weights considered here.

Auxiliary calibration around frozen backbones connects OTSF and TSF-TTA through streaming learning and adapter design (Kim et al., 2025; Medeiros et al., 2025). In this setting, candidates adjust the same base forecast, so weighting their corrections differs from selecting among complete predictors. MATE studies this credit-allocation problem using matured historical losses.

2.2 Test-Time Adaptation for Time-Series Forecasting

Test-time adaptation (TTA) adapts pretrained models to shifted test data (Liang et al., 2025). Vision approaches include auxiliary self-supervision (Sun et al., 2020), entropy minimization in Tent (Wang et al., 2021), and continual adaptation in CoTTA (Wang et al., 2022). Unlike common unlabeled vision settings, forecasting gradually reveals targets, allowing historical errors to supervise adaptation. The challenge is to use this evidence without relying on targets unavailable at prediction time.

TAFAS uses backbone-agnostic gated calibration before and after a frozen forecaster with period-aware scheduling (Kim et al., 2025). PETSA combines low-rank adaptation, dynamic gating, and losses addressing robustness, frequency content, and local structure (Medeiros et al., 2025). DynaTTA adjusts learning rates and correction gates using prediction errors and representation shifts, and introduces TTFBench (Grover & Etemad, 2025). COSA uses recent statistical context for output correction (Im & Kwon, 2026), while FAC learns frequency-domain corrections from fully matured targets (Wang et al., 2026).

These approaches provide complementary correction mechanisms and adaptation signals, but aggregate shift magnitude does not determine each correction's utility across leads and channels. Under the same shift, a correction may help one position and overcorrect another. Position-specific weights can reflect this difference, but must share evidence when feedback is sparse. MATE therefore treats credit allocation as a separate task: matured losses evaluate residual combinations, while a global reference regularizes lead–channel weights to balance shared evidence and positional differences.

3 Problem Setup

At deployment, let $x_t \in \mathbb{R}^C$ denote the observation at time t, where C is the number of variables (channels). Given a history window $X_t = (x_{t-L+1}, \ldots, x_t) \in \mathbb{R}^{L\times C}$ of length L, the task is to predict the next H observations, $Y_t = (x_{t+1}, \ldots, x_{t+H}) \in \mathbb{R}^{H\times C}$. Each forecast thus contains $H \times C$ values, indexed by forecast lead and channel.

The pretrained backbone f_θ produces the base forecast $B_t = f_\theta(X_t)$. An adaptation module with learnable parameters ϕ_t calibrates this forecast, yielding $\widehat{Y}_t = F_{\theta,\phi_t}(X_t)$, where F_{θ,ϕ_t} denotes the combined forecasting system. Dependence on the available historical information is implicit in this notation. The backbone parameters θ remain fixed, and supervised updates to ϕ_t use only fully matured historical feedback.

At time t, the system may use only information that has already arrived. Under the full-window feedback protocol (Wang et al., 2026), a historical window with forecast origin s becomes eligible for supervised updates only once all H targets are observed, i.e., when $s + H \le t$. The eligible historical records are

$$\mathcal{D}_t = \left\{ (X_s, \widehat{Y}_s, Y_s) \mid s \in \mathcal{T}_t,\ s + H \le t \right\}, \tag{1}$$

where $\mathcal{T}_t$ is the set of historical origins at which forecasts have already been issued, and $\widehat{Y}_s$ is the forecast saved at origin s. Windows that have not fully matured contribute no partially supervised loss, although their already observed values may enter subsequent inputs. Evaluation uses forecasts as originally issued; later adaptation cannot revise past predictions. Within this setting, we study how historical feedback can determine lead–channel credit weights for subsequent forecasts.

4 Method

4.1 Overview

To address position-dependent correction utility under delayed feedback, MATE separates candidate generation from credit allocation through three components (Figure 1). At prediction time, a structured residual dictionary constructs complementary corrections around the frozen backbone. A credit controller combines them using lead–channel weights learned from matured historical errors. After all targets in a saved window arrive, a delayed-feedback update revises credit statistics, historical error statistics, and calibrator parameters for subsequent predictions. This separates the available directions of correction from the evidence used to determine their contributions.

MATE combines the frozen forecast B_t with five candidate residuals in $\mathcal{K}$—local, global, vintage, input, and context—using credit weights learned from matured feedback:

$$\widehat{Y}_t = B_t + \sum_{k \in \mathcal{K}} W_t^{(k)} \odot R_t^{(k)}. \tag{2}$$

where $R_t^{(k)} \in \mathbb{R}^{H \times C}$ is a candidate residual, $W_t^{(k)} \in [0,1]^{H \times C}$ sets its contribution, and $\odot$ denotes elementwise multiplication. These independently box-constrained weights control additive corrections and need not sum to one. Inputs, base forecasts, and candidates saved at prediction time support subsequent updates once their targets fully arrive.

4.2 Structured Residual Dictionary

A single calibration mechanism may struggle to capture the different effects of complex, abrupt shifts. We therefore retain distinct correction directions from output structure, overlapping historical forecasts, and current observations. Local and global residuals capture different temporal structures; vintage, input-induced, and context residuals add evidence from forecast history and recent inputs. These five candidates form the dictionary $Q_t \in \mathbb{R}^{H \times C \times 5}$; the controller subsequently determines their contributions.

Output-structure corrections. Forecast errors can reflect both short-range dependencies and smooth horizon-wide bias. We separate these effects into local and global residuals: the local component models neighboring leads and channel interactions, while the global component supplies smooth adjustments across the horizon:

$$R_t^{\text{local}} = \text{Conv}_{\text{dw}}(B_t) + a \odot B_t + b + B_t M_{\text{off}}. \tag{3}$$

$$R_t^{\text{global}}[:, c] = P V_c^\top B_t[:, c]. \tag{4}$$

The depthwise convolution shares a kernel across leads within each channel; a scales channels, b provides position-specific biases, and the zero-diagonal matrix M_{off} models cross-channel interactions. For the global residual, fixed orthogonalized discrete Legendre bases $P \in \mathbb{R}^{H \times r}$ restrict corrections to a smooth polynomial subspace; $V_c \in \mathbb{R}^{H \times r}$ is a learnable projection and r the calibration rank. Zero initialization of the local parameters and V_c makes the output calibrator initially an identity mapping.

Historical-version correction. Forecasts issued at different origins can cover the same absolute target, providing additional predictive evidence. Their errors may be correlated, so we account for shared errors when fusing them. We cached only base forecasts to avoid recursively reusing corrected outputs. For current lead h, lead $h + d$ of the forecast issued at $t - d$ refers to the same target. Let $\mathcal{D}_{t,h}$ contain the available aligned origin offsets, including $d = 0$. Using the shrinkage estimate $\widehat{\mu}_{h,c}$ of the mean matured base-forecast residual, we debiased each aligned forecast and then computed correlation-aware fusion weights:

$$z_d = B_{t-d}[h + d, c] + \widehat{\mu}_{h+d,c},\ d \in \mathcal{D}_{t,h}. \tag{5}$$

$$\Sigma = D\mathcal{R}(\rho_c)D,\ \mathcal{R}(\rho_c)_{ij} = \rho_c^{|d_i - d_j|},\ \alpha = \frac{[\Sigma^{-1}\mathbf{1}]_+}{\mathbf{1}^\top [\Sigma^{-1}\mathbf{1}]_+}. \tag{6}$$

The diagonal entries of D are square roots of shrunk error second moments. We estimated ρ_c from aligned errors of adjacent forecast versions and shrank it according to the number of matured adjacent-origin pairs. Thus, Σ is a structured covariance proxy, not the exact empirical covariance. The operator $[\cdot]_+$ truncates negative entries before normalization. The resulting correction is

$$R_t^{\text{vintage}}[h, c] = \sum_{d \in \mathcal{D}_{t,h}} \alpha_d z_d - \left(B_t[h, c] + \widehat{\mu}_{h,c}\right). \tag{7}$$

Subtracting the current debiased forecast isolates the incremental correction from version fusion; without an overlapping historical forecast, this residual is zero. Alignment requires no target labels, whereas the error statistics use only fully matured feedback. The fusion weights α combine forecast versions; the credit weights W_t separately control the resulting correction.

Input-induced and context corrections. Output corrections act on the base forecast, whereas input calibration can change how the frozen forecaster processes recent history. We equipped the input calibrator C_ϕ with analogous local, channel, and low-rank structure. Its low-rank left factor was initialized from a smooth basis but remained trainable. The input-induced residual is

$$R_t^{\text{input}} = f_\theta(C_{\phi_1}(X_t)) - B_t. \tag{8}$$

This is the direct difference between two forward predictions, not a first-order approximation. To exploit recent persistence without additional trainable parameters, we also formed

$$p_c = \text{clip}_{[0,1]}\left(\widehat{\rho}_c - \frac{q_c}{\max(\sigma_c, \epsilon)}\right),\ R_t^{\text{context}}[h,c] = p_c\,(x_{t,c} - B_t[h,c])\,. \tag{9}$$

where $\widehat{\rho}_c$ is the clipped lag-one coefficient of the centered recent window; q_c is its mean absolute difference, σ_c its standard deviation, and ϵ a numerical floor. We compute p_c from the current input, and the controller weights this residual.

4.3 Lead–Channel Credit Allocation

Correction utility can vary across leads and channels. We use matured losses to estimate their joint utility at different positions. Because positional feedback can be sparse, a global credit reference pools evidence across leads and channels and regularizes position-specific weights toward that shared estimate (Figure 1c). At position (h, c), let $Q_{s,h,c} \in \mathbb{R}^5$ denote the saved candidate slice $Q_s[h, c, :]$, represented as a column vector, and let $e_{s,h,c} = Y_s[h, c] - B_s[h, c]$. We accumulated

$$G_t = \sum_{s,h,c} Q_{s,h,c} Q_{s,h,c}^\top,\ m_t = \sum_{s,h,c} Q_{s,h,c} e_{s,h,c}. \tag{10}$$

The sums include only released historical records processed by time t, with each record counted once. The Gram matrix G_t captures interactions among candidates, while m_t measures their alignment with base-forecast errors. For weights $w \in \mathbb{R}^5$, the corrected error is $e - Q^\top w$; its accumulated squared loss, up to a constant, is $w^\top G_t w - 2m_t^\top w$. Crucially, we used saved candidates rather than recomputing them after calibrator updates.

Following the follow-the-regularized-leader (FTRL) formulation (McMahan, 2017), we obtained the global reference with regularization strength $\lambda > 0$:

$$g_t = \arg\min_{w \in [0,1]^5} \left\{ w^\top G_t w - 2m_t^\top w + \lambda \|w\|_2^2 \right\}. \tag{11}$$

Aggregating over channels at fixed lead h gives $G_{t,h}^{\text{lead}}$ and $m_{t,h}^{\text{lead}}$; aggregating over leads at fixed channel c gives $G_{t,c}^{\text{chan}}$ and $m_{t,c}^{\text{chan}}$. We solved

$$u_{t,h} = \arg\min_{w \in [0,1]^5} \left\{ w^\top G_{t,h}^{\text{lead}} w - 2(m_{t,h}^{\text{lead}})^\top w + \lambda \|w - g_t\|_2^2 \right\}. \tag{12}$$

$$a_{t,c} = \arg\min_{w \in [0,1]^5} \left\{ w^\top G_{t,c}^{\text{chan}} w - 2(m_{t,c}^{\text{chan}})^\top w + \lambda \|w - g_t\|_2^2 \right\}. \tag{13}$$

Both $u_{t,h}$ and $a_{t,c}$ are five-dimensional. A shared reference stabilizes sparse positions, while lead- and channel-specific statistics retain heterogeneity. We solve each five-variable convex quadratic program by enumerating bound/free patterns.

To avoid counting a shared baseline twice, we centered the channel weights before combining them with the lead weights:

$$v_{t,c} = a_{t,c} - \frac{1}{C}\sum_{j=1}^{C} a_{t,j},\ W_t[h,c,:] = \text{clip}(u_{t,h} + v_{t,c}, 0, 1)\,. \tag{14}$$

The zero-sum channel offsets fix the additive baseline before clipping. The resulting $W_t \in [0,1]^{H \times C \times 5}$ assigns each candidate residual a credit weight at every lead–channel position. Without matured evidence, we set $W_t = 0$, recovering the frozen backbone forecast.

4.4 DELAYED-FEEDBACK UPDATES

Delayed feedback serves two purposes: assessing the candidates used for past predictions and training calibrators to generate future candidates. We therefore separate statistical updates from gradient training after each window matures. Credit statistics use saved Q_s and errors $Y_s - B_s$; historical-version statistics accumulate error means, second moments, and aligned correlations without back-propagation. Only input and output calibrators receive gradient updates; context coefficients are recomputed from the current input.

For the output calibrator, we recomputed local and global residuals from the saved base forecast; for the input calibrator, we recomputed predictions from the saved input. The output loss, input prediction error, and scale-adaptive pseudo-Huber loss (Charbonnier et al., 1997) are

$$\mathcal{L}_{\text{out}} = \text{mean}\left[\left(B + R_{\phi_0}^{(\text{local})} + R_{\phi_0}^{(\text{global})} - Y\right)^2\right]. \tag{15}$$

$$\delta = f_\theta(C_{\phi_1}(X)) - Y. \tag{16}$$

$$\mathcal{L}_{\text{in}} = \text{mean}\left[2\tau^2\left(\sqrt{1 + (\delta/\tau)^2} - 1\right)\right],\ \tau = \max(\text{median}(|\delta|), \epsilon)\,. \tag{17}$$

where ϕ_0 and ϕ_1 parameterize the output and input calibrators, respectively; X, B, and Y come from released historical records. Means and medians span batch, lead, and channel dimensions. The scale τ is detached from gradients; the pseudo-Huber loss is quadratic near zero and approximately linear for large residuals. With Ω_{out} and Ω_{in} denoting mean squared second differences of convolution kernels and position biases, the joint objective is

$$\mathcal{L}_{\text{cal}} = \mathcal{L}_{\text{out}} + \mathcal{L}_{\text{in}} + \eta\,(\Omega_{\text{out}} + \Omega_{\text{in}})\,, \tag{18}$$

Here, η sets the smoothness penalty. One AdamW step (Loshchilov & Hutter, 2019) updated the calibrators per released feedback batch; the backbone remained frozen, so only subsequent forecasts were affected.

Table 1: MSE by backbone and adaptation method in the Natural scenario.

Dataset	H	DLinear					FreTS					iTransformer					PatchTST				
		Frozen	TAFAS	PETSA	DynaTTA	MATE	Frozen	TAFAS	PETSA	DynaTTA	MATE	Frozen	TAFAS	PETSA	DynaTTA	MATE	Frozen	TAFAS	PETSA	DynaTTA	MATE
ETTh1	96	0.4583	0.4523	0.4581	0.4522	**0.4474**	0.4370	0.4328	0.4368	0.4345	**0.4268**	0.4410	0.4352	0.4406	0.4321	**0.4292**	0.4250	0.4201	0.4248	0.4182	**0.4158**
	192	0.5113	0.5005	0.5110	0.5078	**0.4972**	0.4942	0.4857	0.4939	0.4956	**0.4786**	0.4982	0.4880	0.4979	0.4916	**0.4806**	0.4810	0.4725	0.4806	0.4736	**0.4697**
	336	0.5593	0.5468	0.5589	0.5598	**0.5448**	0.5464	0.5366	0.5461	0.5617	**0.5299**	0.5534	0.5419	0.5531	0.5632	**0.5345**	0.5440	0.5344	0.5436	0.5342	**0.5300**
	720	0.7100	**0.6787**	0.7088	0.6935	0.6987	0.7152	0.6847	0.7141	**0.6836**	0.6993	0.7051	**0.6754**	0.7042	0.6921	0.6881	0.7155	**0.6862**	0.7143	0.6983	0.6960
ETTh2	96	0.1805	**0.1780**	0.1804	0.1794	0.1802	0.1842	0.1823	0.1841	0.1823	**0.1781**	0.1969	0.1934	0.1967	0.1927	**0.1872**	0.1849	0.1840	0.1848	0.1859	**0.1817**
	192	0.2221	0.2175	0.2219	0.2196	**0.2174**	0.2244	0.2203	0.2242	0.2223	**0.2157**	0.2324	0.2284	0.2323	0.2313	**0.2224**	0.2180	0.2126	0.2177	0.2157	**0.2098**
	336	0.2507	**0.2426**	0.2503	0.2463	0.2440	0.2553	0.2461	0.2549	0.2468	**0.2459**	0.2852	0.2647	0.2842	0.2682	**0.2612**	0.2414	0.2368	0.2411	0.2462	**0.2352**
	720	0.3148	**0.2951**	0.3141	0.3061	0.2972	0.3252	**0.3009**	0.3246	0.3048	0.3071	0.3303	0.3041	0.3295	0.3119	**0.3024**	0.2981	0.2914	0.2977	0.3053	**0.2829**
ETTm1	96	0.3624	0.3480	0.3617	0.3450	**0.3404**	0.3625	0.3556	0.3620	0.3463	**0.3383**	0.3825	0.3671	0.3810	**0.3366**	0.3426	0.3898	0.3829	0.3895	0.3614	**0.3528**
	192	0.4325	0.4125	0.4315	0.4123	**0.4097**	0.4242	0.4153	0.4237	0.4107	**0.4046**	0.4281	0.4169	0.4272	0.4067	**0.3964**	0.4461	0.4365	0.4452	0.4339	**0.4186**
	336	0.5052	0.4746	0.5033	0.4808	**0.4724**	0.4906	0.4756	0.4897	0.4729	**0.4683**	0.4989	0.4743	0.4971	0.4639	**0.4606**	0.4900	0.4743	0.4890	0.4752	**0.4626**
	720	0.5800	**0.5374**	0.5764	0.5523	0.5429	0.5584	0.5360	0.5565	0.5520	**0.5323**	0.5881	0.5399	0.5837	0.5466	**0.5204**	0.5560	0.5275	0.5523	0.5349	**0.5215**
ETTm2	96	0.1212	0.1197	0.1211	0.1205	**0.1170**	0.1193	0.1179	0.1192	0.1177	**0.1138**	0.1240	0.1222	0.1238	0.1212	**0.1164**	0.1180	0.1174	0.1180	0.1179	**0.1153**
	192	0.1494	0.1469	0.1493	0.1475	**0.1450**	0.1486	0.1460	0.1485	0.1471	**0.1427**	0.1737	0.1676	0.1730	0.1602	**0.1510**	0.1549	0.1536	0.1547	0.1539	**0.1503**
	336	0.1827	0.1782	0.1825	0.1786	**0.1777**	0.1812	0.1762	0.1810	0.1789	**0.1739**	0.2010	0.1947	0.2002	0.1954	**0.1837**	0.1916	0.1893	0.1914	0.1915	**0.1827**
	720	0.2410	0.2316	0.2402	0.2383	**0.2294**	0.2369	0.2264	0.2361	0.2346	**0.2223**	0.2621	0.2456	0.2607	0.2585	**0.2362**	0.2508	0.2427	0.2485	0.2449	**0.2312**
Weather	96	0.1954	0.1896	0.1952	0.1862	**0.1657**	0.1857	0.1796	0.1853	0.1745	**0.1614**	0.1711	0.1675	0.1704	0.1663	**0.1568**	0.1740	0.1716	0.1738	0.1767	**0.1584**
	192	0.2403	0.2291	0.2397	0.2288	**0.2077**	0.2310	0.2199	0.2303	0.2187	**0.2034**	0.2225	0.2130	0.2211	0.2122	**0.2027**	0.2193	0.2139	0.2189	0.2190	**0.2017**
	336	0.2918	0.2736	0.2904	0.2765	**0.2552**	0.2844	0.2668	0.2830	0.2679	**0.2521**	0.2796	0.2627	0.2780	0.2648	**0.2532**	0.2760	0.2659	0.2747	0.2726	**0.2497**
	720	0.3644	0.3466	0.3625	0.3550	**0.3360**	0.3599	0.3425	0.3581	0.3565	**0.3337**	0.3573	0.3395	0.3556	0.3448	**0.3320**	0.3512	0.3413	0.3483	0.3365	**0.3280**
Exchange	96	0.0913	0.0892	0.0913	0.0901	**0.0820**	0.0828	0.0805	0.0827	**0.0794**	0.0796	0.0869	0.0863	0.0869	0.0890	**0.0835**	0.0857	0.0835	0.0856	0.0816	**0.0812**
	192	0.1829	0.1779	0.1828	0.1803	**0.1702**	0.1737	0.1682	0.1736	0.1684	**0.1643**	0.1825	0.1760	0.1823	0.1761	**0.1675**	0.1873	0.1799	0.1871	0.1735	**0.1697**
	336	0.3281	0.3175	0.3279	0.3235	**0.3116**	0.3246	0.3120	0.3243	**0.3060**	0.3084	0.3396	0.3315	0.3394	0.3253	**0.3236**	0.3389	0.3207	0.3386	**0.2859**	0.3181

5 EXPERIMENTS

5.1 EXPERIMENTAL SETUP

Datasets. We evaluated MATE on six TSF-TTA benchmarks (Kim et al., 2025; Wang et al., 2026) spanning different sampling rates, channel counts, and time spans: ETTh1, ETTh2, ETTm1, ETTm2 (Zhou et al., 2021), Weather (Max Planck Institute for Biogeochemistry, n.d.), and Exchange (Lai et al., 2018).

Protocol. Following FAC (Wang et al., 2026), we used chronological 7:1:2 training/validation/test splits and training-only normalization statistics. The look-back length was 96; forecast horizons were 96, 192, 336, and 720, excluding 720 for Exchange. Supervision was released only after the full target window matured; forecasts were evaluated as issued, without later revision.

Backbones and adaptation methods. We used patch-based PatchTST (Nie et al., 2023), decomposition-based linear DLinear (Zeng et al., 2023), frequency-domain FreTS (Yi et al., 2023), and variable-interaction iTransformer (Liu et al., 2024). For each backbone, we compared the frozen model (Frozen) with TAFAS (Kim et al., 2025), PETSA (Medeiros et al., 2025), DynaTTA (Grover & Etemad, 2025), and MATE. We adapted public implementations to the shared full-window feedback protocol by disabling partial-label updates and post-hoc forecast replacement. These baselines are protocol-aligned adaptations, not unmodified official implementations; Appendix A.2 details the changes. We do not include COSA or FAC as baselines. COSA updates from targets revealed in the current mini-batch rather than waiting for the full forecast window to mature. The official code for FAC is not publicly available, so we cannot re-evaluate it under our shared protocol. Their published results are therefore not directly comparable (Im & Kwon, 2026; Wang et al., 2026).

Scenarios and evaluation. We evaluated the unperturbed Natural stream, the official TTFBench benchmark (Grover & Etemad, 2025), and three controlled scenarios: Level, Dynamic, and Profile. We report mean squared error (MSE), our primary metric, averaged over three test seeds; mean absolute error (MAE) and per-configuration ablations appear in the appendix. All experiments ran on an NVIDIA GeForce RTX 4080 SUPER GPU with 16 GB memory. Appendix A details scenario construction, hyperparameters, and implementation.

5.2 Main Comparisons

Tables 1–2 report MSE for Natural and TTFBench; Appendix B covers Level, Dynamic, and Profile. The comparisons span 460 dataset–backbone–horizon configurations (92 per scenario) under the same protocol. Throughout the paper, best results within each comparison group are bold and second-best results are underlined.

Table 2: MSE by backbone and adaptation method in TTFBench.

Dataset	H	DLinear					FreTS					iTransformer					PatchTST				
		Frozen	TAFAS	PETSA	DynaTTA	MATE	Frozen	TAFAS	PETSA	DynaTTA	MATE	Frozen	TAFAS	PETSA	DynaTTA	MATE	Frozen	TAFAS	PETSA	DynaTTA	MATE
ETTh1	96	0.4731	0.4706	0.4730	0.4713	**0.4667**	0.4523	0.4504	0.4522	0.4670	**0.4450**	0.4573	0.4530	0.4571	0.4633	**0.4484**	0.4418	0.4390	0.4417	0.4435	**0.4339**
	192	0.5422	0.5398	0.5421	0.5473	**0.5349**	0.5254	0.5233	0.5252	0.5501	**0.5146**	0.5315	0.5283	0.5313	0.5488	**0.5190**	0.5136	0.5121	0.5133	0.5203	**0.5050**
	336	0.6176	0.6281	0.6177	0.6323	**0.6161**	0.6047	0.6137	0.6046	0.6754	**0.5959**	0.6158	0.6239	0.6158	0.6808	**0.6070**	0.6024	0.6078	0.6022	0.6237	**0.5957**
	720	**0.8737**	0.9307	0.8740	0.9080	0.8869	**0.8798**	0.9333	0.8799	1.1761	0.8808	**0.8713**	0.9225	0.8717	1.0988	0.8791	0.8857	0.9259	0.8856	0.9716	**0.8820**
ETTh2	96	0.1885	**0.1883**	0.1885	0.1899	0.1907	0.1921	0.1914	0.1920	0.1935	**0.1883**	0.2059	0.2044	0.2058	0.2071	**0.1988**	0.1943	0.1945	0.1943	0.1976	**0.1933**
	192	0.2421	0.2430	0.2420	0.2456	**0.2410**	0.2454	0.2453	0.2453	0.2549	**0.2395**	0.2543	0.2547	0.2543	0.2624	**0.2472**	0.2389	0.2373	0.2386	0.2471	**0.2346**
	336	0.2919	0.2975	**0.2917**	0.2946	0.2924	0.2964	0.2992	0.2962	0.3164	**0.2925**	0.3288	0.3230	0.3280	0.3495	**0.3146**	0.2826	0.2855	**0.2824**	0.3208	0.2831
	720	0.4441	0.4902	**0.4438**	0.4660	0.4451	0.4546	0.4920	0.4543	0.6452	**0.4505**	0.4605	0.5002	0.4600	0.6508	**0.4464**	0.4267	0.4592	**0.4264**	0.5659	0.4277
ETTm1	96	0.3641	0.3537	0.3636	0.3535	**0.3462**	0.3641	0.3549	0.3634	0.3540	**0.3387**	0.3845	0.3629	0.3824	0.3450	**0.3424**	0.3918	0.3851	0.3913	0.3648	**0.3536**
	192	0.4369	0.4245	0.4362	0.4267	**0.4214**	0.4283	0.4193	0.4277	0.4247	**0.4090**	0.4331	0.4206	0.4319	0.4232	**0.4013**	0.4504	0.4402	0.4489	0.4417	**0.4176**
	336	0.5145	0.4977	0.5135	0.5029	**0.4936**	0.4997	0.4881	0.4988	0.4986	**0.4792**	0.5089	0.4857	0.5065	0.4908	**0.4705**	0.5001	0.4895	0.4990	0.4927	**0.4730**
	720	0.6037	0.5869	0.6016	0.5967	**0.5806**	0.5821	0.5737	0.5801	0.6202	**0.5599**	0.6146	0.5874	0.6110	0.6246	**0.5545**	0.5809	0.5667	0.5780	0.5739	**0.5514**
ETTm2	96	0.1216	0.1207	0.1215	0.1217	**0.1180**	0.1198	0.1188	0.1198	0.1193	**0.1150**	0.1248	0.1231	0.1246	0.1238	**0.1175**	0.1186	0.1183	0.1185	0.1196	**0.1165**
	192	0.1507	0.1497	0.1507	0.1505	**0.1474**	0.1501	0.1488	0.1500	0.1523	**0.1454**	0.1748	0.1707	0.1744	0.1674	**0.1543**	0.1566	0.1563	0.1565	0.1590	**0.1531**
	336	0.1867	0.1858	0.1866	0.1858	**0.1846**	0.1853	0.1834	0.1851	0.1910	**0.1806**	0.2054	0.2026	0.2046	0.2119	**0.1909**	0.1959	0.1962	0.1958	0.2028	**0.1904**
	720	0.2547	0.2571	0.2542	0.2594	**0.2478**	0.2508	0.2516	0.2504	0.2798	**0.2413**	0.2774	0.2752	0.2763	0.3107	**0.2577**	0.2649	0.2660	0.2632	0.2699	**0.2520**
Weather	96	0.1973	0.1924	0.1971	0.1903	**0.1688**	0.1874	0.1821	0.1870	0.1795	**0.1642**	0.1726	0.1694	0.1725	0.1698	**0.1589**	0.1755	0.1737	0.1754	0.1792	**0.1612**
	192	0.2432	0.2342	0.2427	0.2345	**0.2129**	0.2337	0.2248	0.2331	0.2258	**0.2088**	0.2248	0.2171	0.2237	0.2189	**0.2072**	0.2218	0.2181	0.2215	0.2236	**0.2072**
	336	0.2970	0.2824	0.2958	0.2858	**0.2641**	0.2893	0.2753	0.2881	0.2807	**0.2611**	0.2840	0.2704	0.2830	0.2763	**0.2607**	0.2808	0.2738	0.2796	0.2805	**0.2590**
	720	0.3784	0.3696	0.3768	0.3759	**0.3541**	0.3736	0.3649	0.3720	0.3930	**0.3515**	0.3708	0.3606	0.3697	0.3810	**0.3494**	0.3647	0.3593	0.3620	0.3575	**0.3467**
Exchange	96	0.1032	0.1024	0.1032	0.1025	**0.0941**	0.0906	**0.0896**	0.0905	0.0901	0.0905	0.0954	0.0960	0.0954	0.1012	**0.0936**	0.0945	0.0932	0.0944	0.0927	**0.0925**
	192	0.2175	0.2157	0.2174	0.2166	**0.2076**	0.2010	**0.1988**	0.2009	0.2025	0.2017	0.2124	0.2106	0.2123	0.2164	**0.2065**	0.2129	0.2083	0.2128	0.2069	**0.2061**
	336	0.3919	0.3869	0.3917	0.3891	**0.3781**	0.3810	0.3753	0.3809	0.3770	**0.3733**	0.3952	0.3923	0.3950	0.3981	**0.3818**	0.3934	0.3817	0.3932	**0.3619**	0.3797

Overall performance. Table 3 reports equally weighted mean MSE across configurations and the count (share) of configurations in which each method attains the lowest MSE. MATE has the lowest mean MSE in every scenario, with an overall MSE of 0.3187 and 396 wins out of 460 configurations (86.1%).

Table 3: Mean MSE and win count (share) across scenarios.

Scenario / N	Frozen		TAFAS		PETSA		DynaTTA		MATE	
	MSE	Win count (share)	MSE	Win count (share)	MSE	Win count (share)	MSE	Win count (share)	MSE	Win count (share)
Natural / 92	0.3228	0 (0.0%)	0.3116	8 (8.7%)	0.3221	0 (0.0%)	0.3134	5 (5.4%)	**0.3051**	**79 (85.9%)**
TTFBench / 92	0.3512	3 (3.3%)	0.3510	3 (3.3%)	0.3507	4 (4.3%)	0.3669	1 (1.1%)	**0.3385**	**81 (88.0%)**
Level / 92	0.3337	0 (0.0%)	0.3251	7 (7.6%)	0.3330	0 (0.0%)	0.3307	5 (5.4%)	**0.3177**	**80 (87.0%)**
Dynamic / 92	0.3351	0 (0.0%)	0.3231	10 (10.9%)	0.3343	0 (0.0%)	0.3258	6 (6.5%)	**0.3180**	**76 (82.6%)**
Profile / 92	0.3296	0 (0.0%)	0.3203	8 (8.7%)	0.3289	0 (0.0%)	0.3242	4 (4.3%)	**0.3141**	**80 (87.0%)**
Overall / 460	0.3345	3 (0.7%)	0.3262	36 (7.8%)	0.3338	4 (0.9%)	0.3322	21 (4.6%)	**0.3187**	**396 (86.1%)**

To account for differing error scales, we report relative MSE reduction for method m against comparator b on configuration i (positive for improvement, negative for degradation):

$$\Delta_i(m \mid b) = \frac{\mathrm{MSE}_{i,b} - \mathrm{MSE}_{i,m}}{\mathrm{MSE}_{i,b}} \times 100\%. \tag{19}$$

Figure 2(a) plots the share of configurations whose relative excess, $\frac{\mathrm{MSE}_i - \mathrm{MSE}_{i,\min}}{\mathrm{MSE}_{i,\min}}$, falls within each threshold. MATE's share rises from 86.1% at zero excess to 92.2% within 1% of the minimum. In panel (b), mean and median reductions against all four comparators exceed 2%, indicating gains beyond a few large improvements. Boxes show the median and interquartile range; whiskers reach the furthest observations within 1.5 interquartile ranges of each quartile. Dots mark all 460 configurations, and labeled values give the median and mean.

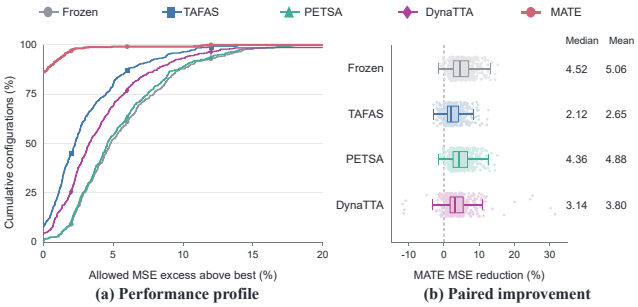


Figure 2: Overall performance distributions. (a) Cumulative configuration share by relative excess MSE over the per-configuration minimum. (b) MATE's MSE reduction relative to each baseline.

Across conditions. MATE has the highest win share across scenario, dataset, backbone, and horizon groups (Figure 3), winning every configuration on ETTm2 and Weather across all five scenarios and 71.0% at horizon 720. Beyond win frequency, Figure 4 shows positive median MSE reductions against Frozen and TAFAS in every group: 8.2% against Frozen on Weather, and 3.1% and 1.0% against TAFAS with iTransformer and DLinear, respectively.

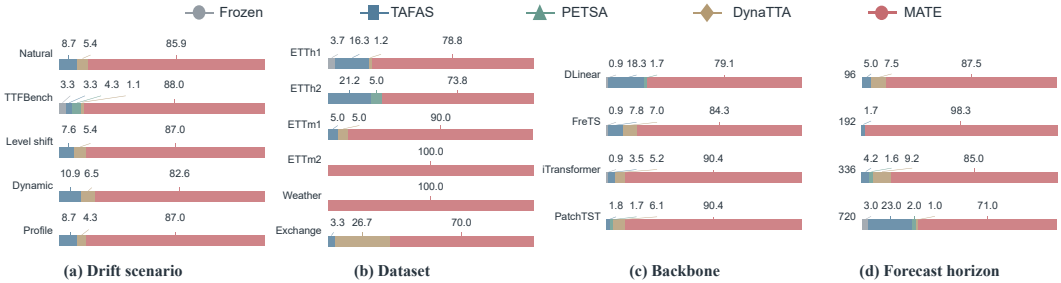


Figure 3: Win composition across conditions. Bars show within-group win shares (each row sums to 100%); nonzero shares are labeled.

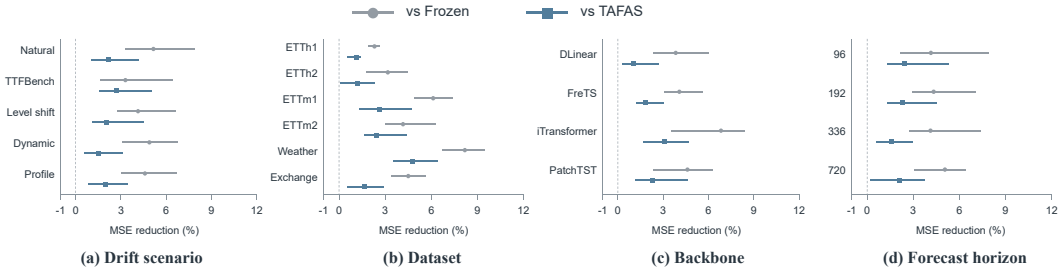


Figure 4: Grouped MSE reduction of MATE relative to Frozen and TAFAS. Panels (a)–(d) group results by scenario, dataset, backbone, and horizon. Points show medians; horizontal intervals show the first-to-third-quartile range.

Dataset–scenario interactions. MATE's median MSE reduction relative to TAFAS is positive in every dataset–scenario pair, with larger gains on Weather and the ETTm datasets (Figure 5). Relative to Frozen, its mean reduction is positive in all 30 pairs and largest among the four TTA methods in 29, reaching 9.98% (Figure 6).

5.3 Mechanism Ablations

We varied credit granularity and removed individual residual sources over 36 configurations: ETTh2, ETTm2, and Weather; PatchTST and DLinear; horizons 96, 336, and 720; and Natural

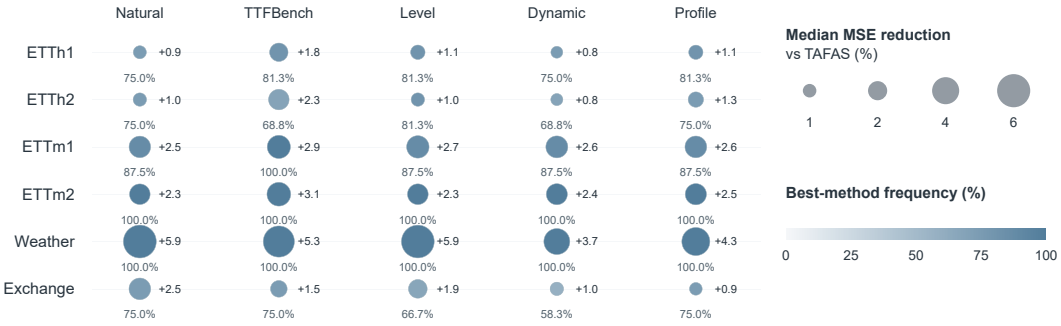


Figure 5: Dataset–scenario results. Color shows MATE's win share; bubble size shows its median MSE reduction relative to TAFAS.

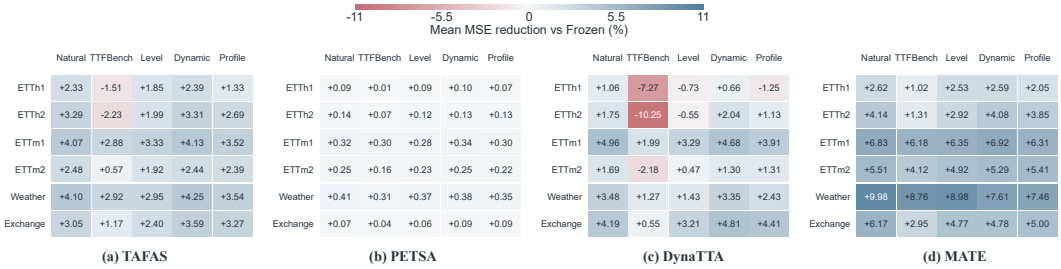


Figure 6: Mean MSE reduction of four TTA methods relative to Frozen. Panels (a)–(d) show TAFAS, PETSA, DynaTTA, and MATE, respectively.

and Level. Table 4 averages three test seeds; variant definitions and per-configuration results appear in Appendix C. Appendix C.4 analyzes learned credit weights.

Full MATE achieves the lowest mean MSE (0.2258). Uniform and Global increase MSE by 2.79% and 1.28%, respectively; joint lead–channel allocation also outperforms either single-axis variant. Removing Vintage or Context increases MSE by 0.97% each, versus at most 0.22% for Local, Global, or Input, with other components fixed. These results support complementary residual evidence from historical overlap and recent observations, together with joint lead–channel credit allocation.

Table 4: Mechanism ablations of credit-control granularity and structured residual sources.

Group	Setting	MSE	MSE increase vs. full MATE (%)
Credit allocation	Uniform	0.2321	2.79
	Global	0.2287	1.28
	Lead-only	0.2280	0.97
	Channel-only	0.2263	0.22
Residual source	w/o Local	0.2263	0.22
	w/o Global	0.2259	0.04
	w/o Vintage	0.2280	0.97
	w/o Input	0.2263	0.22
	w/o Context	0.2280	0.97
Reference	Full MATE	**0.2258**	–

6 Conclusion

MATE separates residual generation from lead–channel credit allocation. It uses stored candidates and matured errors to weight complementary corrections. Across six datasets, four backbones, and five scenarios, MATE achieves broad forecasting gains. Controlled ablations support the benefit of joint lead–channel credit allocation with fixed residual candidates.

Adaptation remains constrained by feedback delay, candidate coverage, and online computation and memory costs. Future work will combine partial and matured feedback, expand the candidate space, and evaluate longer real-world streams to better balance accuracy, adaptation latency, and resource use.

AI USE STATEMENT

We utilize AI of the ChatGPT type as an auxiliary tool for code writing, data analysis, and English translation and revision. The auxiliary functions include code writing and debugging, assisting in organizing and interpreting experimental results, as well as enhancing the clarity and consistency of the paper. We are responsible for the overall work of the research, the design of the research ideas, reviewing the code, analysis and text generated by the AI assistance, and bearing full responsibility for the final content, results and conclusions.

REFERENCES

Pierre Charbonnier, Laure Blanc-Féraud, Gilles Aubert, and Michel Barlaud. Deterministic edge-preserving regularization in computed imaging. *IEEE Transactions on Image Processing*, 6(2): 298–311, 1997. doi: 10.1109/83.551699.

João Gama, Indrė Žliobaitė, Albert Bifet, Mykola Pechenizkiy, and Abdelhamid Bouchachia. A survey on concept drift adaptation. *ACM Computing Surveys*, 46(4):44:1–44:37, 2014. doi: 10.1145/2523813.

Shivam Grover and Ali Etemad. Shift-aware test-time adaptation and benchmarking for time-series forecasting. In *Second Workshop on Test-Time Adaptation: Putting Updates to the Test! at ICML*, 2025. URL https://openreview.net/forum?id=a399SmgWGl.

Xiannan Huang, Shuhan Qiu, Jiayuan Du, and Chao Yang. Online time series prediction using feature adjustment. In *International Conference on Learning Representations*, 2026. doi: 10.48550/arXiv.2509.03810.

Jeonghwan Im and Hyuk-Yoon Kwon. COSA: Context-aware output-space adapter for test-time adaptation in time series forecasting. In *International Conference on Learning Representations*, 2026. URL https://openreview.net/forum?id=L7Z5wBMPrW.

Pooria Joulani, Andras Gyorgy, and Csaba Szepesvari. Online learning under delayed feedback. In *Proceedings of the 30th International Conference on Machine Learning*, volume 28 of *Proceedings of Machine Learning Research*, pp. 1453–1461, 2013. URL https://proceedings.mlr.press/v28/joulani13.html.

HyunGi Kim, Siwon Kim, Jisoo Mok, and Sungroh Yoon. Battling the non-stationarity in time series forecasting via test-time adaptation. In *Proceedings of the AAAI Conference on Artificial Intelligence*, volume 39, pp. 17868–17876, 2025. doi: 10.1609/aaai.v39i17.33965.

Guokun Lai, Wei-Cheng Chang, Yiming Yang, and Hanxiao Liu. Modeling long- and short-term temporal patterns with deep neural networks. In *Proceedings of the 41st International ACM SIGIR Conference on Research and Development in Information Retrieval*, pp. 95–104, 2018. doi: 10.1145/3209978.3210006.

Ying-yee Ava Lau, Zhiwen Shao, and Dit-Yan Yeung. Fast and slow streams for online time series forecasting without information leakage. In *International Conference on Learning Representations*, 2025. URL https://openreview.net/forum?id=I0n3EyogMi.

Daojun Liang, Haixia Zhang, Jing Wang, Dongfeng Yuan, and Minggao Zhang. Act now: A novel online forecasting framework for large-scale streaming data. *arXiv preprint arXiv:2412.00108*, 2024. doi: 10.48550/arXiv.2412.00108.

Jian Liang, Ran He, and Tieniu Tan. A comprehensive survey on test-time adaptation under distribution shifts. *International Journal of Computer Vision*, 133:31–64, 2025. doi: 10.1007/s11263-024-02181-w.

Yong Liu, Haixu Wu, Jianmin Wang, and Mingsheng Long. Non-stationary transformers: Exploring the stationarity in time series forecasting. In *Advances in Neural Information Processing Systems*, volume 35, pp. 9881–9893, 2022. doi: 10.52202/068431-0718.

Yong Liu, Tengge Hu, Haoran Zhang, Haixu Wu, Shiyu Wang, Lintao Ma, and Mingsheng Long. itransformer: Inverted transformers are effective for time series forecasting. In *International Conference on Learning Representations*, 2024. doi: 10.48550/arXiv.2310.06625.

Ilya Loshchilov and Frank Hutter. Decoupled weight decay regularization. In *International Conference on Learning Representations*, 2019. doi: 10.48550/arXiv.1711.05101.

Max Planck Institute for Biogeochemistry. Weather station data, jena. https://weather.bgc-jena.mpg.de/, n.d. Dataset; accessed September 23, 2026.

H. Brendan McMahan. A survey of algorithms and analysis for adaptive online learning. *Journal of Machine Learning Research*, 18(90):1–50, 2017. URL https://www.jmlr.org/papers/v18/14-428.html.

Heitor R. Medeiros, Hossein Sharifi-Noghabi, Gabriel L. Oliveira, and Saghar Irandoust. Accurate parameter-efficient test-time adaptation for time series forecasting. In *Second Workshop on Test-Time Adaptation: Putting Updates to the Test! at ICML*, 2025. doi: 10.48550/arXiv.2506.23424.

Yuqi Nie, Nam H. Nguyen, Phanwadee Sinthong, and Jayant Kalagnanam. A time series is worth 64 words: Long-term forecasting with transformers. In *International Conference on Learning Representations*, 2023. doi: 10.48550/arXiv.2211.14730.

Quang Pham, Chenghao Liu, Doyen Sahoo, and Steven C. H. Hoi. Learning fast and slow for online time series forecasting. In *International Conference on Learning Representations*, 2023. doi: 10.48550/arXiv.2202.11672.

Yu Sun, Xiaolong Wang, Zhuang Liu, John Miller, Alexei A. Efros, and Moritz Hardt. Test-time training with self-supervision for generalization under distribution shifts. In *Proceedings of the 37th International Conference on Machine Learning*, volume 119 of *Proceedings of Machine Learning Research*, pp. 9229–9248, 2020. doi: 10.48550/arXiv.1909.13231.

Dequan Wang, Evan Shelhamer, Shaoteng Liu, Bruno Olshausen, and Trevor Darrell. Tent: Fully test-time adaptation by entropy minimization. In *International Conference on Learning Representations*, 2021. doi: 10.48550/arXiv.2006.10726.

Haochun Wang, Ruichen Xu, Georgios Kementzidis, Karen Cho, Sebastian Ramirez Villarreal, and Yuefan Deng. Towards principled test-time adaptation for time series forecasting. *arXiv preprint arXiv:2605.17250*, 2026. doi: 10.48550/arXiv.2605.17250.

Qin Wang, Olga Fink, Luc Van Gool, and Dengxin Dai. Continual test-time domain adaptation. In *Proceedings of the IEEE/CVF Conference on Computer Vision and Pattern Recognition*, 2022. doi: 10.1109/CVPR52688.2022.00706.

Kun Yi, Qi Zhang, Wei Fan, Shoujin Wang, Pengyang Wang, Hui He, Ning An, Defu Lian, Longbing Cao, and Zhendong Niu. Frequency-domain mlps are more effective learners in time series forecasting. In *Advances in Neural Information Processing Systems*, volume 36, pp. 76656–76679, 2023. doi: 10.52202/075280-3349.

Ailing Zeng, Muxi Chen, Lei Zhang, and Qiang Xu. Are transformers effective for time series forecasting? In *Proceedings of the AAAI Conference on Artificial Intelligence*, volume 37, pp. 11121–11128, 2023. doi: 10.1609/aaai.v37i9.26317.

Yi-Fan Zhang, Qingsong Wen, Xue Wang, Weiqi Chen, Liang Sun, Zhang Zhang, Liang Wang, Rong Jin, and Tieniu Tan. OneNet: Enhancing time series forecasting models under concept drift by online ensembling. In *Advances in Neural Information Processing Systems*, volume 36, 2023. doi: 10.52202/075280-3066.

Haoyi Zhou, Shanghang Zhang, Jieqi Peng, Shuai Zhang, Jianxin Li, Hui Xiong, and Wancai Zhang. Informer: Beyond efficient transformer for long sequence time-series forecasting. In *Proceedings of the AAAI Conference on Artificial Intelligence*, volume 35, pp. 11106–11115, 2021. doi: 10.1609/aaai.v35i12.17325.

A Experimental Setup and Reproducibility Details

A.1 Data Splits and Scenario Construction

We split each of the six datasets chronologically into training, validation, and test segments in a 7:1:2 ratio. Model standardization used training-set statistics only, and forecast targets remained within their respective evaluation segments. Synthetic shifts were applied to the test data object, which included the L historical observations preceding the test boundary; the training and validation objects were unchanged. Below, $x_{i,c}$ denotes a training-standardized observation, $i = 0, \dots, n-1$ indexes the test data object, c indexes channels, and $u_i = i/(n-1)$. The custom scenarios used perturbation strength $\eta = 0.8$, where η denotes scenario severity, not the smoothness coefficient in Equation 18.

Natural and Level. Natural retained the original test stream without synthetic perturbations, preserving its inherent nonstationarity. Level added a fixed channel-specific offset after the midpoint:

$$\widetilde{x}_{i,c} = x_{i,c} + \eta b_c \mathbf{1}(i \geq \lfloor n/2 \rfloor), \qquad b_c \sim \mathcal{U}(-1, 1). \tag{20}$$

The offset remained constant within each channel over the second half. Because it was generated in training-standardized space, η specifies its magnitude relative to the training scale, rather than a common offset in the original units.

Dynamic. We first added a quadratic trend, four cumulative level changes, and a multifrequency sinusoidal perturbation. We then applied a gradual scale transformation to their sum and added noise:

$$\widetilde{x}^{D}_{i,c} = S_{0.25\eta}\big[x + T^{D} + J_{0.35\eta} + F_{0.30\eta}\big]_{i,c} + \epsilon^{D}_{i,c}, \tag{21}$$

$$T^{D}_{i,c} = 0.30\eta s_c a_c u_i^2, \qquad s_c \in \{-1, 1\}, \quad a_c \sim \mathcal{U}(0.4, 0.9). \tag{22}$$

The four switching locations τ_j were centered at $0.2n$, $0.4n$, $0.6n$, and $0.8n$, respectively, with independent jitter sampled from $\mathcal{U}(-0.04, 0.04)$ of the series length. Each switch introduced a persistent channel-specific increment:

$$J_{\beta,i,c} = \sum_{j=1}^{4} \frac{\beta}{2} \xi_{j,c} \mathbf{1}(i \geq \tau_j), \qquad \xi_{j,c} \sim \mathcal{N}(0, 0.55^2). \tag{23}$$

The sinusoidal perturbation used periods $P_1 = P$, $P_2 = \max(4, \lfloor P/2 \rfloor)$, and $P_3 = \max(4, \lfloor 1.5P \rfloor)$, with $P = \max(8, \lfloor 0.2n \rfloor)$. Amplitude magnitudes were sampled from $\mathcal{U}(0.25, 0.75)$ with random signs, and phases from $\mathcal{U}(0, 2\pi)$. Its envelope increased over time:

$$F_{\beta,i,c} = \frac{\beta(0.5 + 0.5u_i)}{\sqrt{3}} \sum_{k=1}^{3} A_{k,c} \sin\left(\frac{2\pi i}{P_k} + \phi_{k,c}\right). \tag{24}$$

The scale transformation was centered on the channel mean m_c of the combined sequence before the midpoint. It left the first half unchanged and transformed the second half as

$$S_\beta[v]_{i,c} = m_c + \big[1 + r_i(f_c - 1)\big](v_{i,c} - m_c), \qquad i \geq \lfloor n/2 \rfloor, \tag{25}$$

where r_i increased linearly from zero to one over the second half, and

$$f_c = \max(0.2, 1 + 0.5\beta s_c a_c), \qquad a_c \sim \mathcal{U}(0.7, 1.3), \quad s_c \in \{-1, 1\}. \tag{26}$$

Finally, we added independent noise $\epsilon^{D}_{i,c} \sim \mathcal{N}(0, (0.08\eta)^2)$. Dynamic therefore combined smooth trends, abrupt state changes, frequency perturbations, scale changes, and random noise in a single test stream.

Profile. Profile used the same composition of perturbations, but derived its trend direction and periods from the original sequence:

$$\widetilde{x}^{P}_{i,c} = S_{0.20\eta}\big[x + T^{P} + F^{P} + J_{0.30\eta}\big]_{i,c} + \epsilon^{P}_{i,c}, \tag{27}$$

$$T^{P}_{i,c} = 0.28\eta d_c(0.55u_i + 0.45u_i^2). \tag{28}$$

where d_c was the sign of the difference between the channel means over the last and first 20% of the original sequence; a zero difference was assigned a random sign. After adding the trend, we centered each channel and computed its real Fourier transform. We selected the three dominant periods P_k with the largest mean spectral amplitudes across channels and formed

$$F_{i,c}^{P} = \frac{0.30\eta(0.35 + 0.65u_i)}{\sqrt{3}} \sum_{k=1}^{3} \Bigg[A_{k,c} \sin\left(\frac{2\pi i}{P_k} + \phi_{k,c}\right) + B_k \sin\left(\frac{2\pi i}{P_k} + \phi_{k,1}\right) \Bigg]. \tag{29}$$

We sampled $A_{k,c} \sim \mathcal{U}(0.20, 0.65)$, $B_k \sim \mathcal{U}(0.10, 0.35)$, and $\phi_{k,c} \sim \mathcal{U}(0, 2\pi)$. The second sinusoidal term was shared across channels. We then added $\epsilon_{i,c}^{P} \sim \mathcal{N}(0, (0.06\eta)^2)$. Profile thus combined the sequence's trend direction, dominant periods, and shared cross-channel structure to produce data-dependent shifts. For both Dynamic and Profile, structural perturbations were applied to the test-input and target arrays, while their Gaussian noise was sampled independently.

TTFBench. We used the authors' generator (Grover & Etemad, 2025), independently of the custom severity parameter η. The following equations summarize that implementation. Each raw perturbation combined continuous piecewise polynomials, sinusoids and double-frequency cosines, multiple steps, and Gaussian noise:

$$g_i = a \Bigg[p(i) + \sum_k A_k \left\{ \sin\left(\frac{2\pi i}{P_k} + \phi_k\right) + 0.5 \cos\left(\frac{4\pi i}{P_k} + \frac{\phi_k}{2}\right) \right\} + \sum_j b_j \mathbf{1}(i \geq \tau_j) + \epsilon_i \Bigg] + b. \tag{30}$$

The polynomial had two to six segments of degree one to three, joined by constant translations. Sampling ranges for coefficients, periods, amplitudes, switch counts, and noise scales were determined from training-prefix trends, spectra, change points, and residuals, with channel-specific adjustments. Independent components also used random scaling a and translation b. The generator rescaled each perturbation by its standard deviation to a sampled target amplitude, yielding a shared component $g^{(0)}$ and independent channel components $g^{(c)}$. The final perturbation was

$$h_{i,c} = \omega_c s_c g_i^{(0)} + \nu_c g_{i,c}^{(c)}, \qquad \delta_{i,c} = h_{i,c} - h_{0,c}. \tag{31}$$

The shared component was enabled with probability 0.5. We had $\nu_c \sim \mathcal{U}(0.4, 1.0)$, and s_c was the sign of channel c's mean correlation with the other channels. Shared-component weights were sampled randomly and adjusted according to channel correlation; they were further attenuated for flat or outlier-dominated channels. Subtracting $h_{0,c}$ sets the perturbation to zero at the test-stream boundary, ensuring continuity at the onset; it does not guarantee preservation of the original cross-channel correlation structure.

The official generator first normalized the cleaned full sequence, perturbed its final 20%, and then restored the original units. For forecasting, we restored the original training and validation segments and the historical observations preceding the test boundary, then standardized model inputs using training-set statistics. The original benchmark covered ETTh1, ETTh2, ETTm1, Weather, and Exchange; we extended it to ETTm2 using the same generator. Each seed in our TTFBench evaluation includes ten perturbation instances.

A.2 Feedback Scheduling and Implementation Parameters

MATE used a batch length of 32, calibration rank 8, and AdamW (Loshchilov & Hutter, 2019) with learning rate 10^{-4} and weight decay 10^{-5}. The credit regularization strength was 32, and the smoothness coefficient was 10^{-4}. We performed one calibrator update after each release of matured feedback.

TAFAS (Kim et al., 2025), PETSA (Medeiros et al., 2025), and DynaTTA (Grover & Etemad, 2025) used settings from their public implementations, retaining their calibration structures, loss designs,

and period-aware batch partitions. Where DynaTTA did not specify separate calibration settings, we used the TAFAS reference configuration. To enforce a common supervision rule, we removed updates driven by partial targets and paths that subsequently replaced already issued forecasts. Supervised updates occurred only after all targets in a historical batch had arrived. DynaTTA's label-dependent error statistics and memory writes followed the same rule, while its label-free measures based on current inputs were retained.

All methods used the same data splits, test streams, and pretrained checkpoint for each frozen backbone. Only DynaTTA's drift-measurement interface required backbone-specific handling: DLinear used control driven by matured errors, while FreTS used representations before the prediction head to compute feature distances. These changes did not alter the backbone's forecasting architecture or parameters. Issued forecasts were scored without subsequent replacement. The results therefore concern versions adapted to the full-window feedback protocol. Each method retained its own batch schedule, so the supervision rule was shared, but update frequencies and computational budgets were not identical.

B Additional Main Results

For the eight mean tables, each cell places the mean across three test seeds above the sample standard deviation (denominator 2); the captioned 10^{-3} factor applies only to the standard deviation. For TTFBench, we first average the ten perturbation instances within each seed before computing the cross-seed standard deviation.

MSE results. Tables B1–B3 report MSE under the Level, Dynamic, and Profile shifts. Each row gives a dataset–horizon pair; columns compare five methods for each backbone.

MAE results. Tables B4–B8 report MAE for Natural, TTFBench, Level, Dynamic, and Profile. Rows give dataset–horizon pairs, and columns compare methods within each backbone. MATE attains the lowest MAE in 77, 77, 75, 74, and 73 of 92 configurations in those scenarios, respectively. Its scenario-level mean MAE is 0.3585, 0.3794, 0.3667, 0.3740, and 0.3676, respectively.

MSE standard deviations. Tables B9 and B10 report cross-seed MSE variability for Natural and TTFBench. The corresponding means appear in Tables 1 and 2; values are reported in 10^{-3} units.

Table B1: MSE by backbone and adaptation method in the Level scenario (SD values $\times 10^{-3}$).

Dataset	H	DLinear					FreTS					iTransformer					PatchTST				
		Frozen	TAFAS	PETSA	DynaTTA	MATE	Frozen	TAFAS	PETSA	DynaTTA	MATE	Frozen	TAFAS	PETSA	DynaTTA	MATE	Frozen	TAFAS	PETSA	DynaTTA	MATE
ETTh1	96	0.4622 ± 3.03	0.4569 ± 2.57	0.4620 ± 3.05	0.4562 ± 2.84	**0.4523** ± 2.88	0.4410 ± 2.95	0.4372 ± 2.70	0.4408 ± 2.99	0.4458 ± 2.66	**0.4317** ± 3.09	0.4446 ± 2.83	0.4389 ± 2.56	0.4442 ± 2.91	0.4436 ± 0.727	**0.4331** ± 2.51	0.4304 ± 3.54	0.4268 ± 3.58	0.4302 ± 3.59	0.4271 ± 4.98	**0.4219** ± 3.40
	192	0.5199 ± 8.31	0.5102 ± 5.00	0.5196 ± 8.25	0.5158 ± 6.00	**0.5064** ± 6.05	0.5032 ± 8.19	0.4953 ± 5.43	0.5029 ± 8.12	0.5103 ± 2.79	**0.4885** ± 6.66	0.5068 ± 8.27	0.4974 ± 5.80	0.5065 ± 8.24	0.5099 ± 6.95	**0.4895** ± 5.87	0.4910 ± 9.77	0.4857 ± 9.48	0.4907 ± 9.81	0.4870 ± 9.65	**0.4803** ± 8.42
	336	0.5762 ± 19.8	0.5636 ± 6.72	0.5757 ± 19.6	0.5694 ± 8.63	**0.5601** ± 9.81	0.5638 ± 19.3	0.5530 ± 7.22	0.5634 ± 19.1	0.5811 ± 15.3	**0.5468** ± 13.7	0.5703 ± 22.2	0.5584 ± 10.5	0.5699 ± 22.0	0.5804 ± 2.04	**0.5504** ± 14.1	0.5618 ± 22.2	0.5565 ± 17.6	0.5614 ± 22.1	0.5584 ± 14.9	**0.5469** ± 16.7
	720	0.7539 ± 56.0	**0.7256** ± 13.7	0.7524 ± 55.0	0.7330 ± 19.1	0.7418 ± 30.9	0.7592 ± 55.3	**0.7307** ± 13.5	0.7579 ± 54.3	0.7945 ± 55.7	0.7429 ± 41.2	0.7484 ± 64.2	**0.7203** ± 17.1	0.7473 ± 63.2	0.7843 ± 47.0	0.7316 ± 43.2	0.7630 ± 65.5	0.7574 ± 50.9	0.7620 ± 65.0	0.7843 ± 55.2	**0.7430** ± 53.1
ETTh2	96	0.1852 ± 2.29	**0.1832** ± 1.83	0.1851 ± 2.31	0.1844 ± 1.11	0.1860 ± 1.83	0.1894 ± 1.68	0.1877 ± 1.42	0.1893 ± 1.68	0.1881 ± 1.74	**0.1843** ± 1.90	0.2014 ± 4.17	0.1985 ± 3.65	0.2012 ± 4.19	0.1986 ± 2.70	**0.1924** ± 3.98	0.1900 ± 3.20	0.1894 ± 3.12	0.1900 ± 3.21	0.1912 ± 3.49	**0.1876** ± 3.02
	192	0.2309 ± 2.20	**0.2274** ± 2.30	0.2307 ± 2.22	0.2292 ± 1.23	0.2281 ± 2.66	0.2340 ± 2.46	0.2307 ± 2.82	0.2338 ± 2.46	0.2316 ± 5.17	**0.2268** ± 3.14	0.2408 ± 7.63	0.2379 ± 6.56	0.2407 ± 7.66	0.2402 ± 6.19	**0.2322** ± 7.26	0.2266 ± 2.60	0.2221 ± 1.62	0.2262 ± 2.58	0.2256 ± 1.29	**0.2199** ± 2.43
	336	0.2650 ± 3.37	**0.2595** ± 6.26	0.2646 ± 3.36	0.2621 ± 4.32	0.2617 ± 5.43	0.2697 ± 4.05	0.2629 ± 6.97	0.2694 ± 4.07	0.2672 ± 7.28	**0.2627** ± 5.52	0.2984 ± 3.22	0.2818 ± 5.69	0.2975 ± 3.25	0.2929 ± 12.4	**0.2794** ± 3.85	0.2549 ± 2.62	0.2516 ± 2.08	0.2546 ± 2.59	0.2603 ± 0.769	**0.2516** ± 2.88
	720	0.3475 ± 17.3	0.3391 ± 20.7	0.3468 ± 17.1	0.3468 ± 22.6	**0.3352** ± 19.0	0.3578 ± 20.3	0.3446 ± 24.3	0.3572 ± 20.2	0.3793 ± 45.3	**0.3438** ± 21.5	0.3577 ± 16.4	0.3453 ± 19.9	0.3570 ± 16.2	0.3789 ± 30.8	**0.3363** ± 17.9	0.3300 ± 13.6	0.3270 ± 14.9	0.3295 ± 13.6	0.3406 ± 4.51	**0.3201** ± 14.5
ETTm1	96	0.3640 ± 1.17	0.3508 ± 1.54	0.3633 ± 1.14	0.3489 ± 1.22	**0.3436** ± 1.59	0.3640 ± 1.15	0.3575 ± 1.10	0.3635 ± 1.10	0.3521 ± 2.90	**0.3402** ± 1.61	0.3844 ± 1.41	0.3683 ± 1.58	0.3828 ± 1.34	**0.3422** ± 3.60	0.3433 ± 1.57	0.3916 ± 0.972	0.3861 ± 1.52	0.3914 ± 0.926	0.3651 ± 2.06	**0.3555** ± 4.02
	192	0.4352 ± 1.85	0.4177 ± 2.67	0.4342 ± 1.75	0.4184 ± 1.86	**0.4151** ± 2.21	0.4267 ± 1.85	0.4188 ± 2.06	0.4263 ± 1.83	0.4179 ± 3.27	**0.4080** ± 2.08	0.4309 ± 1.85	0.4205 ± 2.91	0.4301 ± 1.89	0.4166 ± 4.65	**0.3994** ± 2.65	0.4487 ± 2.01	0.4416 ± 2.80	0.4479 ± 2.03	0.4422 ± 4.40	**0.4205** ± 2.32
	336	0.5093 ± 2.76	0.4838 ± 4.32	0.5076 ± 2.70	0.4888 ± 3.99	**0.4822** ± 4.04	0.4946 ± 2.84	0.4820 ± 3.46	0.4939 ± 2.85	0.4860 ± 2.75	**0.4742** ± 3.10	0.5032 ± 2.68	0.4799 ± 3.72	0.5013 ± 2.73	0.4766 ± 7.04	**0.4660** ± 3.19	0.4943 ± 2.42	0.4829 ± 3.53	0.4935 ± 2.40	0.4868 ± 5.26	**0.4687** ± 4.03
	720	0.5879 ± 3.08	**0.5559** ± 8.89	0.5847 ± 2.99	0.5682 ± 14.9	0.5586 ± 6.72	0.5665 ± 3.66	0.5512 ± 7.19	0.5649 ± 3.56	0.5813 ± 22.7	**0.5433** ± 5.33	0.5965 ± 3.23	0.5585 ± 9.04	0.5927 ± 3.17	0.5876 ± 26.2	**0.5327** ± 6.67	0.5642 ± 3.50	0.5452 ± 6.57	0.5615 ± 3.72	0.5531 ± 7.04	**0.5346** ± 7.46
ETTm2	96	0.1223 ± 0.392	0.1211 ± 0.525	0.1223 ± 0.394	0.1214 ± 0.363	**0.1186** ± 0.663	0.1206 ± 0.419	0.1194 ± 0.517	0.1205 ± 0.427	0.1197 ± 0.503	**0.1156** ± 0.594	0.1250 ± 0.348	0.1232 ± 0.457	0.1248 ± 0.341	0.1231 ± 1.25	**0.1176** ± 0.541	0.1193 ± 0.438	0.1187 ± 0.352	0.1193 ± 0.431	0.1193 ± 0.636	**0.1170** ± 0.578
	192	0.1515 ± 0.714	0.1496 ± 1.02	0.1515 ± 0.714	0.1507 ± 0.682	**0.1477** ± 1.37	0.1508 ± 0.707	0.1487 ± 0.936	0.1507 ± 0.710	0.1504 ± 2.04	**0.1456** ± 1.02	0.1759 ± 0.843	0.1702 ± 0.927	0.1752 ± 0.948	0.1646 ± 0.964	**0.1541** ± 1.04	0.1572 ± 0.870	0.1559 ± 0.563	0.1570 ± 0.822	0.1564 ± 0.885	**0.1532** ± 1.06
	336	0.1860 ± 0.707	0.1829 ± 2.38	0.1859 ± 0.728	0.1832 ± 1.56	**0.1819** ± 2.96	0.1845 ± 0.687	0.1807 ± 2.19	0.1843 ± 0.715	0.1856 ± 4.47	**0.1782** ± 2.24	0.2046 ± 1.27	0.1994 ± 2.41	0.2038 ± 1.31	0.2028 ± 2.33	**0.1880** ± 2.00	0.1950 ± 0.785	0.1928 ± 0.894	0.1947 ± 0.732	0.1953 ± 1.26	**0.1876** ± 2.36
	720	0.2473 ± 2.76	0.2415 ± 8.03	0.2466 ± 2.77	0.2472 ± 9.36	**0.2364** ± 7.36	0.2431 ± 2.76	0.2362 ± 7.87	0.2424 ± 2.79	0.2509 ± 11.3	**0.2302** ± 6.42	0.2681 ± 0.865	0.2563 ± 8.19	0.2668 ± 1.01	0.2784 ± 20.4	**0.2449** ± 5.34	0.2573 ± 2.09	0.2496 ± 4.15	0.2550 ± 2.45	0.2519 ± 3.68	**0.2398** ± 6.56
Weather	96	0.1969 ± 0.285	0.1917 ± 0.348	0.1967 ± 0.263	0.1895 ± 0.795	**0.1684** ± 1.02	0.1872 ± 0.316	0.1816 ± 0.484	0.1868 ± 0.336	0.1792 ± 1.55	**0.1639** ± 0.944	0.1723 ± 0.212	0.1690 ± 0.515	0.1716 ± 0.297	0.1707 ± 2.01	**0.1584** ± 0.405	0.1752 ± 0.359	0.1734 ± 0.382	0.1751 ± 0.377	0.1796 ± 2.29	**0.1607** ± 1.03
	192	0.2426 ± 0.497	0.2328 ± 0.628	0.2421 ± 0.447	0.2342 ± 1.97	**0.2119** ± 1.60	0.2333 ± 0.516	0.2236 ± 0.782	0.2327 ± 0.511	0.2239 ± 1.94	**0.2075** ± 1.42	0.2246 ± 0.516	0.2162 ± 0.254	0.2232 ± 0.479	0.2184 ± 2.14	**0.2062** ± 1.30	0.2215 ± 0.608	0.2177 ± 0.796	0.2212 ± 0.627	0.2248 ± 3.82	**0.2059** ± 1.33
	336	0.2959 ± 1.08	0.2806 ± 1.85	0.2946 ± 1.20	0.2844 ± 3.03	**0.2619** ± 2.84	0.2884 ± 1.07	0.2735 ± 1.88	0.2871 ± 1.18	0.2777 ± 5.90	**0.2586** ± 2.61	0.2833 ± 1.01	0.2693 ± 1.71	0.2818 ± 1.11	0.2738 ± 4.52	**0.2589** ± 2.16	0.2800 ± 1.15	0.2735 ± 1.54	0.2789 ± 1.11	0.2793 ± 1.74	**0.2562** ± 2.98
	720	0.3731 ± 2.73	0.3641 ± 7.74	0.3715 ± 2.86	0.3715 ± 9.75	**0.3502** ± 8.06	0.3687 ± 2.71	0.3598 ± 7.77	0.3670 ± 2.81	0.3884 ± 14.7	**0.3478** ± 7.75	0.3656 ± 2.72	0.3568 ± 7.02	0.3640 ± 2.66	0.3696 ± 9.91	**0.3450** ± 6.81	0.3598 ± 2.70	0.3594 ± 3.78	0.3575 ± 2.75	0.3508 ± 4.92	**0.3421** ± 8.16
Exchange	96	0.1011 ± 6.01	0.0994 ± 5.69	0.1010 ± 6.02	0.0999 ± 6.04	**0.0914** ± 5.47	0.0916 ± 3.46	0.0898 ± 3.38	0.0916 ± 3.47	**0.0894** ± 4.69	0.0899 ± 5.23	0.0956 ± 4.21	0.0953 ± 4.47	0.0957 ± 4.23	0.0982 ± 3.67	**0.0929** ± 5.42	0.0946 ± 3.75	0.0925 ± 3.59	0.0946 ± 3.75	**0.0904** ± 1.35	0.0911 ± 4.41
	192	0.2039 ± 17.7	0.1996 ± 16.8	0.2038 ± 17.7	0.2014 ± 17.7	**0.1921** ± 17.2	0.1934 ± 14.2	0.1886 ± 13.7	0.1933 ± 14.2	0.1905 ± 14.4	**0.1868** ± 16.7	0.2018 ± 16.0	0.1960 ± 15.4	0.2016 ± 16.1	0.1974 ± 18.2	**0.1890** ± 16.2	0.2098 ± 14.0	0.2022 ± 13.3	0.2096 ± 14.0	0.1947 ± 8.92	**0.1928** ± 15.6
	336	0.3701 ± 37.7	0.3610 ± 36.7	0.3699 ± 37.7	0.3661 ± 38.0	**0.3556** ± 35.4	0.3659 ± 35.1	0.3548 ± 34.0	0.3657 ± 35.1	**0.3523** ± 42.1	0.3538 ± 34.9	0.3777 ± 37.4	0.3730 ± 37.9	0.3775 ± 37.4	0.3697 ± 35.5	**0.3647** ± 37.7	0.3824 ± 35.5	0.3641 ± 33.3	0.3822 ± 35.5	**0.3282** ± 20.4	0.3637 ± 35.9

Table B2: MSE by backbone and adaptation method in the Dynamic scenario (SD values $\times 10^{-3}$).

Dataset	H	DLinear					FreTS					iTransformer					PatchTST				
		Frozen	TAFAS	PETSA	DynaTTA	MATE	Frozen	TAFAS	PETSA	DynaTTA	MATE	Frozen	TAFAS	PETSA	DynaTTA	MATE	Frozen	TAFAS	PETSA	DynaTTA	MATE
ETTh1	96	0.4719 ± 5.20	0.4655 ± 5.41	0.4716 ± 5.24	0.4653 ± 8.82	**0.4609** ± 5.98	0.4507 ± 5.09	0.4463 ± 5.26	0.4506 ± 5.11	0.4532 ± 6.00	**0.4401** ± 5.61	0.4548 ± 5.01	0.4486 ± 4.97	0.4544 ± 5.06	0.4477 ± 7.17	**0.4427** ± 5.34	0.4385 ± 4.75	0.4335 ± 5.24	0.4383 ± 4.80	0.4325 ± 5.55	**0.4294** ± 5.34
	192	0.5273 ± 7.18	0.5158 ± 7.18	0.5269 ± 7.20	0.5236 ± 14.2	**0.5131** ± 7.55	0.5104 ± 7.14	0.5012 ± 7.17	0.5101 ± 7.17	0.5161 ± 9.39	**0.4947** ± 7.63	0.5143 ± 6.90	0.5033 ± 6.87	0.5139 ± 6.89	0.5094 ± 5.12	**0.4961** ± 7.28	0.4966 ± 6.49	0.4877 ± 7.68	0.4962 ± 6.53	0.4895 ± 8.29	**0.4853** ± 6.82
	336	0.5775 ± 7.81	0.5637 ± 8.37	0.5770 ± 7.76	0.5766 ± 11.5	**0.5630** ± 9.09	0.5649 ± 7.77	0.5538 ± 8.34	0.5645 ± 7.73	0.5871 ± 9.26	**0.5479** ± 8.18	0.5710 ± 7.90	0.5583 ± 8.46	0.5706 ± 7.89	0.5849 ± 13.2	**0.5519** ± 8.13	0.5629 ± 6.12	0.5518 ± 9.66	0.5623 ± 6.27	0.5526 ± 10.6	**0.5486** ± 6.80
	720	0.7302 ± 9.93	**0.6989** ± 12.0	0.7288 ± 9.99	0.7143 ± 9.95	0.7190 ± 11.4	0.7357 ± 9.98	**0.7051** ± 12.4	0.7345 ± 10.1	0.7113 ± 14.9	0.7198 ± 10.9	0.7250 ± 10.4	**0.6946** ± 12.5	0.7240 ± 10.6	0.7174 ± 17.3	0.7075 ± 10.6	0.7373 ± 12.2	**0.7057** ± 20.3	0.7358 ± 12.6	0.7182 ± 29.4	0.7161 ± 11.6
ETTh2	96	0.1898 ± 3.71	**0.1873** ± 3.70	0.1898 ± 3.70	0.1888 ± 4.30	0.1894 ± 4.64	0.1938 ± 3.68	0.1919 ± 3.54	0.1937 ± 3.67	0.1919 ± 4.28	**0.1876** ± 4.24	0.2057 ± 3.25	0.2020 ± 3.15	0.2054 ± 3.28	0.2020 ± 4.80	**0.1959** ± 3.78	0.1946 ± 3.23	0.1938 ± 3.17	0.1945 ± 3.23	0.1952 ± 3.37	**0.1915** ± 4.08
	192	0.2349 ± 5.72	0.2302 ± 5.88	0.2347 ± 5.74	0.2326 ± 7.62	**0.2299** ± 6.41	0.2376 ± 5.72	0.2334 ± 5.71	0.2374 ± 5.73	0.2341 ± 4.89	**0.2289** ± 5.97	0.2449 ± 4.70	0.2406 ± 5.18	0.2447 ± 4.71	0.2424 ± 6.32	**0.2344** ± 4.90	0.2317 ± 5.56	0.2258 ± 5.15	0.2313 ± 5.53	0.2284 ± 7.14	**0.2231** ± 6.04
	336	0.2665 ± 5.88	**0.2574** ± 5.95	0.2661 ± 5.87	0.2614 ± 6.45	0.2594 ± 6.31	0.2709 ± 5.88	**0.2610** ± 5.93	0.2706 ± 5.87	0.2617 ± 7.10	0.2613 ± 6.00	0.3007 ± 4.81	0.2790 ± 5.34	0.2998 ± 4.79	0.2811 ± 12.1	**0.2765** ± 4.80	0.2575 ± 5.58	0.2522 ± 4.68	0.2572 ± 5.55	0.2615 ± 5.40	**0.2504** ± 5.82
	720	0.3314 ± 4.84	**0.3104** ± 6.49	0.3306 ± 4.85	0.3214 ± 5.86	0.3121 ± 4.96	0.3420 ± 5.36	**0.3163** ± 7.09	0.3413 ± 5.38	0.3190 ± 5.16	0.3229 ± 5.27	0.3468 ± 4.64	0.3196 ± 5.50	0.3459 ± 4.70	0.3244 ± 5.26	**0.3178** ± 4.27	0.3155 ± 5.22	0.3081 ± 4.37	0.3151 ± 5.19	0.3207 ± 5.48	**0.2997** ± 5.46
ETTm1	96	0.3741 ± 3.84	0.3594 ± 3.71	0.3733 ± 3.85	0.3574 ± 4.73	**0.3518** ± 3.92	0.3755 ± 3.28	0.3682 ± 3.60	0.3750 ± 3.35	0.3597 ± 3.69	**0.3502** ± 3.52	0.3981 ± 3.19	0.3805 ± 3.07	0.3965 ± 3.26	**0.3495** ± 3.46	0.3550 ± 3.56	0.4050 ± 3.01	0.3980 ± 3.35	0.4046 ± 3.07	0.3742 ± 1.83	**0.3652** ± 4.32
	192	0.4451 ± 4.69	0.4249 ± 4.92	0.4440 ± 4.79	0.4255 ± 7.07	**0.4224** ± 5.30	0.4374 ± 4.11	0.4283 ± 4.68	0.4369 ± 4.14	0.4252 ± 5.49	**0.4171** ± 4.62	0.4410 ± 4.15	0.4290 ± 4.54	0.4400 ± 4.24	0.4202 ± 5.76	**0.4084** ± 4.73	0.4612 ± 3.46	0.4516 ± 4.14	0.4602 ± 3.53	0.4498 ± 3.33	**0.4322** ± 4.18
	336	0.5193 ± 5.55	0.4887 ± 6.57	0.5173 ± 5.60	0.4944 ± 11.3	**0.4867** ± 7.50	0.5051 ± 5.08	0.4898 ± 6.38	0.5042 ± 5.09	0.4901 ± 7.99	**0.4821** ± 5.99	0.5167 ± 5.22	0.4887 ± 6.53	0.5145 ± 5.22	0.4820 ± 7.23	**0.4745** ± 6.38	0.5059 ± 4.28	0.4903 ± 5.57	0.5048 ± 4.42	0.4924 ± 5.55	**0.4775** ± 5.75
	720	0.5965 ± 6.66	**0.5534** ± 8.73	0.5926 ± 6.86	0.5669 ± 10.5	0.5587 ± 8.98	0.5751 ± 6.35	0.5517 ± 8.44	0.5730 ± 6.65	0.5759 ± 16.4	**0.5479** ± 7.93	0.6084 ± 5.52	0.5543 ± 9.40	0.6032 ± 6.06	0.5707 ± 12.1	**0.5351** ± 8.44	0.5745 ± 5.63	0.5454 ± 7.92	0.5706 ± 6.08	0.5521 ± 5.49	**0.5386** ± 7.44
ETTm2	96	0.1273 ± 1.79	0.1258 ± 1.73	0.1273 ± 1.79	0.1270 ± 1.75	**0.1228** ± 1.78	0.1255 ± 1.69	0.1241 ± 1.67	0.1254 ± 1.69	0.1240 ± 2.21	**0.1199** ± 1.68	0.1295 ± 1.86	0.1276 ± 1.79	0.1292 ± 1.87	0.1269 ± 1.99	**0.1220** ± 1.92	0.1241 ± 1.81	0.1233 ± 1.77	0.1240 ± 1.81	0.1241 ± 1.64	**0.1212** ± 1.91
	192	0.1561 ± 2.58	0.1536 ± 2.50	0.1560 ± 2.58	0.1548 ± 2.59	**0.1513** ± 2.64	0.1555 ± 2.53	0.1529 ± 2.53	0.1554 ± 2.54	0.1541 ± 1.35	**0.1492** ± 2.57	0.1751 ± 2.94	0.1701 ± 3.07	0.1747 ± 2.94	0.1670 ± 3.53	**0.1562** ± 2.89	0.1613 ± 2.64	0.1598 ± 2.54	0.1610 ± 2.65	0.1602 ± 2.56	**0.1563** ± 2.74
	336	0.1908 ± 4.07	0.1861 ± 4.25	0.1905 ± 4.03	0.1862 ± 4.37	**0.1856** ± 4.55	0.1896 ± 3.96	0.1842 ± 4.06	0.1893 ± 3.94	0.1875 ± 5.22	**0.1817** ± 4.19	0.2055 ± 4.42	0.1994 ± 4.36	0.2051 ± 4.40	0.2031 ± 4.06	**0.1900** ± 4.36	0.1986 ± 4.42	0.1961 ± 4.15	0.1983 ± 4.44	0.1987 ± 4.21	**0.1896** ± 4.38
	720	0.2530 ± 8.14	0.2434 ± 8.88	0.2520 ± 8.25	0.2491 ± 8.80	**0.2413** ± 8.51	0.2495 ± 7.92	0.2382 ± 8.36	0.2485 ± 8.03	0.2480 ± 10.4	**0.2339** ± 7.73	0.2739 ± 8.35	0.2564 ± 9.33	0.2722 ± 8.60	0.2710 ± 8.12	**0.2470** ± 8.42	0.2629 ± 8.00	0.2542 ± 7.28	0.2601 ± 7.94	0.2565 ± 6.44	**0.2419** ± 8.07
Weather	96	0.1953 ± 4.02	0.1898 ± 3.66	0.1951 ± 3.98	0.1883 ± 3.31	**0.1786** ± 3.40	0.1867 ± 3.82	0.1811 ± 3.49	0.1864 ± 3.81	0.1785 ± 3.86	**0.1715** ± 3.33	0.1783 ± 3.73	0.1711 ± 3.33	0.1777 ± 3.65	0.1701 ± 3.90	**0.1630** ± 3.33	0.1785 ± 3.69	0.1761 ± 3.65	0.1783 ± 3.68	0.1791 ± 3.27	**0.1668** ± 3.51
	192	0.2404 ± 5.00	0.2298 ± 4.51	0.2399 ± 5.01	0.2310 ± 4.58	**0.2193** ± 4.51	0.2326 ± 4.81	0.2219 ± 4.42	0.2320 ± 4.82	0.2225 ± 3.24	**0.2131** ± 4.36	0.2270 ± 4.68	0.2168 ± 4.49	0.2262 ± 4.72	0.2168 ± 5.26	**0.2116** ± 4.41	0.2238 ± 4.60	0.2185 ± 4.41	0.2233 ± 4.62	0.2206 ± 4.60	**0.2098** ± 4.61
	336	0.2936 ± 6.22	0.2763 ± 5.61	0.2924 ± 6.35	0.2800 ± 5.10	**0.2665** ± 5.58	0.2875 ± 6.05	0.2703 ± 5.51	0.2862 ± 6.16	0.2727 ± 8.26	**0.2625** ± 5.46	0.2862 ± 6.06	0.2678 ± 5.79	0.2845 ± 6.21	0.2703 ± 8.47	**0.2622** ± 5.60	0.2808 ± 5.59	0.2703 ± 5.17	0.2794 ± 5.56	0.2732 ± 4.15	**0.2600** ± 5.58
	720	0.3716 ± 7.31	0.3532 ± 7.56	0.3698 ± 7.44	0.3633 ± 9.19	**0.3481** ± 8.78	0.3680 ± 7.20	0.3496 ± 7.42	0.3662 ± 7.23	0.3676 ± 11.1	**0.3456** ± 8.60	0.3718 ± 7.69	0.3505 ± 8.58	0.3697 ± 7.75	0.3591 ± 8.48	**0.3426** ± 8.13	0.3596 ± 6.65	0.3481 ± 5.53	0.3568 ± 6.49	0.3474 ± 4.43	**0.3391** ± 7.55
Exchange	96	0.1027 ± 4.36	0.0997 ± 5.13	0.1026 ± 4.41	0.1007 ± 5.38	**0.0984** ± 4.09	0.0955 ± 4.30	0.0924 ± 4.56	0.0954 ± 4.31	**0.0912** ± 5.15	0.0921 ± 4.10	0.0987 ± 4.53	0.0971 ± 4.26	0.0986 ± 4.52	0.0992 ± 4.46	**0.0971** ± 3.88	0.1010 ± 5.00	0.0977 ± 5.10	0.1009 ± 5.02	**0.0954** ± 4.12	0.0957 ± 4.64
	192	0.1966 ± 7.94	0.1901 ± 8.73	0.1965 ± 7.98	0.1938 ± 8.53	**0.1868** ± 8.73	0.1892 ± 8.60	0.1820 ± 9.12	0.1890 ± 8.62	0.1827 ± 7.48	**0.1786** ± 7.12	0.1973 ± 11.1	0.1883 ± 10.5	0.1971 ± 11.1	0.1877 ± 11.0	**0.1862** ± 10.1	0.2074 ± 12.7	0.1983 ± 12.8	0.2072 ± 12.8	0.1909 ± 11.0	**0.1883** ± 10.3
	336	0.3415 ± 13.6	0.3300 ± 11.8	0.3413 ± 13.6	0.3351 ± 13.4	**0.3293** ± 12.4	0.3407 ± 14.4	0.3282 ± 12.5	0.3405 ± 14.3	**0.3190** ± 14.2	0.3254 ± 12.7	0.3633 ± 26.7	0.3492 ± 23.6	0.3630 ± 26.6	**0.3440** ± 18.4	0.3484 ± 25.1	0.3602 ± 18.2	0.3420 ± 16.3	0.3600 ± 18.2	**0.3060** ± 9.65	0.3418 ± 16.4

Table B3: MSE by backbone and adaptation method in the Profile scenario (SD values $\times 10^{-3}$).

Dataset	H	DLinear					FreTS					iTransformer					PatchTST				
		Frozen	TAFAS	PETSA	DynaTTA	MATE	Frozen	TAFAS	PETSA	DynaTTA	MATE	Frozen	TAFAS	PETSA	DynaTTA	MATE	Frozen	TAFAS	PETSA	DynaTTA	MATE
ETTh1	96	0.4588 ± 6.37	0.4542 ± 6.95	0.4586 ± 6.40	0.4549 ± 8.91	**0.4496** ± 6.72	0.4380 ± 5.98	0.4348 ± 6.46	0.4379 ± 5.98	0.4408 ± 6.67	**0.4289** ± 6.16	0.4438 ± 4.30	0.4386 ± 5.47	0.4434 ± 4.36	0.4407 ± 8.70	**0.4320** ± 5.50	0.4271 ± 5.84	0.4234 ± 6.33	0.4270 ± 5.88	0.4214 ± 6.98	**0.4184** ± 6.35
	192	0.5124 ± 8.03	0.5053 ± 9.49	0.5121 ± 8.13	0.5166 ± 14.5	**0.5016** ± 9.23	0.4959 ± 7.59	0.4904 ± 8.92	0.4956 ± 7.69	0.5073 ± 12.1	**0.4828** ± 8.34	0.5016 ± 6.05	0.4941 ± 7.71	0.5012 ± 6.11	0.5069 ± 12.9	**0.4858** ± 7.90	0.4837 ± 6.46	0.4778 ± 7.89	0.4834 ± 6.54	0.4785 ± 9.68	**0.4737** ± 7.96
	336	0.5626 ± 10.8	0.5571 ± 13.5	0.5623 ± 10.8	0.5714 ± 15.2	**0.5544** ± 13.5	0.5504 ± 10.3	0.5465 ± 12.9	0.5502 ± 10.4	0.5952 ± 29.8	**0.5370** ± 11.9	0.5590 ± 8.43	0.5532 ± 11.6	0.5588 ± 8.52	0.5961 ± 37.6	**0.5445** ± 11.2	0.5485 ± 8.76	0.5443 ± 11.0	0.5483 ± 8.91	0.5438 ± 12.9	**0.5369** ± 11.3
	720	0.7213 ± 19.1	**0.7045** ± 22.7	0.7203 ± 19.3	0.7181 ± 19.3	0.7181 ± 21.7	0.7272 ± 18.8	**0.7112** ± 22.6	0.7264 ± 18.9	0.7249 ± 24.5	0.7168 ± 21.1	0.7183 ± 16.4	**0.7022** ± 20.2	0.7177 ± 16.7	0.7374 ± 26.7	0.7077 ± 19.2	0.7252 ± 15.2	0.7105 ± 19.8	0.7244 ± 15.4	0.7381 ± 26.4	**0.7096** ± 18.9
ETTh2	96	0.1825 ± 1.89	**0.1802** ± 1.72	0.1825 ± 1.89	0.1815 ± 2.27	0.1826 ± 2.03	0.1861 ± 1.87	0.1844 ± 1.62	0.1860 ± 1.86	0.1843 ± 1.55	**0.1803** ± 1.75	0.1988 ± 2.48	0.1955 ± 2.31	0.1985 ± 2.46	0.1952 ± 2.28	**0.1895** ± 2.53	0.1870 ± 2.07	0.1863 ± 2.10	0.1869 ± 2.06	0.1877 ± 2.35	**0.1839** ± 2.12
	192	0.2257 ± 3.31	0.2217 ± 2.66	0.2255 ± 3.31	0.2237 ± 3.09	**0.2214** ± 2.69	0.2280 ± 3.43	0.2245 ± 2.77	0.2278 ± 3.42	0.2263 ± 4.29	**0.2194** ± 3.04	0.2368 ± 2.91	0.2330 ± 2.69	0.2366 ± 2.90	0.2361 ± 1.74	**0.2265** ± 2.93	0.2222 ± 3.95	0.2176 ± 3.86	0.2218 ± 3.92	0.2214 ± 6.91	**0.2138** ± 3.52
	336	0.2572 ± 5.15	**0.2504** ± 3.32	0.2568 ± 5.11	0.2537 ± 3.36	0.2510 ± 3.75	0.2620 ± 4.84	0.2542 ± 3.09	0.2617 ± 4.83	0.2564 ± 2.08	**0.2530** ± 4.03	0.2938 ± 4.19	0.2755 ± 2.76	0.2929 ± 4.19	0.2804 ± 6.28	**0.2704** ± 4.59	0.2483 ± 5.22	0.2448 ± 5.56	0.2480 ± 5.22	0.2550 ± 8.61	**0.2423** ± 4.28
	720	0.3253 ± 5.90	**0.3091** ± 2.00	0.3245 ± 5.83	0.3189 ± 2.82	0.3093 ± 3.09	0.3370 ± 5.47	**0.3165** ± 1.34	0.3363 ± 5.38	0.3223 ± 7.24	0.3201 ± 3.79	0.3449 ± 3.99	0.3219 ± 1.60	0.3441 ± 3.93	0.3310 ± 13.0	**0.3179** ± 2.59	0.3088 ± 6.28	0.3057 ± 7.62	0.3084 ± 6.23	0.3173 ± 4.19	**0.2951** ± 4.63
ETTm1	96	0.3642 ± 5.29	0.3507 ± 5.41	0.3635 ± 5.31	0.3495 ± 6.28	**0.3436** ± 5.47	0.3644 ± 5.69	0.3583 ± 5.96	0.3640 ± 5.65	0.3517 ± 5.86	**0.3413** ± 5.32	0.3903 ± 2.52	0.3743 ± 0.801	0.3887 ± 2.22	**0.3440** ± 3.15	0.3494 ± 2.22	0.3917 ± 6.74	0.3861 ± 7.07	0.3914 ± 6.75	0.3659 ± 6.59	**0.3594** ± 6.15
	192	0.4343 ± 5.78	0.4162 ± 5.92	0.4332 ± 5.87	0.4187 ± 7.60	**0.4141** ± 5.95	0.4264 ± 5.79	0.4191 ± 6.27	0.4260 ± 5.83	0.4178 ± 7.43	**0.4081** ± 5.87	0.4321 ± 1.03	0.4218 ± 0.603	0.4311 ± 0.926	0.4150 ± 4.92	**0.4016** ± 0.843	0.4491 ± 6.17	0.4421 ± 7.00	0.4483 ± 6.27	0.4402 ± 6.97	**0.4234** ± 5.84
	336	0.5067 ± 6.43	0.4802 ± 6.67	0.5049 ± 6.45	0.4879 ± 8.98	**0.4792** ± 6.48	0.4930 ± 6.12	0.4811 ± 6.97	0.4923 ± 6.16	0.4833 ± 8.90	**0.4730** ± 6.03	0.5140 ± 6.64	0.4854 ± 4.28	0.5116 ± 6.27	0.4765 ± 5.55	**0.4702** ± 3.90	0.4948 ± 5.87	0.4820 ± 7.11	0.4939 ± 6.00	0.4830 ± 7.82	**0.4698** ± 6.03
	720	0.5814 ± 7.74	**0.5490** ± 9.91	0.5781 ± 7.83	0.5606 ± 12.0	0.5521 ± 8.12	0.5613 ± 7.37	0.5477 ± 10.3	0.5597 ± 7.61	0.5704 ± 20.0	**0.5402** ± 8.84	0.6071 ± 7.67	0.5615 ± 6.99	0.6023 ± 7.42	0.5769 ± 16.6	**0.5372** ± 4.88	0.5624 ± 6.20	0.5388 ± 8.93	0.5595 ± 6.66	0.5465 ± 12.2	**0.5337** ± 9.12
ETTm2	96	0.1238 ± 0.856	0.1223 ± 0.778	0.1238 ± 0.857	0.1228 ± 0.458	**0.1193** ± 0.891	0.1216 ± 0.980	0.1202 ± 0.911	0.1215 ± 0.968	0.1199 ± 1.02	**0.1161** ± 0.912	0.1248 ± 1.76	0.1230 ± 1.47	0.1245 ± 1.68	0.1220 ± 0.750	**0.1176** ± 1.51	0.1204 ± 1.02	0.1197 ± 1.03	0.1203 ± 1.01	0.1200 ± 0.930	**0.1176** ± 0.968
	192	0.1519 ± 1.01	0.1493 ± 0.901	0.1518 ± 1.02	0.1504 ± 0.778	**0.1471** ± 0.888	0.1509 ± 1.13	0.1484 ± 1.00	0.1508 ± 1.13	0.1490 ± 1.41	**0.1447** ± 1.05	0.1710 ± 2.47	0.1656 ± 2.66	0.1706 ± 2.47	0.1618 ± 2.54	**0.1509** ± 1.95	0.1568 ± 1.21	0.1555 ± 1.15	0.1566 ± 1.21	0.1561 ± 1.20	**0.1519** ± 1.06
	336	0.1854 ± 1.47	0.1809 ± 1.11	0.1852 ± 1.47	0.1824 ± 0.848	**0.1802** ± 1.01	0.1839 ± 1.75	0.1789 ± 1.31	0.1837 ± 1.75	0.1826 ± 1.50	**0.1763** ± 1.29	0.1996 ± 2.62	0.1935 ± 2.30	0.1992 ± 2.60	0.1962 ± 2.52	**0.1837** ± 1.99	0.1920 ± 2.20	0.1900 ± 2.01	0.1918 ± 2.21	0.1925 ± 2.03	**0.1839** ± 1.43
	720	0.2447 ± 3.21	0.2355 ± 1.73	0.2439 ± 3.18	0.2432 ± 3.36	**0.2335** ± 1.65	0.2412 ± 3.66	0.2308 ± 2.15	0.2403 ± 3.58	0.2398 ± 5.13	**0.2254** ± 2.53	0.2664 ± 3.96	0.2499 ± 1.05	0.2650 ± 3.80	0.2631 ± 5.89	**0.2394** ± 2.04	0.2538 ± 3.87	0.2463 ± 3.30	0.2518 ± 3.70	0.2486 ± 1.99	**0.2342** ± 2.37
Weather	96	0.2013 ± 2.22	0.1960 ± 2.22	0.2011 ± 2.17	0.1937 ± 1.87	**0.1816** ± 1.97	0.1917 ± 2.05	0.1860 ± 1.96	0.1914 ± 2.05	0.1819 ± 4.86	**0.1741** ± 1.93	0.1813 ± 1.90	0.1744 ± 1.67	0.1806 ± 1.85	0.1734 ± 2.04	**0.1669** ± 2.05	0.1817 ± 1.72	0.1798 ± 1.84	0.1815 ± 1.73	0.1836 ± 4.17	**0.1694** ± 1.51
	192	0.2475 ± 2.78	0.2373 ± 2.62	0.2470 ± 2.73	0.2381 ± 2.58	**0.2241** ± 2.42	0.2386 ± 2.72	0.2285 ± 2.49	0.2380 ± 2.72	0.2283 ± 1.37	**0.2174** ± 2.37	0.2319 ± 2.33	0.2218 ± 2.21	0.2311 ± 2.35	0.2221 ± 2.38	**0.2161** ± 2.14	0.2280 ± 2.54	0.2238 ± 2.82	0.2276 ± 2.58	0.2277 ± 4.33	**0.2142** ± 2.33
	336	0.3014 ± 3.53	0.2853 ± 3.32	0.3001 ± 3.66	0.2892 ± 2.69	**0.2731** ± 2.86	0.2943 ± 3.57	0.2786 ± 3.36	0.2930 ± 3.73	0.2815 ± 7.56	**0.2689** ± 2.74	0.2914 ± 3.24	0.2740 ± 3.27	0.2895 ± 3.38	0.2792 ± 5.81	**0.2679** ± 2.75	0.2863 ± 3.28	0.2787 ± 3.77	0.2851 ± 3.43	0.2833 ± 7.16	**0.2661** ± 2.97
	720	0.3795 ± 5.86	0.3673 ± 7.04	0.3780 ± 5.97	0.3765 ± 8.16	**0.3595** ± 4.27	0.3752 ± 5.91	0.3633 ± 7.16	0.3738 ± 6.00	0.3884 ± 14.7	**0.3565** ± 4.54	0.3781 ± 5.37	0.3619 ± 7.24	0.3762 ± 5.46	0.3712 ± 4.92	**0.3527** ± 4.40	0.3663 ± 5.80	0.3605 ± 7.45	0.3642 ± 6.23	0.3614 ± 12.8	**0.3505** ± 4.53
Exchange	96	0.0968 ± 3.62	0.0942 ± 3.94	0.0967 ± 3.63	0.0954 ± 3.20	**0.0908** ± 3.37	0.0890 ± 2.25	0.0861 ± 2.88	0.0889 ± 2.28	0.0854 ± 2.33	**0.0854** ± 3.47	0.0927 ± 1.73	0.0911 ± 2.48	0.0926 ± 1.71	0.0934 ± 5.04	**0.0909** ± 2.70	0.0937 ± 2.66	0.0912 ± 3.04	0.0936 ± 2.68	0.0890 ± 3.51	**0.0886** ± 3.96
	192	0.1936 ± 8.38	0.1880 ± 9.59	0.1934 ± 8.38	0.1909 ± 9.35	**0.1823** ± 10.2	0.1855 ± 7.24	0.1792 ± 8.71	0.1854 ± 7.27	0.1810 ± 9.04	**0.1749** ± 11.6	0.1934 ± 6.33	0.1848 ± 8.73	0.1932 ± 6.31	0.1842 ± 8.65	**0.1832** ± 8.26	0.2014 ± 5.38	0.1935 ± 5.94	0.2012 ± 5.39	0.1861 ± 5.31	**0.1803** ± 11.2
	336	0.3459 ± 6.43	0.3365 ± 7.26	0.3457 ± 6.38	0.3413 ± 6.08	**0.3346** ± 8.17	0.3439 ± 5.61	0.3330 ± 6.59	0.3437 ± 5.57	**0.3265** ± 7.00	0.3308 ± 10.2	0.3691 ± 13.2	0.3566 ± 8.93	0.3687 ± 13.1	**0.3461** ± 12.3	0.3573 ± 14.5	0.3616 ± 5.80	0.3434 ± 5.82	0.3613 ± 5.82	**0.3096** ± 3.97	0.3449 ± 10.7

Table B4: MAE by dataset and forecast horizon, grouped by backbone and adaptation method, in the Natural scenario (SD values $\times 10^{-3}$).

Dataset	H	DLinear					FreTS					iTransformer					PatchTST				
		Frozen	TAFAS	PETSA	DynaTTA	MATE	Frozen	TAFAS	PETSA	DynaTTA	MATE	Frozen	TAFAS	PETSA	DynaTTA	MATE	Frozen	TAFAS	PETSA	DynaTTA	MATE
ETTh1	96	0.4632 ±0	0.4589 ±0	0.4630 ±0	0.4600 ±1.91	**0.4562** ±0	0.4476 ±0	0.4444 ±0	0.4475 ±0	0.4492 ±0.923	**0.4408** ±0	0.4578 ±0	0.4534 ±0	0.4575 ±0	0.4555 ±0.819	**0.4500** ±0	0.4534 ±0	0.4486 ±0	0.4532 ±0	**0.4463** ±0.370	0.4477 ±0
	192	0.4985 ±0	0.4925 ±0	0.4982 ±0	0.4968 ±2.51	**0.4916** ±0	0.4875 ±0	0.4828 ±0	0.4873 ±0	0.4926 ±1.02	**0.4787** ±0	0.4963 ±0	0.4911 ±0	0.4960 ±0	0.4978 ±0.392	**0.4875** ±0	0.4900 ±0	0.4848 ±0	0.4896 ±0	0.4876 ±1.10	**0.4832** ±0
	336	0.5287 ±0	0.5260 ±0	0.5284 ±0	0.5328 ±1.61	**0.5242** ±0	0.5208 ±0	0.5194 ±0	0.5206 ±0	0.5387 ±0.376	**0.5127** ±0	0.5312 ±0	0.5300 ±0	0.5310 ±0	0.5490 ±3.72	**0.5231** ±0	0.5288 ±0	0.5276 ±0	0.5285 ±0	0.5302 ±0.856	**0.5222** ±0
	720	0.6176 ±0	**0.6092** ±0	0.6171 ±0	0.6153 ±1.76	0.6153 ±0	0.6219 ±0	0.6145 ±0	0.6214 ±0	**0.6112** ±0.965	0.6149 ±0	0.6230 ±0	0.6166 ±0	0.6226 ±0	0.6256 ±0.964	**0.6159** ±0	0.6259 ±0	0.6248 ±0	0.6253 ±0	0.6374 ±3.72	**0.6180** ±0
ETTh2	96	0.2862 ±0	**0.2842** ±0	0.2861 ±0	0.2856 ±0.412	0.2864 ±0	0.2908 ±0	0.2891 ±0	0.2907 ±0	0.2905 ±0.410	**0.2857** ±0	0.3059 ±0	0.3020 ±0	0.3056 ±0	0.3025 ±0.357	**0.2975** ±0	0.2880 ±0	**0.2871** ±0	0.2879 ±0	0.2888 ±0.443	0.2872 ±0
	192	0.3188 ±0	**0.3147** ±0	0.3186 ±0	0.3169 ±1.46	0.3160 ±0	0.3240 ±0	0.3201 ±0	0.3238 ±0	0.3222 ±1.57	**0.3175** ±0	0.3335 ±0	0.3291 ±0	0.3333 ±0	0.3319 ±0.908	**0.3258** ±0	0.3212 ±0	0.3157 ±0	0.3208 ±0	0.3192 ±1.97	**0.3145** ±0
	336	0.3415 ±0	**0.3344** ±0	0.3412 ±0	0.3379 ±0.714	0.3363 ±0	0.3481 ±0	**0.3398** ±0	0.3478 ±0	0.3402 ±1.89	0.3406 ±0	0.3792 ±0	0.3601 ±0.103	0.3783 ±0	0.3592 ±3.23	**0.3587** ±0	0.3369 ±0	0.3339 ±0	0.3366 ±0	0.3435 ±1.57	**0.3316** ±0
	720	0.3872 ±0	**0.3714** ±0	0.3866 ±0	0.3805 ±1.35	0.3737 ±0	0.3972 ±0	**0.3777** ±0	0.3967 ±0	0.3806 ±4.31	0.3831 ±0	0.4053 ±0	0.3845 ±0.226	0.4047 ±0	0.3886 ±3.53	**0.3836** ±0	0.3775 ±0	0.3756 ±0	0.3771 ±0	0.3854 ±6.93	**0.3658** ±0
ETTm1	96	0.3908 ±0	0.3794 ±0	0.3902 ±0	0.3792 ±0.835	**0.3706** ±0	0.3931 ±0	0.3875 ±0	0.3927 ±0	0.3855 ±0.312	**0.3749** ±0	0.4056 ±0	0.3971 ±0	0.4047 ±0	**0.3840** ±0.684	0.3864 ±0	0.4080 ±0	0.4024 ±0	0.4077 ±0	0.3934 ±0.227	**0.3854** ±0
	192	0.4265 ±0	0.4127 ±0	0.4257 ±0	0.4155 ±1.14	**0.4104** ±0	0.4273 ±0	0.4212 ±0	0.4270 ±0	0.4219 ±0.471	**0.4136** ±0	0.4361 ±0	0.4298 ±0	0.4356 ±0	0.4266 ±0.616	**0.4175** ±0	0.4422 ±0	0.4353 ±0	0.4414 ±0	0.4345 ±0.557	**0.4253** ±0
	336	0.4654 ±0	**0.4479** ±0	0.4642 ±0	0.4544 ±1.60	0.4483 ±0	0.4647 ±0	0.4567 ±0	0.4642 ±0	0.4597 ±1.25	**0.4526** ±0	0.4774 ±0	0.4654 ±0	0.4764 ±0	0.4641 ±0.558	**0.4584** ±0	0.4732 ±0	0.4629 ±0	0.4724 ±0	0.4654 ±0.234	**0.4579** ±0
	720	0.5144 ±0	**0.4957** ±0	0.5123 ±0	0.5049 ±3.20	0.4987 ±0	0.5117 ±0	0.5036 ±0	0.5107 ±0	0.5172 ±3.62	**0.4999** ±0	0.5334 ±0	0.5167 ±0	0.5313 ±0.131	0.5249 ±0.931	**0.5060** ±0	0.5230 ±0	0.5078 ±0	0.5205 ±0.119	0.5136 ±1.10	**0.5043** ±0
ETTm2	96	0.2341 ±0	0.2326 ±0	0.2341 ±0	0.2335 ±0.369	**0.2289** ±0	0.2311 ±0	0.2298 ±0	0.2310 ±0	0.2301 ±0.436	**0.2257** ±0	0.2359 ±0	0.2337 ±0	0.2356 ±0	0.2331 ±0.339	**0.2280** ±0	0.2300 ±0	0.2293 ±0	0.2299 ±0	0.2299 ±0.367	**0.2274** ±0
	192	0.2600 ±0	0.2577 ±0	0.2599 ±0	0.2585 ±0.475	**0.2555** ±0	0.2599 ±0	0.2575 ±0	0.2598 ±0	0.2591 ±0.903	**0.2543** ±0	0.2760 ±0	0.2710 ±0	0.2755 ±0	0.2675 ±0.286	**0.2611** ±0	0.2654 ±0	0.2641 ±0	0.2652 ±0	0.2641 ±0.354	**0.2612** ±0
	336	0.2871 ±0	0.2841 ±0	0.2869 ±0	0.2848 ±0.231	**0.2836** ±0	0.2873 ±0	0.2834 ±0	0.2870 ±0	0.2864 ±0.530	**0.2815** ±0	0.3028 ±0	0.2979 ±0	0.3022 ±0	0.2984 ±0.513	**0.2897** ±0	0.2948 ±0	0.2939 ±0	0.2946 ±0	0.2971 ±0.279	**0.2884** ±0
	720	0.3292 ±0	0.3242 ±0	0.3286 ±0	0.3275 ±0.624	**0.3223** ±0	0.3291 ±0	0.3218 ±0	0.3284 ±0	0.3289 ±1.80	**0.3188** ±0	0.3545 ±0	0.3415 ±0	0.3532 ±0	0.3538 ±3.29	**0.3336** ±0	0.3411 ±0	0.3381 ±0	0.3392 ±0	0.3380 ±1.68	**0.3264** ±0
Weather	96	0.2350 ±0	0.2338 ±0	0.2348 ±0	0.2350 ±0.494	**0.2162** ±0	0.2247 ±0	0.2238 ±0	0.2244 ±0	0.2274 ±0.580	**0.2115** ±0	0.2093 ±0	0.2101 ±0	0.2088 ±0.176	0.2180 ±1.73	**0.2037** ±0	0.2153 ±0	0.2173 ±0	0.2153 ±0	0.2294 ±1.34	**0.2076** ±0
	192	0.2707 ±0	0.2684 ±0	0.2704 ±0	0.2696 ±0.858	**0.2561** ±0	0.2624 ±0	0.2599 ±0	0.2620 ±0	0.2628 ±0.240	**0.2522** ±0	0.2561 ±0	0.2541 ±0	0.2554 ±0	0.2608 ±1.06	**0.2492** ±0	0.2565 ±0	0.2591 ±0	0.2564 ±0	0.2726 ±5.50	**0.2501** ±0
	336	0.3066 ±0	0.3027 ±0	0.3059 ±0	0.3037 ±1.11	**0.2929** ±0	0.3002 ±0	0.2960 ±0	0.2995 ±0	0.3033 ±1.50	**0.2901** ±0	0.2980 ±0	0.2942 ±0	0.2973 ±0	0.3038 ±2.12	**0.2895** ±0	0.2959 ±0	0.3002 ±0	0.2955 ±0	0.3160 ±1.37	**0.2874** ±0
	720	0.3533 ±0	0.3585 ±0	0.3524 ±0	0.3565 ±0.942	**0.3497** ±0	0.3488 ±0	0.3532 ±0	0.3479 ±0	0.3650 ±2.63	**0.3470** ±0	0.3488 ±0	0.3520 ±0	0.3481 ±0.140	0.3605 ±3.89	**0.3450** ±0	0.3447 ±0	0.3609 ±0	0.3435 ±0	0.3584 ±2.31	**0.3428** ±0
Exchange	96	0.2128 ±0	0.2113 ±0	0.2128 ±0	0.2119 ±0.509	**0.1998** ±0	0.1995 ±0	**0.1975** ±0	0.1995 ±0	**0.1975** ±2.28	0.1984 ±0	0.2084 ±0	0.2088 ±0	0.2084 ±0	0.2143 ±2.76	**0.2053** ±0	0.2035 ±0	0.2009 ±0	0.2033 ±0	0.2013 ±1.84	**0.2008** ±0
	192	0.3048 ±0	0.3023 ±0	0.3048 ±0	0.3034 ±0.778	**0.2931** ±0	0.2948 ±0	0.2917 ±0	0.2948 ±0	0.2931 ±1.36	**0.2899** ±0	0.3061 ±0	0.3025 ±0.237	0.3059 ±0	0.3044 ±1.59	**0.2947** ±0	0.3070 ±0	0.3007 ±0	0.3068 ±0	0.2996 ±0.918	**0.2958** ±0
	336	0.4143 ±0	0.4102 ±0	0.4142 ±0	0.4124 ±1.92	**0.4025** ±0	0.4110 ±0	0.4054 ±0	0.4109 ±0	0.4042 ±6.75	**0.4017** ±0	0.4238 ±0	0.4200 ±0.123	0.4237 ±0	0.4195 ±3.72	**0.4140** ±0	0.4235 ±0	0.4112 ±0	0.4233 ±0	**0.3905** ±0	0.4098 ±0

Table B5: MAE by dataset and forecast horizon, grouped by backbone and adaptation method, in the TTFBench scenario (SD values $\times 10^{-3}$).

Dataset	H	DLinear					FreTS					iTransformer					PatchTST				
		Frozen	TAFAS	PETSA	DynaTTA	MATE	Frozen	TAFAS	PETSA	DynaTTA	MATE	Frozen	TAFAS	PETSA	DynaTTA	MATE	Frozen	TAFAS	PETSA	DynaTTA	MATE
ETTh1	96	0.4730 ±0	0.4721 ±0	0.4730 ±0	0.4734 ±1.04	**0.4694** ±0	0.4584 ±0	0.4576 ±0	0.4584 ±0	0.4724 ±1.16	**0.4542** ±0	0.4689 ±0	0.4663 ±0	0.4687 ±0	0.4776 ±1.17	**0.4635** ±0	0.4647 ±0	0.4626 ±0	0.4646 ±0	0.4655 ±0.972	**0.4605** ±0
	192	0.5180 ±0	0.5184 ±0	0.5180 ±0	0.5221 ±1.52	**0.5160** ±0	0.5078 ±0	0.5080 ±0	0.5077 ±0	0.5264 ±1.82	**0.5028** ±0	0.5172 ±0	0.5170 ±0	0.5171 ±0	0.5332 ±1.92	**0.5118** ±0	0.5109 ±0	0.5112 ±0	0.5107 ±0	0.5169 ±2.08	**0.5067** ±0
	336	**0.5639** ±0	0.5736 ±0	0.5640 ±0	0.5741 ±0.628	0.5663 ±0	0.5566 ±0	0.5652 ±0	0.5566 ±0	0.5978 ±3.10	**0.5533** ±0	0.5677 ±0	0.5765 ±0	0.5678 ±0	0.6086 ±4.25	**0.5653** ±0	0.5639 ±0	0.5702 ±0	0.5638 ±0	0.5776 ±1.42	**0.5621** ±0
	720	**0.6951** ±0	0.7179 ±0	0.6953 ±0	0.7107 ±3.58	0.6999 ±0	0.6992 ±0	0.7209 ±0	0.6993 ±0	0.7902 ±6.35	**0.6987** ±0	**0.6996** ±0	0.7221 ±0	0.6998 ±0	0.7851 ±6.18	0.7017 ±0	0.7033 ±0	0.7242 ±0	0.7033 ±0	0.7403 ±12.9	**0.7013** ±0
ETTh2	96	**0.2935** ±0	0.2938 ±0	**0.2935** ±0	0.2950 ±0.816	0.2955 ±0	0.2976 ±0	0.2973 ±0	0.2976 ±0	0.3000 ±0.424	**0.2947** ±0	0.3131 ±0	0.3111 ±0	0.3128 ±0	0.3142 ±0.463	**0.3069** ±0	**0.2959** ±0	0.2960 ±0	**0.2959** ±0	0.2991 ±0.704	0.2969 ±0
	192	0.3344 ±0	0.3354 ±0	**0.3343** ±0	0.3376 ±0.950	0.3348 ±0	0.3398 ±0	0.3397 ±0	0.3397 ±0	0.3471 ±2.30	**0.3362** ±0	0.3487 ±0	0.3485 ±0	0.3487 ±0	0.3552 ±1.14	**0.3441** ±0	0.3369 ±0	**0.3343** ±0	0.3366 ±0	0.3429 ±4.44	**0.3343** ±0
	336	0.3701 ±0	0.3741 ±0	**0.3699** ±0	0.3721 ±0.915	0.3714 ±0	0.3762 ±0	0.3776 ±0	0.3760 ±0	0.3887 ±3.28	**0.3738** ±0	0.4061 ±0	0.3987 ±0.105	0.4055 ±0	0.4136 ±2.52	**0.3946** ±0	0.3651 ±0	0.3664 ±0	**0.3649** ±0	0.3922 ±3.79	0.3661 ±0
	720	0.4573 ±0	0.4788 ±0	**0.4571** ±0	0.4679 ±1.07	0.4581 ±0	0.4662 ±0	0.4815 ±0	0.4660 ±0	0.5334 ±1.09	**0.4634** ±0	0.4740 ±0	0.4899 ±0.356	0.4737 ±0	0.5385 ±5.06	**0.4637** ±0	0.4482 ±0	0.4628 ±0	**0.4480** ±0	0.5014 ±20.6	0.4492 ±0
ETTm1	96	0.3923 ±0	0.3849 ±0	0.3918 ±0	0.3862 ±0.466	**0.3750** ±0	0.3946 ±0	0.3896 ±0	0.3942 ±0	0.3932 ±0.713	**0.3777** ±0	0.4073 ±0	0.3974 ±0	0.4062 ±0	0.3919 ±0.325	**0.3888** ±0	0.4099 ±0	0.4065 ±0	0.4096 ±0	0.3976 ±0.420	**0.3898** ±0
	192	0.4297 ±0	0.4227 ±0	0.4292 ±0	0.4256 ±0.864	**0.4182** ±0	0.4306 ±0	0.4262 ±0	0.4303 ±0	0.4333 ±0.278	**0.4185** ±0	0.4399 ±0	0.4351 ±0	0.4394 ±0	0.4401 ±0.979	**0.4240** ±0	0.4453 ±0	0.4405 ±0	0.4443 ±0	0.4422 ±0.451	**0.4290** ±0
	336	0.4713 ±0	0.4644 ±0	0.4707 ±0	0.4684 ±0.712	**0.4618** ±0	0.4709 ±0	0.4672 ±0	0.4705 ±0	0.4785 ±1.91	**0.4617** ±0	0.4839 ±0	0.4751 ±0	0.4828 ±0	0.4830 ±0.735	**0.4667** ±0	0.4797 ±0	0.4751 ±0	0.4790 ±0	0.4780 ±0.550	**0.4681** ±0
	720	0.5281 ±0	0.5264 ±0	0.5272 ±0	0.5301 ±0.731	**0.5208** ±0	0.5263 ±0	0.5282 ±0	0.5255 ±0	0.5559 ±1.71	**0.5179** ±0	0.5491 ±0	0.5446 ±0	0.5477 ±0.104	0.5670 ±0.636	**0.5265** ±0	0.5374 ±0	0.5324 ±0	0.5358 ±0	0.5370 ±1.47	**0.5257** ±0
ETTm2	96	0.2346 ±0	0.2338 ±0	0.2346 ±0	0.2346 ±0.236	**0.2300** ±0	0.2318 ±0	0.2307 ±0	0.2317 ±0	0.2319 ±0.233	**0.2269** ±0	0.2367 ±0	0.2347 ±0	0.2364 ±0	0.2363 ±0.467	**0.2290** ±0	0.2306 ±0	0.2302 ±0	0.2305 ±0	0.2316 ±0.477	**0.2287** ±0
	192	0.2615 ±0	0.2607 ±0	0.2614 ±0	0.2615 ±0.212	**0.2579** ±0	0.2616 ±0	0.2603 ±0	0.2614 ±0	0.2639 ±1.23	**0.2571** ±0	0.2774 ±0	0.2740 ±0	0.2770 ±0	0.2746 ±0.342	**0.2645** ±0	0.2670 ±0	0.2666 ±0	0.2669 ±0	0.2687 ±0.297	**0.2639** ±0
	336	0.2907 ±0	0.2907 ±0	0.2906 ±0	0.2911 ±0.468	**0.2890** ±0	0.2910 ±0	0.2897 ±0	0.2909 ±0	0.2962 ±0.206	**0.2871** ±0	0.3064 ±0	0.3044 ±0.114	0.3058 ±0	0.3118 ±1.61	**0.2955** ±0	0.2985 ±0	0.2989 ±0	0.2984 ±0	0.3049 ±0.775	**0.2945** ±0
	720	0.3399 ±0	0.3431 ±0	0.3397 ±0	0.3436 ±0.690	**0.3362** ±0	0.3398 ±0	0.3407 ±0	0.3394 ±0	0.3586 ±2.47	**0.3334** ±0	0.3649 ±0	0.3625 ±0	0.3640 ±0	0.3871 ±4.57	**0.3495** ±0	0.3515 ±0	0.3527 ±0	0.3501 ±0	0.3550 ±2.92	**0.3419** ±0
Weather	96	0.2382 ±0	0.2376 ±0	0.2380 ±0	0.2387 ±0.350	**0.2186** ±0	0.2279 ±0	0.2272 ±0	0.2276 ±0	0.2326 ±0.749	**0.2141** ±0	0.2122 ±0	0.2133 ±0	0.2120 ±0.106	0.2216 ±1.39	**0.2069** ±0	0.2182 ±0	0.2200 ±0	0.2182 ±0	0.2314 ±0.812	**0.2107** ±0
	192	0.2751 ±0	0.2740 ±0	0.2748 ±0	0.2751 ±0.773	**0.2604** ±0	0.2668 ±0	0.2654 ±0	0.2664 ±0	0.2700 ±0.101	**0.2567** ±0	0.2603 ±0	0.2592 ±0	0.2596 ±0	0.2671 ±0.887	**0.2543** ±0	0.2605 ±0	0.2629 ±0	0.2604 ±0	0.2730 ±3.88	**0.2555** ±0
	336	0.3131 ±0	0.3113 ±0	0.3125 ±0	0.3123 ±0.941	**0.3002** ±0	0.3068 ±0	0.3044 ±0	0.3061 ±0	0.3146 ±1.65	**0.2975** ±0	0.3042 ±0	0.3021 ±0	0.3037 ±0	0.3132 ±1.89	**0.2970** ±0	0.3024 ±0	0.3058 ±0	0.3019 ±0	0.3173 ±1.41	**0.2959** ±0
	720	0.3664 ±0	0.3756 ±0	0.3657 ±0	0.3725 ±1.38	**0.3627** ±0	0.3622 ±0	0.3704 ±0	0.3614 ±0	0.3897 ±1.01	**0.3602** ±0	0.3616 ±0	0.3682 ±0	0.3611 ±0.128	0.3838 ±3.47	**0.3580** ±0	0.3580 ±0	0.3684 ±0	**0.3565** ±0	0.3692 ±2.00	0.3573 ±0
Exchange	96	0.2287 ±0	0.2283 ±0	0.2286 ±0	0.2282 ±0.325	**0.2151** ±0	0.2105 **0.2099** ±0	0.2104 ±0	0.2118 ±1.80	0.2125 ±0	0.2197 ±0	0.2214 ±0	0.2197 ±0	0.2289 ±2.14	**0.2179** ±0	0.2163 **0.2149** ±0	0.2162 ±0	0.2157 ±1.01	0.2153 ±0		
	192	0.3334 ±0	0.3326 ±0	0.3334 ±0	0.3330 ±0.397	**0.3232** ±0	0.3182 **0.3170** ±0	0.3181 ±0	0.3207 ±0.410	0.3203 ±0	0.3310 ±0	0.3304 ±0.103	0.3309 ±0	0.3366 ±1.70	**0.3259** ±0	0.3289 ±0	0.3253 ±0	0.3288 ±0	0.3270 ±1.20	**0.3246** ±0	
	336	0.4527 ±0	0.4498 ±0	0.4526 ±0	0.4514 ±1.68	**0.4420** ±0	0.4448 ±0	0.4414 ±0	0.4447 ±0	0.4435 ±1.61	**0.4400** ±0	0.4564 ±0	0.4548 ±0.222	0.4563 ±0	0.4587 ±1.33	**0.4489** ±0	0.4548 ±0	0.4473 ±0	0.4547 ±0	**0.4357** ±0	0.4452 ±0

Table B6: MAE by dataset and forecast horizon, grouped by backbone and adaptation method, in the Level scenario (SD values $\times 10^{-3}$).

Dataset	H	DLinear					FreTS					iTransformer					PatchTST				
		Frozen	TAFAS	PETSA	DynaTTA	MATE	Frozen	TAFAS	PETSA	DynaTTA	MATE	Frozen	TAFAS	PETSA	DynaTTA	MATE	Frozen	TAFAS	PETSA	DynaTTA	MATE
ETTh1	96	0.4660 ± 1.16	0.4623 ± 1.22	0.4659 ± 1.19	0.4628 ± 1.50	**0.4591** ± 1.57	0.4508 ± 1.12	0.4480 ± 1.25	0.4507 ± 1.16	0.4572 ± 1.65	**0.4447** ± 1.56	0.4608 ± 1.03	0.4565 ± 0.982	0.4605 ± 1.08	0.4636 ± 0.904	**0.4531** ± 0.765	0.4571 ± 1.75	0.4533 ± 2.29	0.4569 ± 1.82	0.4528 ± 3.49	**0.4519** ± 1.79
	192	0.5040 ± 2.98	0.4986 ± 1.73	0.5037 ± 2.96	0.5013 ± 1.94	**0.4968** ± 2.66	0.4935 ± 3.11	0.4891 ± 2.13	0.4933 ± 3.08	0.5012 ± 0.913	**0.4854** ± 2.83	0.5020 ± 2.79	0.4974 ± 2.05	0.5017 ± 2.80	0.5090 ± 3.84	**0.4931** ± 2.00	0.4962 ± 3.77	0.4934 ± 4.95	0.4960 ± 3.83	0.4959 ± 5.82	**0.4901** ± 3.52
	336	0.5374 ± 7.31	0.5342 ± 1.99	0.5371 ± 7.26	0.5358 ± 1.87	**0.5313** ± 3.04	0.5303 ± 7.37	0.5278 ± 2.36	0.5300 ± 7.27	0.5473 ± 4.65	**0.5220** ± 4.87	0.5397 ± 7.29	0.5378 ± 2.63	0.5394 ± 7.26	0.5567 ± 2.48	**0.5309** ± 3.57	0.5377 ± 8.68	0.5388 ± 8.85	0.5375 ± 8.68	0.5411 ± 7.47	**0.5308** ± 6.27
	720	0.6376 ± 22.5	**0.6289** ± 5.41	0.6370 ± 22.0	0.6312 ± 7.97	0.6342 ± 10.2	0.6419 ± 22.6	**0.6336** ± 5.21	0.6413 ± 22.1	0.6628 ± 23.5	0.6349 ± 15.4	0.6411 ± 23.0	0.6345 ± 5.44	0.6406 ± 22.5	0.6696 ± 17.9	**0.6344** ± 12.3	0.6467 ± 24.2	0.6584 ± 26.6	0.6463 ± 24.1	0.6745 ± 32.6	**0.6391** ± 18.5
ETTh2	96	0.2897 ± 2.15	**0.2880** ± 1.70	0.2896 ± 2.15	0.2894 ± 1.30	0.2908 ± 1.97	0.2947 ± 1.63	0.2932 ± 1.42	0.2946 ± 1.63	0.2950 ± 1.98	**0.2904** ± 1.94	0.3091 ± 2.86	0.3054 ± 2.33	0.3088 ± 2.86	0.3067 ± 1.99	**0.3009** ± 2.78	0.2916 ± 2.58	**0.2908** ± 2.30	0.2915 ± 2.58	0.2926 ± 2.80	0.2912 ± 2.42
	192	0.3246 ± 2.13	**0.3214** ± 2.25	0.3244 ± 2.14	0.3233 ± 1.22	0.3234 ± 2.68	0.3299 ± 2.11	0.3266 ± 2.36	0.3297 ± 2.10	0.3281 ± 4.76	**0.3247** ± 2.67	0.3384 ± 4.17	0.3348 ± 3.30	0.3382 ± 4.19	0.3371 ± 3.59	**0.3317** ± 4.06	0.3269 ± 2.53	**0.3218** ± 1.21	0.3264 ± 2.49	0.3253 ± 1.88	0.3219 ± 2.27
	336	0.3514 ± 2.87	**0.3473** ± 5.16	0.3511 ± 2.91	0.3496 ± 4.16	0.3496 ± 4.80	0.3579 ± 3.14	**0.3522** ± 5.24	0.3576 ± 3.16	0.3565 ± 8.26	0.3528 ± 4.38	0.3885 ± 3.05	0.3726 ± 5.17	0.3876 ± 3.04	0.3798 ± 11.3	**0.3722** ± 4.11	0.3466 ± 2.96	**0.3437** ± 2.45	0.3462 ± 2.89	0.3522 ± 1.14	0.3441 ± 3.14
	720	0.4115 ± 10.7	0.4106 ± 16.6	0.4110 ± 10.7	0.4131 ± 16.8	**0.4050** ± 14.7	0.4208 ± 11.7	0.4161 ± 17.9	0.4205 ± 11.7	0.4458 ± 38.2	**0.4121** ± 14.1	0.4258 ± 9.48	0.4194 ± 15.2	0.4253 ± 9.45	0.4504 ± 27.0	**0.4109** ± 12.7	0.4022 ± 9.25	0.4030 ± 12.8	0.4018 ± 9.26	0.4121 ± 2.77	**0.3966** ± 11.7
ETTm1	96	0.3918 ± 0.633	0.3813 ± 0.325	0.3912 ± 0.560	0.3818 ± 0.718	**0.3728** ± 0.719	0.3942 ± 0.652	0.3890 ± 0.532	0.3938 ± 0.611	0.3897 ± 1.67	**0.3764** ± 0.740	0.4067 ± 0.751	0.3977 ± 0.810	0.4058 ± 0.698	0.3875 ± 1.16	**0.3867** ± 0.781	0.4091 ± 0.663	0.4044 ± 0.186	0.4088 ± 0.597	0.3963 ± 1.25	**0.3872** ± 1.22
	192	0.4283 ± 1.03	0.4163 ± 0.761	0.4275 ± 0.888	0.4191 ± 0.411	**0.4136** ± 0.706	0.4291 ± 1.09	0.4237 ± 0.948	0.4288 ± 1.06	0.4266 ± 1.56	**0.4159** ± 0.832	0.4381 ± 1.04	0.4322 ± 1.45	0.4376 ± 1.05	0.4331 ± 1.75	**0.4198** ± 1.43	0.4438 ± 1.30	0.4383 ± 1.23	0.4431 ± 1.31	0.4401 ± 2.49	**0.4269** ± 1.03
	336	0.4680 ± 1.50	**0.4537** ± 1.27	0.4669 ± 1.36	0.4593 ± 0.658	0.4541 ± 1.31	0.4673 ± 1.66	0.4609 ± 1.44	0.4669 ± 1.62	0.4681 ± 0.763	**0.4565** ± 1.13	0.4801 ± 1.58	0.4689 ± 1.62	0.4790 ± 1.57	0.4721 ± 3.09	**0.4619** ± 1.33	0.4758 ± 1.55	0.4678 ± 0.546	0.4751 ± 1.43	0.4731 ± 3.80	**0.4620** ± 1.33
	720	0.5192 ± 1.60	**0.5066** ± 3.28	0.5173 ± 1.33	0.5136 ± 6.65	0.5068 ± 2.71	0.5168 ± 2.00	0.5129 ± 3.08	0.5160 ± 1.86	0.5319 ± 9.92	**0.5065** ± 2.43	0.5387 ± 1.77	0.5269 ± 3.90	0.5369 ± 1.66	0.5448 ± 10.9	**0.5131** ± 2.91	0.5278 ± 1.71	0.5176 ± 2.50	0.5258 ± 1.56	0.5237 ± 3.19	**0.5119** ± 3.18
ETTm2	96	0.2354 ± 0.382	0.2341 ± 0.444	0.2353 ± 0.379	0.2348 ± 0.343	**0.2306** ± 0.633	0.2325 ± 0.377	0.2313 ± 0.525	0.2324 ± 0.384	0.2325 ± 0.641	**0.2276** ± 0.568	0.2369 ± 0.302	0.2347 ± 0.601	0.2366 ± 0.297	0.2356 ± 1.56	**0.2292** ± 0.643	0.2313 ± 0.461	0.2306 ± 0.275	0.2312 ± 0.438	0.2313 ± 0.789	**0.2292** ± 0.602
	192	0.2622 ± 0.689	0.2606 ± 0.914	0.2622 ± 0.693	0.2618 ± 0.770	**0.2584** ± 1.23	0.2621 ± 0.640	0.2601 ± 0.885	0.2619 ± 0.642	0.2626 ± 2.12	**0.2572** ± 0.982	0.2778 ± 0.738	0.2733 ± 0.945	0.2773 ± 0.803	0.2726 ± 1.79	**0.2639** ± 1.08	0.2676 ± 0.787	0.2659 ± 0.429	0.2673 ± 0.698	0.2660 ± 1.00	**0.2640** ± 0.998
	336	0.2902 ± 0.663	0.2883 ± 2.15	0.2900 ± 0.692	0.2890 ± 1.35	**0.2875** ± 2.32	0.2903 ± 0.656	0.2873 ± 2.12	0.2900 ± 0.679	0.2926 ± 4.67	**0.2854** ± 1.91	0.3056 ± 1.05	0.3016 ± 2.45	0.3050 ± 1.06	0.3054 ± 2.54	**0.2931** ± 2.00	0.2977 ± 0.818	0.2961 ± 0.917	0.2974 ± 0.707	0.2994 ± 0.954	**0.2927** ± 2.19
	720	0.3329 ± 1.09	0.3318 ± 6.06	0.3325 ± 1.14	0.3337 ± 5.47	**0.3273** ± 4.52	0.3327 ± 1.16	0.3294 ± 6.15	0.3322 ± 1.20	0.3435 ± 10.7	**0.3246** ± 4.30	0.3577 ± 0.790	0.3497 ± 7.38	0.3566 ± 0.860	0.3716 ± 17.5	**0.3397** ± 4.37	0.3449 ± 1.06	0.3408 ± 3.36	0.3428 ± 1.18	0.3416 ± 3.32	**0.3326** ± 4.72
Weather	96	0.2372 ± 0.414	0.2369 ± 0.684	0.2370 ± 0.420	0.2389 ± 0.989	**0.2194** ± 0.875	0.2269 ± 0.428	0.2269 ± 0.765	0.2266 ± 0.443	0.2331 ± 1.35	**0.2145** ± 0.827	0.2110 ± 0.260	0.2125 ± 0.701	0.2104 ± 0.431	0.2239 ± 1.10	**0.2061** ± 0.186	0.2171 ± 0.437	0.2203 ± 0.588	0.2171 ± 0.446	0.2346 ± 2.70	**0.2107** ± 0.911
	192	0.2738 ± 0.627	0.2733 ± 0.938	0.2736 ± 0.621	0.2754 ± 2.18	**0.2610** ± 1.14	0.2656 ± 0.647	0.2648 ± 1.11	0.2653 ± 0.657	0.2700 ± 1.95	**0.2569** ± 0.986	0.2589 ± 0.619	0.2585 ± 0.864	0.2582 ± 0.570	0.2684 ± 1.82	**0.2535** ± 0.987	0.2595 ± 0.707	0.2636 ± 0.941	0.2595 ± 0.715	0.2772 ± 6.07	**0.2550** ± 0.671
	336	0.3116 ± 1.05	0.3106 ± 1.58	0.3110 ± 1.14	0.3116 ± 1.79	**0.3003** ± 2.00	0.3052 ± 1.06	0.3037 ± 1.72	0.3046 ± 1.13	0.3137 ± 5.03	**0.2970** ± 1.93	0.3027 ± 0.980	0.3017 ± 1.60	0.3020 ± 1.08	0.3129 ± 3.37	**0.2959** ± 1.64	0.3009 ± 1.14	0.3079 ± 1.47	0.3006 ± 1.10	0.3212 ± 1.32	**0.2945** ± 1.95
	720	0.3629 ± 1.96	0.3725 ± 4.21	0.3622 ± 2.10	0.3695 ± 4.34	**0.3616** ± 4.57	0.3585 ± 2.02	0.3673 ± 4.22	**0.3578** ± 2.10	0.3897 ± 6.77	0.3584 ± 4.30	0.3579 ± 2.01	0.3660 ± 3.54	0.3574 ± 2.03	0.3788 ± 1.15	**0.3557** ± 4.04	0.3544 ± 2.10	0.3745 ± 1.81	**0.3537** ± 2.05	0.3708 ± 5.37	0.3541 ± 4.96
Exchange	96	0.2201 ± 4.20	0.2198 ± 3.72	0.2201 ± 4.20	0.2196 ± 4.48	**0.2085** ± 3.63	0.2071 ± 2.05	**0.2062** ± 1.82	0.2071 ± 2.05	0.2073 ± 3.87	0.2082 ± 2.92	0.2154 ± 3.12	0.2163 ± 3.29	0.2154 ± 3.12	0.2218 ± 1.70	**0.2134** ± 3.79	0.2104 ± 2.48	**0.2083** ± 2.28	0.2103 ± 2.48	0.2102 ± 1.00	0.2093 ± 1.94
	192	0.3143 ± 9.76	0.3133 ± 9.37	0.3143 ± 9.76	0.3133 ± 9.69	**0.3062** ± 9.40	0.3045 ± 7.40	**0.3028** ± 7.13	0.3044 ± 7.40	0.3056 ± 7.10	0.3041 ± 8.67	0.3147 ± 9.08	0.3122 ± 8.91	0.3145 ± 9.11	0.3155 ± 10.2	**0.3070** ± 8.16	0.3177 ± 6.74	0.3122 ± 6.63	0.3176 ± 6.74	0.3138 ± 4.71	**0.3101** ± 7.17
	336	0.4310 ± 18.6	0.4278 ± 18.6	0.4309 ± 18.6	0.4296 ± 19.7	**0.4224** ± 17.6	0.4279 ± 16.7	0.4237 ± 16.7	0.4279 ± 16.7	0.4247 ± 23.0	**0.4227** ± 17.3	0.4390 ± 18.9	0.4367 ± 19.3	0.4388 ± 18.9	0.4373 ± 17.7	**0.4315** ± 18.9	0.4400 ± 16.6	0.4290 ± 16.2	0.4399 ± 16.6	**0.4125** ± 10.5	0.4294 ± 16.9

Table B7: MAE by dataset and forecast horizon, grouped by backbone and adaptation method, in the Dynamic scenario (SD values $\times 10^{-3}$).

Dataset	H	DLinear					FreTS					iTransformer					PatchTST				
		Frozen	TAFAS	PETSA	DynaTTA	MATE	Frozen	TAFAS	PETSA	DynaTTA	MATE	Frozen	TAFAS	PETSA	DynaTTA	MATE	Frozen	TAFAS	PETSA	DynaTTA	MATE
ETTh1	96	0.4717 ± 2.08	0.4674 ± 2.31	0.4716 ± 2.10	0.4683 ± 4.01	**0.4648** ± 2.51	0.4570 ± 2.02	0.4537 ± 2.21	0.4569 ± 2.05	0.4620 ± 2.05	**0.4501** ± 2.23	0.4667 ± 2.09	0.4621 ± 2.17	0.4664 ± 2.13	0.4659 ± 3.25	**0.4591** ± 2.18	0.4625 ± 1.94	0.4577 ± 2.47	0.4623 ± 2.00	**0.4559** ± 3.66	0.4570 ± 2.12
	192	0.5081 ± 2.54	0.5016 ± 2.94	0.5078 ± 2.56	0.5063 ± 6.63	**0.5009** ± 3.03	0.4977 ± 2.45	0.4925 ± 2.80	0.4975 ± 2.47	0.5045 ± 3.39	**0.4887** ± 2.71	0.5060 ± 2.79	0.5003 ± 3.09	0.5057 ± 2.80	0.5081 ± 1.15	**0.4964** ± 3.08	0.4999 ± 2.74	0.4943 ± 4.22	0.4995 ± 2.80	0.4973 ± 5.03	**0.4932** ± 2.90
	336	0.5388 ± 2.74	0.5353 ± 3.88	0.5385 ± 2.79	0.5419 ± 5.52	**0.5340** ± 4.35	0.5315 ± 2.70	0.5292 ± 3.76	0.5312 ± 2.70	0.5520 ± 4.46	**0.5231** ± 3.36	0.5408 ± 3.18	0.5389 ± 4.10	0.5405 ± 3.21	0.5589 ± 8.37	**0.5325** ± 3.70	0.5392 ± 2.85	0.5368 ± 5.95	0.5389 ± 2.94	0.5401 ± 6.77	**0.5328** ± 3.59
	720	0.6266 ± 3.77	**0.6182** ± 5.93	0.6260 ± 4.00	0.6247 ± 4.31	0.6238 ± 5.50	0.6309 ± 3.91	**0.6234** ± 6.19	0.6304 ± 4.13	0.6248 ± 7.16	0.6238 ± 5.06	0.6319 ± 3.53	0.6250 ± 6.36	0.6314 ± 3.75	0.6360 ± 8.99	**0.6246** ± 5.08	0.6361 ± 5.05	0.6338 ± 12.3	0.6354 ± 5.38	0.6454 ± 18.3	**0.6272** ± 5.44
ETTh2	96	0.2997 ± 2.71	**0.2978** ± 2.71	0.2997 ± 2.69	0.2995 ± 2.93	0.2999 ± 3.52	0.3046 ± 2.94	0.3030 ± 2.80	0.3045 ± 2.92	0.3043 ± 3.82	**0.2997** ± 3.48	0.3183 ± 2.36	0.3146 ± 2.28	0.3180 ± 2.40	0.3155 ± 4.24	**0.3102** ± 2.81	0.3019 ± 2.90	**0.3011** ± 2.84	0.3019 ± 2.89	0.3025 ± 3.11	0.3014 ± 3.50
	192	0.3359 ± 3.60	**0.3322** ± 3.88	0.3357 ± 3.61	0.3343 ± 5.38	0.3327 ± 4.41	0.3412 ± 3.67	0.3377 ± 3.88	0.3410 ± 3.68	0.3381 ± 2.43	**0.3350** ± 4.09	0.3496 ± 2.88	0.3455 ± 3.31	0.3495 ± 2.88	0.3472 ± 4.50	**0.3418** ± 3.11	0.3385 ± 3.69	0.3331 ± 3.63	0.3382 ± 3.67	0.3358 ± 5.84	**0.3321** ± 4.27
	336	0.3611 ± 3.07	**0.3541** ± 3.78	0.3608 ± 3.07	0.3576 ± 3.96	0.3556 ± 3.84	0.3670 ± 2.99	**0.3592** ± 3.72	0.3668 ± 2.99	0.3593 ± 4.54	0.3598 ± 3.44	0.3966 ± 2.13	0.3782 ± 2.85	0.3958 ± 2.08	**0.3762** ± 8.17	0.3771 ± 2.63	0.3568 ± 3.28	0.3533 ± 2.91	0.3566 ± 3.25	0.3613 ± 3.64	**0.3511** ± 3.76
	720	0.4077 ± 3.99	**0.3915** ± 5.61	0.4071 ± 4.00	0.4003 ± 5.60	0.3931 ± 4.43	0.4172 ± 4.12	**0.3979** ± 5.94	0.4167 ± 4.14	0.3984 ± 4.15	0.4028 ± 4.22	0.4242 ± 4.35	0.4039 ± 5.24	0.4235 ± 4.39	0.4049 ± 5.15	**0.4026** ± 4.27	0.3986 ± 4.41	0.3959 ± 3.78	0.3983 ± 4.39	0.4037 ± 3.60	**0.3867** ± 4.89
ETTm1	96	0.3995 ± 2.00	0.3883 ± 1.84	0.3989 ± 2.00	0.3888 ± 1.91	**0.3800** ± 2.03	0.4023 ± 1.75	0.3968 ± 1.82	0.4020 ± 1.78	0.3957 ± 1.48	**0.3846** ± 1.88	0.4148 ± 1.90	0.4060 ± 1.76	0.4139 ± 1.94	**0.3936** ± 1.76	0.3958 ± 1.87	0.4175 ± 1.78	0.4122 ± 1.78	0.4171 ± 1.82	0.4028 ± 0.448	**0.3950** ± 1.99
	192	0.4347 ± 2.28	0.4213 ± 2.21	0.4340 ± 2.33	0.4245 ± 3.23	**0.4193** ± 2.65	0.4360 ± 2.09	0.4299 ± 2.25	0.4357 ± 2.10	0.4316 ± 2.62	**0.4225** ± 2.42	0.4438 ± 2.32	0.4375 ± 2.26	0.4433 ± 2.36	0.4356 ± 3.02	**0.4262** ± 2.55	0.4511 ± 1.88	0.4446 ± 1.89	0.4503 ± 1.91	0.4449 ± 1.17	**0.4346** ± 2.09
	336	0.4740 ± 2.41	**0.4568** ± 2.76	0.4727 ± 2.40	0.4631 ± 4.21	0.4575 ± 3.34	0.4737 ± 2.31	0.4655 ± 2.90	0.4731 ± 2.30	0.4703 ± 4.24	**0.4616** ± 2.75	0.4864 ± 2.48	0.4737 ± 3.02	0.4853 ± 2.48	0.4753 ± 2.89	**0.4678** ± 2.79	0.4822 ± 2.16	0.4724 ± 2.41	0.4814 ± 2.20	0.4756 ± 2.16	**0.4672** ± 2.62
	720	0.5242 ± 2.91	**0.5049** ± 3.72	0.5220 ± 2.96	0.5132 ± 2.74	0.5078 ± 3.86	0.5218 ± 2.88	0.5126 ± 3.96	0.5207 ± 3.03	0.5298 ± 8.36	**0.5092** ± 3.79	0.5436 ± 2.73	0.5243 ± 4.40	0.5412 ± 2.90	0.5378 ± 4.73	**0.5146** ± 4.03	0.5331 ± 2.49	0.5175 ± 3.90	0.5305 ± 2.72	0.5227 ± 2.40	**0.5144** ± 3.24
ETTm2	96	0.2453 ± 1.71	0.2437 ± 1.76	0.2453 ± 1.72	0.2451 ± 1.98	**0.2399** ± 1.82	0.2424 ± 1.65	0.2410 ± 1.66	0.2422 ± 1.66	0.2414 ± 2.10	**0.2370** ± 1.78	0.2460 ± 1.79	0.2438 ± 1.79	0.2456 ± 1.80	0.2434 ± 2.05	**0.2386** ± 1.85	0.2406 ± 1.82	0.2400 ± 1.78	0.2405 ± 1.82	0.2407 ± 1.70	**0.2382** ± 1.97
	192	0.2710 ± 2.27	0.2688 ± 2.31	0.2709 ± 2.28	0.2701 ± 2.30	**0.2665** ± 2.48	0.2708 ± 2.33	0.2684 ± 2.38	0.2707 ± 2.34	0.2701 ± 1.29	**0.2652** ± 2.49	0.2833 ± 2.55	0.2792 ± 2.59	0.2830 ± 2.55	0.2785 ± 2.46	**0.2708** ± 2.54	0.2747 ± 2.40	0.2733 ± 2.32	0.2744 ± 2.41	0.2735 ± 2.38	**0.2708** ± 2.54
	336	0.2989 ± 3.34	0.2959 ± 3.49	0.2987 ± 3.30	0.2966 ± 3.53	**0.2957** ± 3.75	0.2992 ± 3.33	0.2951 ± 3.43	0.2989 ± 3.31	0.2985 ± 3.80	**0.2934** ± 3.60	0.3114 ± 3.48	0.3068 ± 3.40	0.3110 ± 3.48	0.3099 ± 2.76	**0.3000** ± 3.38	0.3048 ± 3.61	0.3037 ± 3.58	0.3046 ± 3.64	0.3073 ± 3.77	**0.2987** ± 3.68
	720	0.3447 ± 5.96	0.3396 ± 6.79	0.3440 ± 6.02	0.3426 ± 7.45	**0.3379** ± 6.25	0.3448 ± 5.81	0.3373 ± 6.45	0.3440 ± 5.89	0.3445 ± 7.08	**0.3342** ± 5.61	0.3689 ± 5.44	0.3551 ± 6.94	0.3675 ± 5.67	0.3676 ± 3.64	**0.3480** ± 5.85	0.3555 ± 5.75	0.3519 ± 5.88	0.3532 ± 5.78	0.3519 ± 5.20	**0.3405** ± 5.85
Weather	96	0.2506 ± 2.15	0.2491 ± 1.96	0.2505 ± 2.13	0.2510 ± 1.46	**0.2443** ± 1.86	0.2423 ± 2.10	0.2406 ± 1.77	0.2420 ± 2.09	0.2456 ± 0.687	**0.2371** ± 1.78	0.2327 ± 2.08	0.2296 ± 1.94	0.2321 ± 2.05	0.2367 ± 3.41	**0.2277** ± 1.89	0.2380 ± 2.13	0.2391 ± 2.08	0.2380 ± 2.12	0.2469 ± 3.97	**0.2333** ± 2.01
	192	0.2865 ± 2.44	0.2835 ± 2.03	0.2862 ± 2.45	0.2861 ± 2.25	**0.2808** ± 2.14	0.2802 ± 2.43	0.2767 ± 1.99	0.2798 ± 2.43	0.2812 ± 2.53	**0.2749** ± 1.94	0.2764 ± 2.50	0.2725 ± 2.12	0.2759 ± 2.53	0.2790 ± 2.03	**0.2718** ± 2.08	0.2787 ± 2.36	0.2794 ± 2.25	0.2785 ± 2.36	0.2857 ± 2.88	**0.2733** ± 2.30
	336	0.3244 ± 2.88	0.3193 ± 2.10	0.3237 ± 2.95	0.3217 ± 1.62	**0.3167** ± 1.95	0.3197 ± 2.84	0.3139 ± 2.08	0.3190 ± 2.92	0.3218 ± 2.23	**0.3127** ± 1.75	0.3203 ± 3.01	0.3130 ± 2.28	0.3192 ± 3.10	0.3221 ± 4.27	**0.3125** ± 2.06	0.3185 ± 2.75	0.3187 ± 2.25	0.3178 ± 2.68	0.3277 ± 3.55	**0.3116** ± 2.08
	720	0.3765 ± 3.73	0.3777 ± 2.09	0.3756 ± 3.71	0.3775 ± 3.31	**0.3745** ± 3.36	0.3736 ± 3.62	0.3736 ± 1.90	0.3726 ± 3.54	0.3887 ± 3.13	**0.3714** ± 3.26	0.3774 ± 3.92	0.3749 ± 2.39	0.3761 ± 3.86	0.3863 ± 2.41	**0.3692** ± 2.74	0.3719 ± 3.44	0.3804 ± 0.844	0.3704 ± 3.16	0.3821 ± 1.37	**0.3684** ± 2.56
Exchange	96	0.2321 ± 6.78	0.2294 ± 7.48	0.2320 ± 6.85	0.2304 ± 7.63	**0.2283** ± 6.15	0.2223 ± 5.65	0.2191 ± 5.99	0.2222 ± 5.69	**0.2188** ± 6.77	0.2206 ± 5.57	0.2291 ± 5.16	0.2284 ± 4.62	0.2291 ± 5.15	0.2324 ± 4.37	**0.2283** ± 4.77	0.2296 ± 6.67	0.2256 ± 6.60	0.2294 ± 6.70	**0.2237** ± 4.10	0.2258 ± 6.36
	192	0.3221 ± 8.77	0.3179 ± 9.49	0.3220 ± 8.82	0.3201 ± 8.87	**0.3151** ± 8.77	0.3153 ± 8.56	0.3104 ± 9.15	0.3152 ± 8.60	0.3123 ± 6.58	**0.3088** ± 6.54	0.3251 ± 9.80	0.3194 ± 9.00	0.3250 ± 9.77	0.3207 ± 9.82	**0.3182** ± 8.76	0.3327 ± 11.8	0.3251 ± 11.7	0.3325 ± 11.8	0.3214 ± 9.22	**0.3182** ± 9.30
	336	0.4299 ± 9.85	0.4246 ± 8.90	0.4298 ± 9.82	0.4268 ± 9.83	**0.4222** ± 8.91	0.4294 ± 10.1	0.4233 ± 9.06	0.4293 ± 10.1	**0.4192** ± 11.2	0.4207 ± 9.25	0.4455 ± 16.6	0.4384 ± 15.4	0.4454 ± 16.5	0.4378 ± 12.6	**0.4376** ± 16.6	0.4458 ± 11.9	0.4338 ± 10.9	0.4456 ± 11.9	**0.4116** ± 6.95	0.4343 ± 11.7

Table B8: MAE by dataset and forecast horizon, grouped by backbone and adaptation method, in the Profile scenario (SD values $\times 10^{-3}$).

Dataset	H	DLinear					FreTS					iTransformer					PatchTST				
		Frozen	TAFAS	PETSA	DynaTTA	MATE	Frozen	TAFAS	PETSA	DynaTTA	MATE	Frozen	TAFAS	PETSA	DynaTTA	MATE	Frozen	TAFAS	PETSA	DynaTTA	MATE
ETTh1	96	0.4631 ± 3.63	0.4599 ± 4.22	0.4629 ± 3.66	0.4610 ± 5.20	**0.4570** ± 4.05	0.4481 ± 3.20	0.4457 ± 3.73	0.4480 ± 3.21	0.4523 ± 3.63	**0.4421** ± 3.46	0.4592 ± 2.15	0.4555 ± 3.14	0.4590 ± 2.19	0.4612 ± 5.72	**0.4517** ± 2.94	0.4541 ± 2.31	0.4503 ± 2.71	0.4540 ± 2.34	**0.4477** ± 3.45	0.4490 ± 2.95
	192	0.4985 ± 4.30	0.4951 ± 5.60	0.4983 ± 4.39	0.5016 ± 8.13	**0.4935** ± 5.33	0.4882 ± 3.85	0.4856 ± 5.09	0.4880 ± 3.94	0.4994 ± 6.53	**0.4809** ± 4.57	0.4981 ± 2.98	0.4950 ± 4.29	0.4978 ± 3.04	0.5077 ± 7.46	**0.4906** ± 4.16	0.4908 ± 2.47	0.4874 ± 3.76	0.4906 ± 2.56	0.4897 ± 5.65	**0.4851** ± 3.58
	336	0.5297 ± 5.87	0.5315 ± 7.73	0.5295 ± 5.94	0.5387 ± 7.53	**0.5287** ± 7.92	0.5226 ± 5.43	0.5249 ± 7.28	0.5224 ± 5.51	0.5555 ± 14.2	**0.5163** ± 6.68	0.5337 ± 4.04	0.5365 ± 6.28	0.5336 ± 4.12	0.5648 ± 19.0	**0.5285** ± 5.74	0.5308 ± 3.49	0.5325 ± 5.33	0.5306 ± 3.60	0.5343 ± 7.09	**0.5257** ± 5.32
	720	0.6221 ± 9.31	**0.6199** ± 9.21	0.6216 ± 9.42	0.6254 ± 6.87	0.6227 ± 10.9	0.6267 ± 8.80	0.6252 ± 9.07	0.6263 ± 8.89	0.6301 ± 7.16	**0.6217** ± 10.2	0.6288 ± 6.65	0.6285 ± 7.89	0.6285 ± 6.83	0.6461 ± 9.57	**0.6249** ± 8.60	0.6304 ± 5.72	0.6374 ± 9.26	0.6301 ± 5.87	0.6586 ± 12.2	**0.6245** ± 8.53
ETTh2	96	0.2908 ± 1.75	**0.2890** ± 1.42	0.2907 ± 1.75	0.2903 ± 2.02	0.2913 ± 1.49	0.2952 ± 1.46	0.2938 ± 1.15	0.2951 ± 1.45	0.2949 ± 1.26	**0.2904** ± 1.25	0.3100 ± 2.00	0.3066 ± 1.70	0.3097 ± 1.98	0.3073 ± 1.71	**0.3020** ± 2.04	0.2925 ± 1.68	0.2919 ± 1.69	0.2925 ± 1.67	0.2931 ± 2.03	**0.2918** ± 1.57
	192	0.3250 ± 2.62	**0.3215** ± 1.75	0.3248 ± 2.61	0.3235 ± 2.62	0.3225 ± 1.62	0.3300 ± 2.44	0.3269 ± 1.62	0.3299 ± 2.41	0.3286 ± 1.79	**0.3238** ± 1.85	0.3397 ± 1.91	0.3359 ± 1.36	0.3396 ± 1.88	0.3393 ± 0.554	**0.3319** ± 1.52	0.3278 ± 3.06	0.3235 ± 3.08	0.3274 ± 3.04	0.3278 ± 6.82	**0.3214** ± 2.57
	336	0.3504 ± 4.17	**0.3448** ± 2.19	0.3501 ± 4.11	0.3479 ± 2.78	0.3460 ± 2.34	0.3568 ± 4.03	0.3503 ± 2.28	0.3566 ± 4.00	0.3517 ± 2.20	**0.3501** ± 3.16	0.3882 ± 4.09	0.3720 ± 2.91	0.3874 ± 4.07	0.3729 ± 2.77	**0.3689** ± 4.27	0.3463 ± 3.95	0.3448 ± 4.64	0.3460 ± 3.97	0.3544 ± 6.75	**0.3415** ± 2.67
	720	0.3997 ± 4.49	**0.3867** ± 1.78	0.3991 ± 4.41	0.3947 ± 1.76	0.3875 ± 2.23	0.4101 ± 4.41	**0.3943** ± 1.60	0.4096 ± 4.33	0.3976 ± 6.82	0.3971 ± 3.12	0.4194 ± 3.83	0.4018 ± 1.78	0.4188 ± 3.77	0.4063 ± 10.2	**0.3987** ± 2.39	0.3906 ± 3.99	0.3926 ± 6.50	0.3902 ± 3.97	0.4000 ± 4.36	**0.3800** ± 2.50
ETTm1	96	0.3927 ± 2.78	0.3817 ± 3.02	0.3921 ± 2.81	0.3826 ± 3.80	**0.3739** ± 3.24	0.3956 ± 2.35	0.3903 ± 2.76	0.3953 ± 2.31	0.3896 ± 3.42	**0.3780** ± 2.90	0.4113 ± 2.54	0.4024 ± 1.26	0.4104 ± 2.32	**0.3893** ± 1.72	0.3913 ± 0.113	0.4109 ± 2.05	0.4055 ± 2.65	0.4106 ± 2.05	0.3972 ± 3.49	**0.3900** ± 3.12
	192	0.4278 ± 2.90	0.4149 ± 3.21	0.4271 ± 2.96	0.4192 ± 4.05	**0.4136** ± 3.40	0.4294 ± 2.39	0.4238 ± 2.98	0.4291 ± 2.43	0.4263 ± 4.50	**0.4162** ± 3.13	0.4386 ± 1.68	0.4328 ± 0.932	0.4381 ± 1.57	0.4321 ± 2.93	**0.4215** ± 0.909	0.4445 ± 2.00	0.4386 ± 2.79	0.4438 ± 2.09	0.4386 ± 2.62	**0.4285** ± 2.83
	336	0.4662 ± 3.16	**0.4507** ± 3.62	0.4650 ± 3.21	0.4574 ± 4.79	0.4520 ± 3.67	0.4664 ± 2.55	0.4598 ± 3.52	0.4660 ± 2.61	0.4651 ± 5.96	**0.4552** ± 3.11	0.4830 ± 2.77	0.4703 ± 0.573	0.4817 ± 2.51	0.4706 ± 2.52	**0.4645** ± 1.41	0.4756 ± 1.69	0.4662 ± 3.08	0.4748 ± 1.82	0.4691 ± 3.74	**0.4617** ± 2.48
	720	0.5147 ± 3.84	**0.5016** ± 5.61	0.5127 ± 3.97	0.5087 ± 4.84	0.5026 ± 4.65	0.5134 ± 3.18	0.5098 ± 5.46	0.5125 ± 3.35	0.5245 ± 12.0	**0.5040** ± 4.76	0.5409 ± 2.62	0.5275 ± 2.38	0.5386 ± 2.18	0.5395 ± 8.57	**0.5149** ± 1.63	0.5258 ± 2.08	0.5121 ± 4.78	0.5237 ± 2.45	0.5183 ± 6.40	**0.5103** ± 4.46
ETTm2	96	0.2402 ± 1.53	0.2385 ± 1.39	0.2402 ± 1.52	0.2391 ± 1.18	**0.2345** ± 1.34	0.2367 ± 1.38	0.2353 ± 1.24	0.2365 ± 1.36	0.2354 ± 1.55	**0.2312** ± 1.25	0.2405 ± 2.43	0.2383 ± 1.92	0.2401 ± 2.33	0.2375 ± 1.15	**0.2328** ± 2.06	0.2352 ± 1.70	0.2347 ± 1.75	0.2351 ± 1.70	0.2350 ± 1.33	**0.2328** ± 1.55
	192	0.2654 ± 1.45	0.2631 ± 1.26	0.2653 ± 1.45	0.2641 ± 1.36	**0.2605** ± 1.19	0.2649 ± 1.35	0.2625 ± 1.19	0.2647 ± 1.35	0.2636 ± 0.679	**0.2590** ± 1.22	0.2785 ± 2.17	0.2738 ± 2.11	0.2781 ± 2.13	0.2722 ± 1.85	**0.2643** ± 2.07	0.2693 ± 1.80	0.2682 ± 1.74	0.2691 ± 1.81	0.2682 ± 1.44	**0.2652** ± 1.62
	336	0.2923 ± 1.70	0.2894 ± 1.18	0.2921 ± 1.69	0.2907 ± 0.788	**0.2886** ± 1.44	0.2924 ± 1.74	0.2885 ± 1.26	0.2921 ± 1.73	0.2923 ± 1.27	**0.2863** ± 1.38	0.3057 ± 2.60	0.3008 ± 2.03	0.3053 ± 2.55	0.3030 ± 2.32	**0.2932** ± 2.11	0.2977 ± 2.34	0.2972 ± 2.16	0.2975 ± 2.36	0.3003 ± 1.56	**0.2918** ± 1.56
	720	0.3352 ± 2.77	0.3304 ± 0.982	0.3346 ± 2.71	0.3345 ± 0.918	**0.3285** ± 1.67	0.3355 ± 2.96	0.3286 ± 1.45	0.3348 ± 2.89	0.3364 ± 3.29	**0.3244** ± 1.95	0.3620 ± 4.06	0.3491 ± 1.55	0.3608 ± 3.94	0.3608 ± 4.06	**0.3404** ± 2.40	0.3456 ± 3.14	0.3440 ± 2.57	0.3440 ± 3.07	0.3444 ± 1.18	**0.3313** ± 1.76
Weather	96	0.2462 ± 1.77	0.2448 ± 1.77	0.2460 ± 1.75	0.2453 ± 1.24	**0.2378** ± 1.70	0.2370 ± 1.66	0.2357 ± 1.74	0.2368 ± 1.66	0.2386 ± 2.91	**0.2301** ± 1.47	0.2258 ± 1.47	0.2235 ± 1.21	0.2252 ± 1.40	0.2293 ± 0.619	**0.2213** ± 1.43	0.2312 ± 1.36	0.2330 ± 1.35	0.2312 ± 1.35	0.2413 ± 2.23	**0.2256** ± 1.00
	192	0.2822 ± 2.23	0.2798 ± 2.13	0.2819 ± 2.24	0.2812 ± 2.37	**0.2752** ± 2.01	0.2750 ± 2.17	0.2723 ± 2.02	0.2747 ± 2.18	0.2750 ± 2.08	**0.2692** ± 2.03	0.2705 ± 1.95	0.2671 ± 1.97	0.2699 ± 1.98	0.2725 ± 1.57	**0.2664** ± 1.78	0.2722 ± 2.12	0.2746 ± 2.35	0.2721 ± 2.14	0.2819 ± 2.81	**0.2667** ± 1.65
	336	0.3194 ± 2.93	0.3157 ± 2.86	0.3188 ± 2.97	0.3174 ± 1.40	**0.3117** ± 2.42	0.3139 ± 2.87	0.3097 ± 2.76	0.3132 ± 2.95	0.3171 ± 4.97	**0.3076** ± 2.35	0.3136 ± 2.70	0.3075 ± 2.66	0.3124 ± 2.76	0.3161 ± 4.25	**0.3069** ± 2.39	0.3118 ± 2.84	0.3157 ± 3.41	0.3113 ± 2.92	0.3248 ± 5.43	**0.3056** ± 2.46
	720	0.3717 ± 4.26	0.3770 ± 5.47	**0.3708** ± 4.36	0.3749 ± 5.68	0.3725 ± 3.44	0.3679 ± 4.11	0.3723 ± 5.29	**0.3670** ± 4.24	0.3885 ± 9.36	0.3688 ± 3.26	0.3714 ± 3.73	0.3720 ± 5.33	0.3700 ± 3.77	0.3823 ± 3.32	**0.3665** ± 3.61	0.3657 ± 4.23	0.3800 ± 6.89	**0.3647** ± 4.65	0.3821 ± 12.0	0.3652 ± 3.35
Exchange	96	0.2218 ± 4.67	0.2192 ± 5.17	0.2217 ± 4.68	0.2203 ± 4.46	**0.2150** ± 4.01	0.2112 ± 2.86	**0.2080** ± 3.80	0.2110 ± 2.90	0.2081 ± 3.18	0.2088 ± 4.38	0.2184 ± 2.07	**0.2172** ± 2.95	0.2183 ± 2.03	0.2213 ± 5.59	0.2174 ± 3.32	0.2178 ± 3.23	0.2144 ± 3.80	0.2176 ± 3.27	**0.2130** ± 5.06	0.2137 ± 5.26
	192	0.3157 ± 7.46	0.3117 ± 8.21	0.3156 ± 7.43	0.3139 ± 8.19	**0.3063** ± 8.38	0.3079 ± 5.87	0.3031 ± 7.02	0.3078 ± 5.87	0.3055 ± 7.46	**0.3003** ± 9.57	0.3170 ± 5.25	0.3106 ± 7.29	0.3168 ± 5.19	0.3112 ± 7.14	**0.3095** ± 6.01	0.3231 ± 4.34	0.3160 ± 5.15	0.3229 ± 4.37	0.3121 ± 4.93	**0.3068** ± 8.88
	336	0.4290 ± 6.77	0.4242 ± 6.28	0.4289 ± 6.70	0.4264 ± 5.54	**0.4216** ± 6.97	0.4272 ± 6.10	0.4214 ± 5.79	0.4271 ± 6.04	**0.4188** ± 0.789	0.4196 ± 8.52	0.4439 ± 10.4	0.4366 ± 7.73	0.4437 ± 10.3	**0.4314** ± 9.31	0.4379 ± 12.6	0.4426 ± 5.95	0.4300 ± 6.45	0.4424 ± 5.96	**0.4082** ± 4.92	0.4316 ± 8.65

Table B9: MSE standard deviations for Natural (10^{-3} units; means in Table 1).

Dataset	H	DLinear					FreTS					iTransformer					PatchTST				
		Frozen	TAFAS	PETSA	DynaTTA	MATE	Frozen	TAFAS	PETSA	DynaTTA	MATE	Frozen	TAFAS	PETSA	DynaTTA	MATE	Frozen	TAFAS	PETSA	DynaTTA	MATE
ETTh1	96	0	0	0	2.87	0	0	0	0	0.754	0	0	0	0	0.594	0	0	0	0	0.878	0
	192	0	0	0	4.14	0	0	0	0	0.335	0	0	0	0	1.01	0	0	0	0	0.818	0
	336	0	0	0	2.15	0	0	0	0	0.630	0	0	0	0	4.38	0	0	0	0	0.861	0
	720	0	0	0	3.82	0	0	0	0.117	1.04	0	0	0.123	0.125	1.53	0	0	0.101	0.169	5.15	0
ETTh2	96	0	0	0	0.662	0	0	0	0	0.225	0	0	0	0	0.221	0	0	0	0	0.379	0
	192	0	0	0	1.90	0	0	0	0	2.20	0	0	0	0	0.458	0	0	0	0	1.76	0
	336	0	0	0	1.69	0	0	0	0	1.31	0	0	0.126	0	4.98	0	0	0	0	1.20	0
	720	0	0	0	2.30	0	0	0	0	3.41	0	0	0.167	0	3.96	0	0	0	0	7.95	0
ETTm1	96	0	0	0	1.06	0	0	0	0	0.389	0	0	0	0	1.04	0	0	0	0	0.552	0
	192	0	0	0.122	1.52	0	0	0	0	0.146	0	0	0	0	0.675	0	0	0	0	0.646	0
	336	0	0	0	3.06	0	0	0	0	1.32	0	0	0	0	0.605	0	0	0	0	0.235	0
	720	0	0	0.201	6.95	0	0	0	0.179	5.00	0	0	0.160	0.305	2.21	0	0	0	0.172	1.77	0
ETTm2	96	0	0	0	0.293	0	0	0	0	0.371	0	0	0	0	0.215	0	0	0	0	0.111	0
	192	0	0	0	0.646	0	0	0	0	0.796	0	0	0.132	0.114	0.566	0	0	0	0	0.353	0
	336	0	0	0	0.547	0	0	0	0	0.900	0	0	0.125	0	0.274	0	0	0	0	0.112	0
	720	0	0	0	0.542	0	0	0	0	2.47	0	0	0	0	2.97	0	0	0	0.127	1.76	0
Weather	96	0	0	0	0.721	0	0	0	0	1.05	0	0	0	0.110	1.45	0	0	0	0	0.666	0
	192	0	0	0	1.08	0	0	0	0	0.934	0	0	0	0	0.934	0	0	0	0	3.00	0
	336	0	0	0	2.36	0	0	0	0.110	2.59	0	0	0.109	0	2.38	0	0	0	0	0.549	0
	720	0	0	0	4.35	0	0	0	0.106	3.00	0	0	0.135	0.201	3.01	0	0	0	0.177	2.24	0
Exchange	96	0	0	0	0.408	0	0	0	0	1.69	0	0	0	0	2.15	0	0	0	0	0.752	0
	192	0	0	0	0.978	0	0	0	0	0.794	0	0	0.270	0	1.95	0	0	0	0	0.463	0
	336	0	0	0	2.15	0	0	0	0	9.58	0	0	0.427	0	6.67	0	0	0	0	0	0

Table B10: MSE standard deviations for TTFBench (10^{-3} units; means in Table 2).

Dataset	H	DLinear					FreTS					iTransformer					PatchTST				
		Frozen	TAFAS	PETSA	DynaTTA	MATE	Frozen	TAFAS	PETSA	DynaTTA	MATE	Frozen	TAFAS	PETSA	DynaTTA	MATE	Frozen	TAFAS	PETSA	DynaTTA	MATE
ETTh1	96	0	0	0	1.72	0	0	0	0	1.62	0	0	0	0	1.29	0	0	0	0	1.37	0
	192	0	0	0	3.04	0	0	0	0	2.81	0	0	0	0	3.01	0	0	0	0	2.85	0
	336	0	0	0	2.25	0	0	0	0	5.91	0	0	0	0	7.09	0	0	0	0	2.35	0
	720	0	0	0	12.2	0	0	0	0	19.1	0	0	0.177	0	17.9	0	0	0.222	0	35.1	0
ETTh2	96	0	0	0	0.923	0	0	0	0	0.165	0	0	0	0	0.583	0	0	0	0	0.775	0
	192	0	0	0	1.38	0	0	0	0	2.35	0	0	0	0	1.97	0	0	0	0	5.27	0
	336	0	0	0	1.24	0	0	0	0	4.73	0	0	0.131	0	5.24	0	0	0	0	5.05	0
	720	0	0	0	4.34	0	0	0	0	8.42	0	0	0.563	0	7.64	0	0	0	0	51.2	0
ETTm1	96	0	0	0	0.495	0	0	0	0	0.886	0	0	0.123	0.169	0.720	0	0	0	0	0.846	0
	192	0	0	0	1.16	0	0	0	0	0.264	0	0	0	0	1.12	0	0	0	0	0.583	0
	336	0	0	0	1.09	0	0	0	0	2.25	0	0	0	0.105	0.550	0	0	0	0	0.782	0
	720	0	0	0.114	4.52	0	0	0	0.159	3.15	0	0	0.156	0.277	0.513	0	0	0	0.143	2.34	0
ETTm2	96	0	0	0	0.137	0	0	0	0	0.198	0	0	0	0	0.195	0	0	0	0	0.191	0
	192	0	0	0	0.408	0	0	0	0	1.06	0	0	0.197	0.114	0.757	0	0	0	0	0.480	0
	336	0	0	0	0.600	0	0	0	0	1.09	0	0	0.154	0	1.99	0	0	0	0	1.08	0
	720	0	0	0	1.94	0	0	0	0	2.99	0	0	0	0	7.58	0	0	0	0	5.58	0
Weather	96	0	0	0	0.705	0	0	0	0	0.820	0	0	0	0	0.922	0	0	0	0	0.517	0
	192	0	0	0	1.01	0	0	0	0	0.533	0	0	0	0	0.360	0	0	0	0	2.27	0
	336	0	0	0	1.42	0	0	0	0	2.82	0	0	0	0	2.35	0	0	0	0	0.883	0
	720	0	0	0	5.08	0	0	0	0	2.72	0	0	0	0.212	3.43	0	0	0	0.168	2.09	0
Exchange	96	0	0	0	0.288	0	0	0	0	1.24	0	0	0	0	1.94	0	0	0	0	0.550	0
	192	0	0	0	0.631	0	0	0	0	0.115	0	0	0.145	0	1.83	0	0	0	0	1.05	0
	336	0	0	0	2.23	0	0	0	0	2.43	0	0	0.359	0	3.84	0	0	0	0	0	0

C Additional Ablation Results

The ablations cover ETTh2, ETTm2, and Weather; PatchTST and DLinear; forecast horizons of 96, 336, and 720; and the Natural and Level scenarios, for 36 configurations in total. Each value is the mean across three test seeds. Credit-allocation ablations hold the residual sources fixed and vary only the weight granularity. Uniform uses one fixed weight for all five residual types; Global shares one five-dimensional vector across leads and channels. Lead-only and Channel-only weights vary along their respective axis and are shared along the other. Residual-source ablations remove one candidate type at a time while keeping all other settings unchanged.

C.1 Results by Dataset

Table C1: Credit-allocation ablation MSE averaged by dataset.

Dataset	Uniform	Global	Lead-only	Channel-only	Full MATE
ETTh2	0.2494	0.2468	**0.2466**	0.2471	0.2469
ETTm2	0.1820	0.1798	0.1793	0.1781	**0.1779**
Weather	0.2648	0.2594	0.2582	0.2537	**0.2527**

Full MATE achieves the lowest mean MSE on ETTm2 and Weather. Differences on ETTh2 are smaller, indicating that the benefit of joint allocation depends on the data.

Table C2: Credit-allocation ablation MAE averaged by dataset.

Dataset	Uniform	Global	Lead-only	Channel-only	Full MATE
ETTh2	0.3397	0.3377	**0.3374**	0.3385	0.3382
ETTm2	0.2849	0.2828	0.2821	0.2819	**0.2814**
Weather	0.2895	0.2948	0.2921	0.2880	**0.2864**

Full MATE also achieves the lowest mean MAE on ETTm2 and Weather, with smaller differences on ETTh2, consistent with the MSE results.

C.2 Credit Allocation by Configuration

Uniform weights assign the same fixed strength to all candidate residuals. Global weights share one five-dimensional vector across all leads and channels. Lead-only and channel-only weights vary along one dimension, whereas full MATE distinguishes both. Comparisons within each backbone group isolate the benefit of position-specific credit allocation. The shortened table headings Uniform, Global, Lead-only, and Channel-only refer to these four weight settings.

Table C3: Credit-allocation ablation MSE in the Natural scenario.

Dataset	H	PatchTST					DLinear				
		Uniform	Global	Lead-only	Channel-only	Full MATE	Uniform	Global	Lead-only	Channel-only	Full MATE
ETTh2	96	**0.1807**	0.1825	0.1822	0.1820	0.1817	**0.1788**	0.1798	0.1798	0.1802	0.1802
	336	0.2373	0.2358	0.2354	0.2355	**0.2352**	0.2470	0.2448	0.2442	0.2445	**0.2440**
	720	0.2925	**0.2819**	0.2823	0.2827	0.2829	0.3078	**0.2945**	**0.2945**	0.2974	0.2972
ETTm2	96	0.1170	0.1162	0.1157	0.1158	**0.1153**	0.1210	0.1180	0.1176	0.1174	**0.1170**
	336	0.1863	0.1858	0.1852	0.1828	**0.1827**	0.1808	0.1789	0.1788	**0.1775**	0.1777
	720	0.2398	0.2339	0.2335	0.2314	**0.2312**	0.2353	0.2323	0.2316	0.2296	**0.2294**
Weather	96	0.1666	0.1630	0.1624	0.1587	**0.1584**	0.1844	0.1753	0.1744	0.1658	**0.1657**
	336	0.2627	0.2553	0.2543	0.2503	**0.2497**	0.2764	0.2651	0.2633	0.2563	**0.2552**
	720	0.3360	0.3315	0.3303	0.3295	**0.3280**	0.3474	0.3414	0.3400	0.3374	**0.3360**

Table C4: Credit-allocation ablation MSE in the Level scenario.

Dataset	H	PatchTST					DLinear				
		Uniform	Global	Lead-only	Channel-only	Full MATE	Uniform	Global	Lead-only	Channel-only	Full MATE
ETTh2	96	**0.1859**	0.1880	0.1877	0.1878	0.1876	**0.1837**	0.1854	0.1854	0.1860	0.1860
	336	**0.2512**	0.2525	0.2521	0.2519	0.2516	**0.2617**	0.2628	0.2621	0.2622	**0.2617**
	720	0.3252	0.3201	0.3203	**0.3198**	0.3201	0.3413	0.3332	**0.3331**	0.3354	0.3352
ETTm2	96	0.1184	0.1178	0.1174	0.1174	**0.1170**	0.1223	0.1195	0.1192	0.1190	**0.1186**
	336	0.1897	0.1900	0.1895	0.1878	**0.1876**	0.1845	0.1830	0.1829	**0.1817**	0.1819
	720	0.2466	0.2421	0.2417	0.2403	**0.2398**	0.2423	0.2397	0.2389	0.2368	**0.2364**
Weather	96	0.1680	0.1651	0.1646	0.1610	**0.1607**	0.1861	0.1781	0.1770	0.1686	**0.1684**
	336	0.2672	0.2619	0.2609	0.2571	**0.2562**	0.2809	0.2719	0.2699	0.2633	**0.2619**
	720	0.3454	0.3468	0.3452	0.3442	**0.3421**	0.3570	0.3578	0.3560	0.3525	**0.3502**

Full MATE achieves a mean MSE of 0.2258, lower than all four restricted settings. This supports the overall benefit of joint lead–channel credit allocation.

Table C5: Credit-allocation ablation MAE in the Natural scenario.

Dataset	H	PatchTST					DLinear				
		Uniform	Global	Lead-only	Channel-only	Full MATE	Uniform	Global	Lead-only	Channel-only	Full MATE
ETTh2	96	**0.2859**	0.2871	0.2866	0.2878	0.2872	**0.2851**	0.2854	0.2852	0.2866	0.2864
	336	0.3340	0.3315	**0.3311**	0.3319	0.3316	0.3387	0.3363	**0.3358**	0.3368	0.3363
	720	0.3733	**0.3646**	0.3648	0.3657	0.3658	0.3820	0.3715	**0.3713**	0.3740	0.3737
ETTm2	96	0.2299	0.2287	0.2277	0.2283	**0.2274**	0.2346	0.2301	0.2297	0.2295	**0.2289**
	336	0.2916	0.2922	0.2909	0.2890	**0.2884**	0.2861	0.2839	**0.2836**	**0.2836**	**0.2836**
	720	0.3329	0.3281	0.3274	0.3269	**0.3264**	0.3259	0.3233	0.3227	0.3226	**0.3223**
Weather	96	0.2120	0.2157	0.2142	0.2084	**0.2076**	0.2294	0.2290	0.2261	0.2173	**0.2162**
	336	0.2904	0.2935	0.2911	0.2886	**0.2874**	0.3005	0.3030	0.2988	0.2952	**0.2929**
	720	**0.3390**	0.3485	0.3457	0.3447	0.3428	**0.3471**	0.3564	0.3537	0.3515	0.3497

Table C6: Credit-allocation ablation MAE in the Level scenario.

Dataset	H	PatchTST					DLinear				
		Uniform	Global	Lead-only	Channel-only	Full MATE	Uniform	Global	Lead-only	Channel-only	Full MATE
ETTh2	96	**0.2895**	0.2911	0.2904	0.2919	0.2912	**0.2887**	0.2896	0.2894	0.2910	0.2908
	336	**0.3440**	0.3445	0.3441	0.3445	0.3441	**0.3491**	0.3501	0.3496	0.3500	0.3496
	720	0.3990	0.3967	0.3968	**0.3965**	0.3966	0.4075	0.4038	**0.4037**	0.4051	0.4050
ETTm2	96	0.2314	0.2304	0.2294	0.2301	**0.2292**	0.2360	0.2318	0.2314	0.2312	**0.2306**
	336	0.2944	0.2957	0.2945	0.2934	**0.2927**	0.2896	0.2877	**0.2873**	0.2876	0.2875
	720	0.3368	0.3335	0.3328	0.3334	**0.3326**	0.3302	0.3283	0.3276	0.3277	**0.3273**
Weather	96	0.2141	0.2186	0.2170	0.2114	**0.2107**	0.2318	0.2326	0.2295	0.2208	**0.2194**
	336	0.2960	0.3008	0.2982	0.2959	**0.2945**	0.3060	0.3102	0.3061	0.3025	**0.3003**
	720	**0.3495**	0.3604	0.3579	0.3561	0.3541	**0.3576**	0.3691	0.3663	0.3637	0.3616

Full MATE achieves a mean MAE of 0.3020, lower than all four restricted settings. This supports the overall benefit of joint lead–channel credit allocation.

C.3 Residual Sources by Configuration

The settings w/o Local, w/o Global, w/o Vintage, w/o Input, and w/o Context remove the local, global, historical-version, input-induced, and context residuals, respectively. Reporting results by backbone and horizon distinguishes each source's aggregate contribution from its effects in individual configurations.

Table C7: Residual-source ablation MSE in the Natural scenario.

Dataset	H	PatchTST						DLinear					
		w/o Local	w/o Global	w/o Vintage	w/o Input	w/o Context	Full MATE	w/o Local	w/o Global	w/o Vintage	w/o Input	w/o Context	Full MATE
ETTh2	96	0.1819	0.1819	0.1830	0.1821	0.1831	**0.1817**	0.1802	0.1803	**0.1788**	0.1808	0.1797	0.1802
	336	0.2350	0.2353	0.2382	0.2363	**0.2348**	0.2352	0.2442	0.2441	0.2447	0.2457	**0.2435**	0.2440
	720	0.2851	0.2853	0.2862	0.2884	**0.2824**	0.2829	0.3004	0.3008	0.2989	0.3041	**0.2966**	0.2972
ETTm2	96	0.1152	0.1156	0.1170	**0.1150**	0.1159	0.1153	**0.1170**	0.1172	0.1196	0.1171	0.1175	**0.1170**
	336	**0.1827**	0.1830	0.1863	0.1839	0.1833	**0.1827**	0.1780	0.1783	0.1791	**0.1774**	0.1779	0.1777
	720	0.2316	0.2314	0.2346	0.2313	0.2330	**0.2312**	0.2306	0.2303	0.2309	**0.2287**	0.2301	0.2294
Weather	96	0.1596	0.1590	0.1607	0.1600	0.1628	**0.1584**	0.1673	0.1665	0.1679	0.1685	0.1806	**0.1657**
	336	0.2504	0.2502	0.2524	0.2505	0.2523	**0.2497**	0.2568	0.2565	0.2589	0.2573	0.2638	**0.2552**
	720	0.3270	0.3256	0.3313	**0.3235**	0.3291	0.3280	0.3351	0.3325	0.3398	**0.3316**	0.3400	0.3360

Table C8: Residual-source ablation MSE in the Level scenario.

Dataset	H	PatchTST						DLinear					
		w/o Local	w/o Global	w/o Vintage	w/o Input	w/o Context	Full MATE	w/o Local	w/o Global	w/o Vintage	w/o Input	w/o Context	Full MATE
ETTh2	96	**0.1875**	0.1876	0.1884	0.1876	0.1893	0.1876	0.1859	0.1860	**0.1844**	0.1861	0.1855	0.1860
	336	**0.2509**	0.2510	0.2542	0.2514	0.2513	0.2516	0.2613	**0.2608**	0.2622	0.2616	0.2612	0.2617
	720	0.3212	0.3207	0.3228	0.3234	**0.3196**	0.3201	0.3374	0.3368	0.3366	0.3397	**0.3347**	0.3352
ETTm2	96	0.1169	0.1172	0.1187	**0.1166**	0.1176	0.1170	**0.1186**	0.1188	0.1212	0.1187	0.1192	**0.1186**
	336	0.1877	**0.1876**	0.1912	0.1882	0.1883	**0.1876**	0.1819	0.1823	0.1833	**0.1816**	0.1821	0.1819
	720	0.2410	0.2401	0.2433	**0.2398**	0.2416	**0.2398**	0.2375	0.2378	0.2376	0.2365	0.2370	**0.2364**
Weather	96	0.1617	0.1611	0.1629	0.1619	0.1649	**0.1607**	0.1698	0.1690	0.1706	0.1706	0.1833	**0.1684**
	336	0.2568	**0.2562**	0.2588	0.2565	0.2588	**0.2562**	0.2632	0.2626	0.2654	0.2632	0.2706	**0.2619**
	720	0.3406	0.3380	0.3451	**0.3361**	0.3435	0.3421	0.3489	0.3461	0.3540	**0.3443**	0.3547	0.3502

Removing either vintage or context corrections increases mean MSE, supporting overlapping historical forecasts and recent observations as useful correction evidence. The other sources have configuration-dependent effects; the complete dictionary achieves the lowest overall MSE.

Table C9: Residual-source ablation MAE in the Natural scenario.

Dataset	H	PatchTST						DLinear					
		w/o Local	w/o Global	w/o Vintage	w/o Input	w/o Context	Full MATE	w/o Local	w/o Global	w/o Vintage	w/o Input	w/o Context	Full MATE
ETTh2	96	0.2873	0.2873	0.2873	**0.2872**	0.2876	**0.2872**	0.2862	0.2865	**0.2852**	0.2865	0.2859	0.2864
	336	0.3318	0.3320	0.3336	0.3331	**0.3309**	0.3316	0.3367	0.3366	0.3366	0.3381	**0.3358**	0.3363
	720	0.3676	0.3677	0.3681	0.3703	**0.3653**	0.3658	0.3763	0.3765	0.3749	0.3792	**0.3733**	0.3737
ETTm2	96	0.2274	0.2278	0.2287	**0.2272**	0.2279	0.2274	**0.2289**	0.2292	0.2324	0.2291	0.2293	**0.2289**
	336	**0.2884**	0.2885	0.2912	0.2893	0.2885	**0.2884**	0.2839	0.2841	0.2852	**0.2829**	0.2837	0.2836
	720	0.3266	0.3265	0.3294	0.3269	0.3271	**0.3264**	0.3233	0.3231	0.3239	**0.3213**	0.3224	0.3223
Weather	96	**0.2062**	0.2078	0.2106	0.2090	0.2122	0.2076	0.2157	**0.2156**	0.2179	0.2185	0.2298	0.2162
	336	**0.2855**	0.2872	0.2899	0.2869	0.2885	0.2874	**0.2919**	0.2922	0.2952	0.2930	0.2981	0.2929
	720	0.3391	0.3394	0.3454	**0.3373**	0.3435	0.3428	0.3462	0.3447	0.3518	**0.3435**	0.3522	0.3497

Table C10: Residual-source ablation MAE in the Level scenario.

Dataset	H	PatchTST						DLinear					
		w/o Local	w/o Global	w/o Vintage	w/o Input	w/o Context	Full MATE	w/o Local	w/o Global	w/o Vintage	w/o Input	w/o Context	Full MATE
ETTh2	96	0.2911	0.2912	0.2912	**0.2910**	0.2917	0.2912	0.2905	0.2907	**0.2895**	0.2904	0.2903	0.2908
	336	0.3438	0.3438	0.3458	0.3442	**0.3434**	0.3441	0.3494	**0.3488**	0.3497	0.3496	0.3491	0.3496
	720	0.3975	0.3965	0.3983	0.3988	**0.3963**	0.3966	0.4064	0.4053	0.4059	0.4075	**0.4049**	0.4050
ETTm2	96	0.2292	0.2294	0.2304	**0.2289**	0.2296	0.2292	**0.2306**	0.2308	0.2341	0.2308	0.2311	**0.2306**
	336	0.2927	**0.2926**	0.2955	0.2931	0.2928	0.2927	0.2873	0.2877	0.2891	**0.2867**	0.2876	0.2875
	720	0.3335	**0.3324**	0.3357	0.3328	0.3334	0.3326	0.3280	0.3279	0.3287	**0.3265**	0.3274	0.3273
Weather	96	**0.2091**	0.2106	0.2135	0.2117	0.2151	0.2107	**0.2186**	0.2188	0.2212	0.2212	0.2333	0.2194
	336	**0.2922**	0.2938	0.2969	0.2938	0.2957	0.2945	**0.2986**	0.2991	0.3024	0.2996	0.3058	0.3003
	720	0.3503	0.3506	0.3569	**0.3491**	0.3550	0.3541	0.3578	0.3572	0.3639	**0.3555**	0.3644	0.3616

Removing either vintage or context corrections also increases mean MAE. Removing local, global, or input-induced corrections has smaller effects, and some removal variants attain slightly lower MAE. Thus, individual sources need not affect MSE and MAE identically.

C.4 Credit-Weight Analysis

Figure C1 reports credit weights averaged within each run over prediction time, leads, and channels, then aggregated by dataset across backbones and horizons. ETTm1 places more weight on Global and Vintage corrections, whereas Exchange places more on Context; allocations also vary between Natural and Level. These averages describe condition-dependent controller use, not causal contributions.

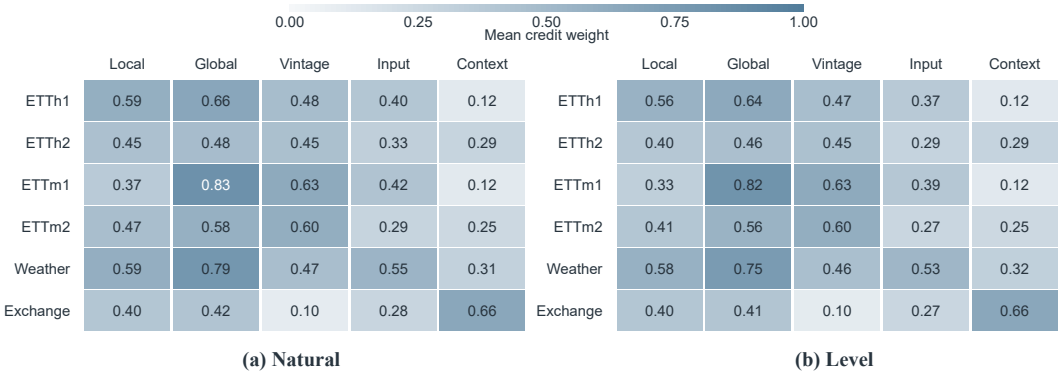


Figure C1: Mean credit weights for the five residual sources in (a) Natural and (b) Level.

D Additional Stress Tests

The stress tests cover ETTh2 and ETTm2, PatchTST and DLinear, and forecast horizons of 96, 336, and 720. Each of the four perturbation types—trend, scale, frequency, and multiple regime shifts—contains 12 configurations evaluated with seed 0. We compare TAFAS, PETSA, and MATE to assess adaptation under targeted perturbations. MATE achieves the lowest mean MSE for all four types; the detailed results show how performance varies across backbones and horizons.

Table D1: Mean MSE under four types of stress-test perturbations.

Scenario	TAFAS	PETSA	MATE
Trend	0.2169	0.2205	**0.2146**
Scale	0.2122	0.2190	**0.2089**
Frequency	0.2484	0.2571	**0.2444**
Multiple regime shifts	0.2189	0.2237	**0.2158**

D.1 Trend Stress Tests

Table D2: MSE under trend perturbations.

Dataset	H	PatchTST			DLinear		
		TAFAS	PETSA	MATE	TAFAS	PETSA	MATE
ETTh2	96	0.1830	0.1843	**0.1818**	**0.1791**	0.1809	0.1817
	336	0.2446	0.2478	**0.2432**	**0.2551**	0.2584	0.2553
	720	0.3174	0.3236	**0.3133**	0.3357	0.3443	**0.3337**
ETTm2	96	0.1174	0.1180	**0.1155**	0.1198	0.1211	**0.1172**
	336	0.1887	0.1916	**0.1840**	0.1795	0.1825	**0.1791**
	720	0.2450	0.2520	**0.2358**	0.2371	0.2415	**0.2341**

MATE attains the lowest MSE in 10 of 12 configurations under trend perturbations.

Table D3: MAE under trend perturbations.

Dataset	H	PatchTST			DLinear		
		TAFAS	PETSA	MATE	TAFAS	PETSA	MATE
ETTh2	96	**0.2882**	0.2887	0.2890	**0.2866**	0.2876	0.2895
	336	0.3484	0.3471	**0.3434**	**0.3489**	0.3516	0.3497
	720	0.4093	0.4072	**0.3989**	0.4123	0.4184	**0.4101**
ETTm2	96	0.2298	0.2300	**0.2284**	0.2329	0.2342	**0.2297**
	336	0.2949	0.2952	**0.2906**	0.2858	0.2873	**0.2857**
	720	0.3455	0.3433	**0.3316**	0.3301	0.3308	**0.3275**

MATE attains the lowest MAE in 9 of 12 configurations under trend perturbations.

D.2 Scale Stress Tests

Table D4: MSE under scale perturbations.

Dataset	H	PatchTST			DLinear		
		TAFAS	PETSA	MATE	TAFAS	PETSA	MATE
ETTh2	96	0.1894	0.1903	**0.1872**	**0.1826**	0.1852	0.1841
	336	0.2423	0.2480	**0.2410**	**0.2461**	0.2561	0.2477
	720	0.2927	0.3014	**0.2858**	**0.2944**	0.3158	0.2977
ETTm2	96	0.1212	0.1219	**0.1188**	0.1235	0.1250	**0.1205**
	336	0.1937	0.1964	**0.1856**	0.1813	0.1867	**0.1796**
	720	0.2478	0.2555	**0.2309**	0.2320	0.2461	**0.2281**

MATE attains the lowest MSE in 9 of 12 configurations under scale perturbations.

Table D5: MAE under scale perturbations.

Dataset	H	PatchTST			DLinear		
		TAFAS	PETSA	MATE	TAFAS	PETSA	MATE
ETTh2	96	0.2871	0.2880	**0.2868**	**0.2833**	0.2857	0.2847
	336	0.3336	0.3367	**0.3308**	**0.3320**	0.3405	0.3341
	720	0.3733	0.3760	**0.3644**	**0.3668**	0.3842	0.3706
ETTm2	96	0.2289	0.2294	**0.2266**	0.2320	0.2336	**0.2281**
	336	0.2934	0.2939	**0.2860**	0.2821	0.2863	**0.2807**
	720	0.3382	0.3390	**0.3206**	0.3189	0.3284	**0.3160**

MATE attains the lowest MAE in 9 of 12 configurations under scale perturbations.

D.3 Frequency Stress Tests

Table D6: MSE under frequency perturbations.

Dataset	H	PatchTST			DLinear		
		TAFAS	PETSA	MATE	TAFAS	PETSA	MATE
ETTh2	96	0.2201	0.2207	**0.2159**	0.2127	0.2152	**0.2121**
	336	0.3016	0.3113	**0.2953**	0.3052	0.3203	**0.3043**
	720	0.3560	0.3662	**0.3452**	**0.3537**	0.3810	0.3562
ETTm2	96	0.1203	0.1209	**0.1189**	0.1225	0.1237	**0.1203**
	336	0.2110	0.2132	**0.2043**	**0.1996**	0.2041	0.2014
	720	0.2969	0.3087	**0.2790**	0.2809	0.3002	**0.2794**

MATE attains the lowest MSE in 10 of 12 configurations under frequency perturbations.

Table D7: MAE under frequency perturbations.

Dataset	H	PatchTST			DLinear		
		TAFAS	PETSA	MATE	TAFAS	PETSA	MATE
ETTh2	96	0.3359	0.3366	**0.3335**	0.3320	0.3340	**0.3304**
	336	0.4096	0.4186	**0.4064**	**0.4112**	0.4239	0.4119
	720	0.4500	0.4562	**0.4412**	**0.4435**	0.4646	0.4475
ETTm2	96	0.2354	0.2359	**0.2345**	0.2383	0.2396	**0.2355**
	336	0.3229	0.3244	**0.3186**	**0.3151**	0.3179	0.3163
	720	0.3960	0.4041	**0.3837**	0.3847	0.3967	**0.3826**

MATE attains the lowest MAE in 9 of 12 configurations under frequency perturbations.

D.4 Multiple Regime Shifts Stress Tests

Table D8: MSE under multiple regime shifts perturbations.

Dataset	H	PatchTST			DLinear		
		TAFAS	PETSA	MATE	TAFAS	PETSA	MATE
ETTh2	96	0.1897	0.1905	**0.1881**	**0.1838**	0.1861	0.1867
	336	0.2515	0.2561	**0.2513**	**0.2566**	0.2632	0.2589
	720	0.3210	0.3251	**0.3099**	0.3244	0.3388	**0.3220**
ETTm2	96	0.1180	0.1186	**0.1161**	0.1203	0.1216	**0.1176**
	336	0.1926	0.1947	**0.1866**	0.1816	0.1856	**0.1811**
	720	0.2492	0.2562	**0.2369**	0.2387	0.2480	**0.2347**

MATE attains the lowest MSE in 10 of 12 configurations under multiple regime shifts perturbations.

Table D9: MAE under multiple regime shifts perturbations.

Dataset	H	PatchTST			DLinear		
		TAFAS	PETSA	MATE	TAFAS	PETSA	MATE
ETTh2	96	**0.2924**	0.2934	0.2931	**0.2894**	0.2916	0.2919
	336	**0.3471**	0.3518	**0.3471**	**0.3482**	0.3547	0.3504
	720	0.4032	0.4059	**0.3948**	0.4024	0.4124	**0.4006**
ETTm2	96	0.2304	0.2310	**0.2286**	0.2338	0.2350	**0.2300**
	336	0.2972	0.2980	**0.2924**	0.2877	0.2902	**0.2870**
	720	0.3431	0.3464	**0.3316**	0.3312	0.3359	**0.3277**

MATE attains the lowest MAE in 9 of 12 configurations under multiple regime shifts perturbations (including ties at the displayed precision).